

https://dspace.org/

# The origin of slope deposits in the southern Drakensberg, eastern Lesotho

**Mills, Stephanie Christiane**

**2008-03-31T09:46:04Z**
http://hdl.handle.net/10539/4726

Downloaded from a DSpace repository. https://dspace.org/

# CHAPTER 5

# Tsatsa-La-Mangaung Results

## 5.1 INTRODUCTION

Only one deposit occurs along the Tsatsa-La-Mangaung mountain range, approximately 2 km from the Great Escarpment. Its position is south-facing and it occurs in the upper portion of the slope. This chapter will describe the morphological, sedimentological and micromorphological results of this deposit. Five pits were additionally sampled on adjacent slopes in order to compare with the sediment from the deposit itself.

## 5.2 MORPHOLOGY

The Tsatsa-La-Mangaung ridge (Figures 5.1 and 5.2) is 224 m in length and varies in width between 14 m to 30 m. The ridge is steepest on its eastern aspect, where it reaches a maximum height of 16 m. The altitudinal range of the deposit varies from 3088 m a.s.l. to 3005 m a.s.l. There is a small secondary ridge to the east of the main ridge which measures 90 m in length, 13 m in width and 2 m in height. The eastern and western main ridge slope gradients are very similar and range from 9º to 26º (cross sections D-D and C-C; Figure 5.2) for the eastern gradient and 10º to 25° for the western gradient (cross sections B-B and C-C respectively; Figure 5.2). The longitudinal profile (cross section A-A) indicates that the slope gradient varies between 15º and 25° and the average gradient for the deposit is 23º. The grass-covered ridge has a large concentration of boulders on the surface and within the deposit itself, ranging from 0.15 m to 1.80 m in length (Figure 5.3). Cross section E-E represents the slope profile containing a range of units related to various types of processes (Figure 5.2) (see Figure 2.2 for comparison to a theoretical slope profile). The interfluve unit has a slope angle of 0º, gradually increasing to 4º on the seepage slope unit. The slope angle then increases to 27º on the convex creep slope and reaches a maximum of 45º on the fall face. On the transportational midslope, the slope angle averages 29º, tapering off to 11º on the colluvial footslope and 4º on the alluvial toeslope. The slope deposit occurs within both the transportational midslope and the colluvial footslope, with a total slope length of 1.2 km down to the small stream.

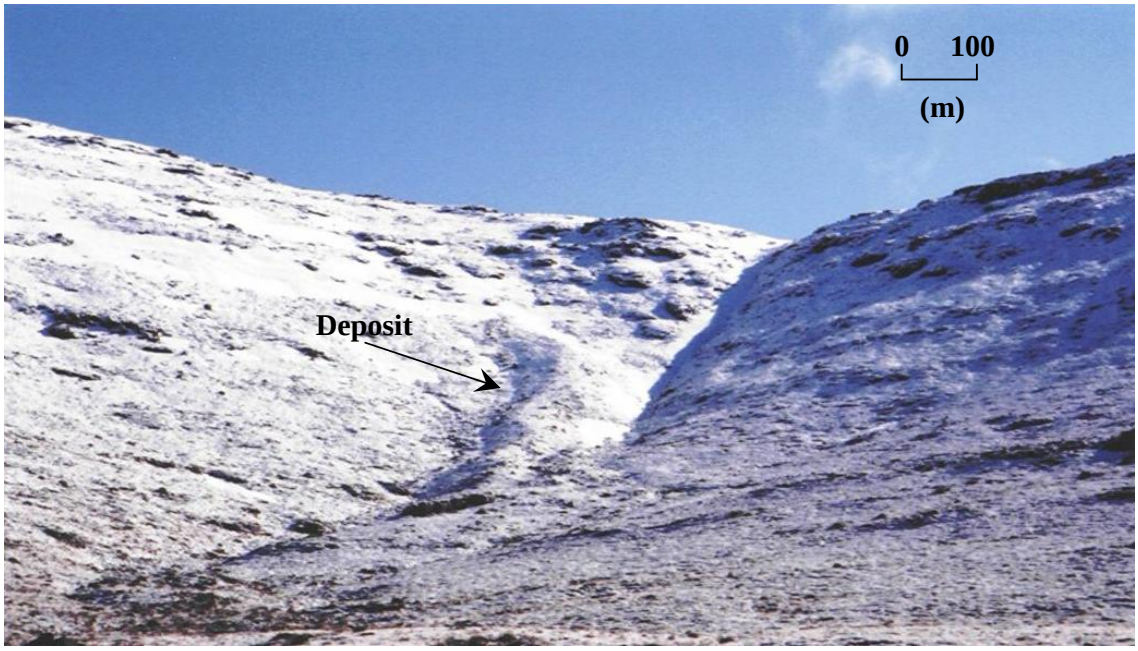



**Figure 5.1** The Tsatsa-La-Mangaung slope deposit (photo by S. Mills).

## 5.3 FIELD OBSERVATIONS

### 5.3.1 Tsatsa-La-Mangaung slope deposit

The lithofacies at the three trenches consist of present-day soil ranging from 25 cm to 60 cm in depth, which is underlain by a gravelly diamict (Figures 5.4 to 5.6). Although the excavation was to a depth between 120 cm and 140 cm, this is not the depth at which bedrock was reached, but the depth at which it became increasingly difficult to excavate boulders. The lithology of the parent material is basalt, which has been discussed in Chapter 3 in relation to its mineralogy. There is no evidence of a weathering front or evidence of distinct weathering rinds on the clasts. Within the diamict, a variety of different sized clasts are present, ranging in size from 2 cm to over 100 cm in length, and which are held together by a sandy matrix. The field characteristics from each trench are summarised in Figure 5.4, 5.5 and 5.6. The diamict unit in all three trenches is predominantly coarse grained, matrix supported with abundant clasts, poorly sorted and yellowish brown in colour.

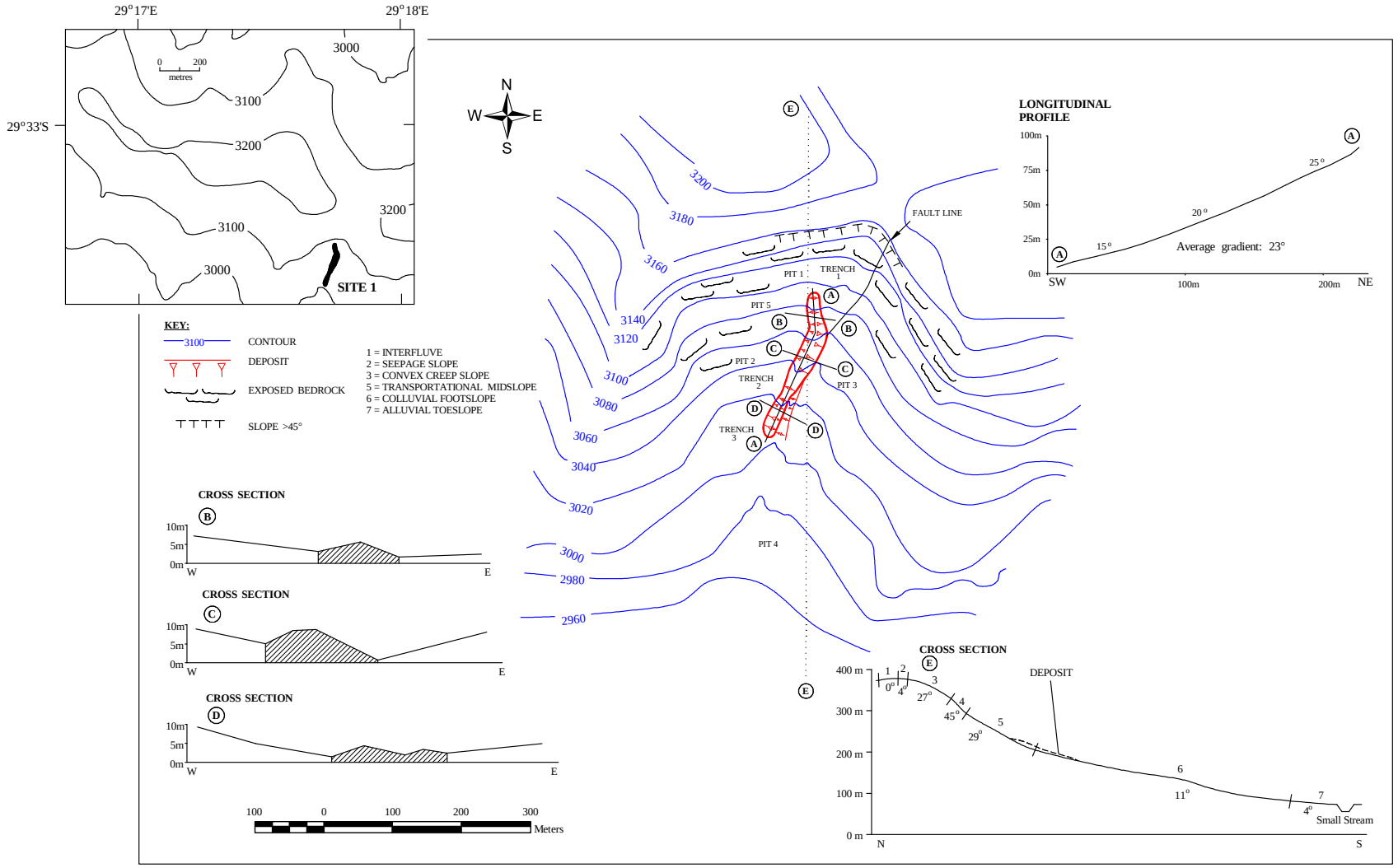



**Figure 5.2** Morphological map of the Tsatsa-La-Mangaung deposit.




**Figure 5.3** Boulders excavated from a trench at the Tsatsa-La-Mangaung deposit (photo by S. Mills).

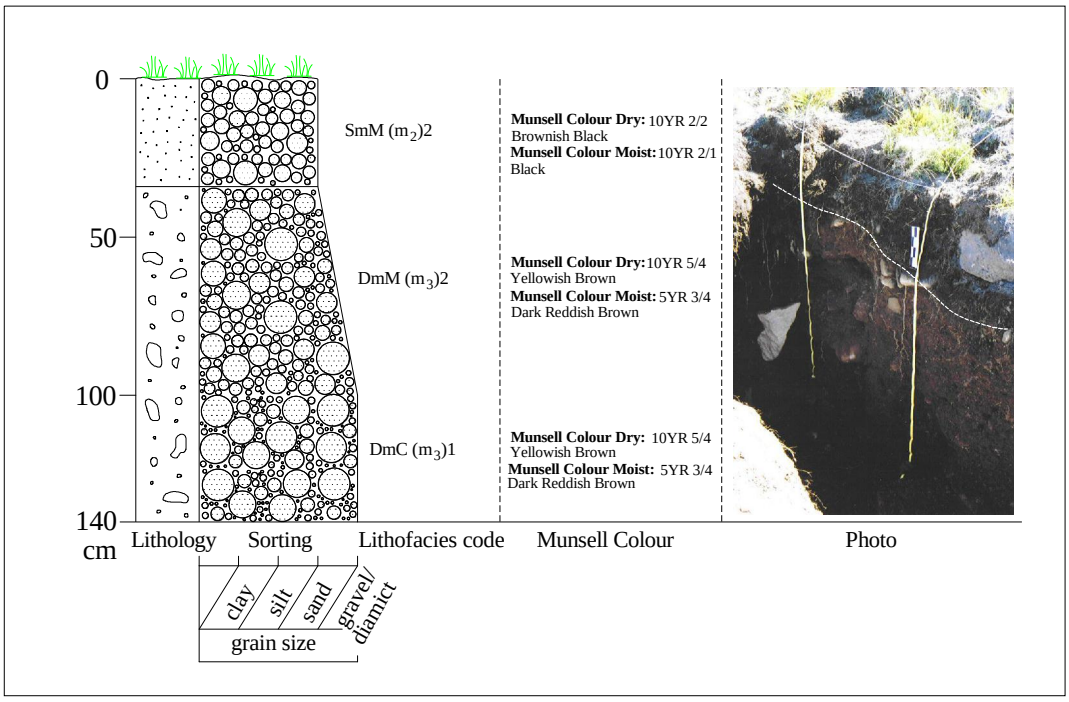



**Figure 5.4** Sedimentological and stratigraphical data for trench 1 at Tsatsa-La-Mangaung.

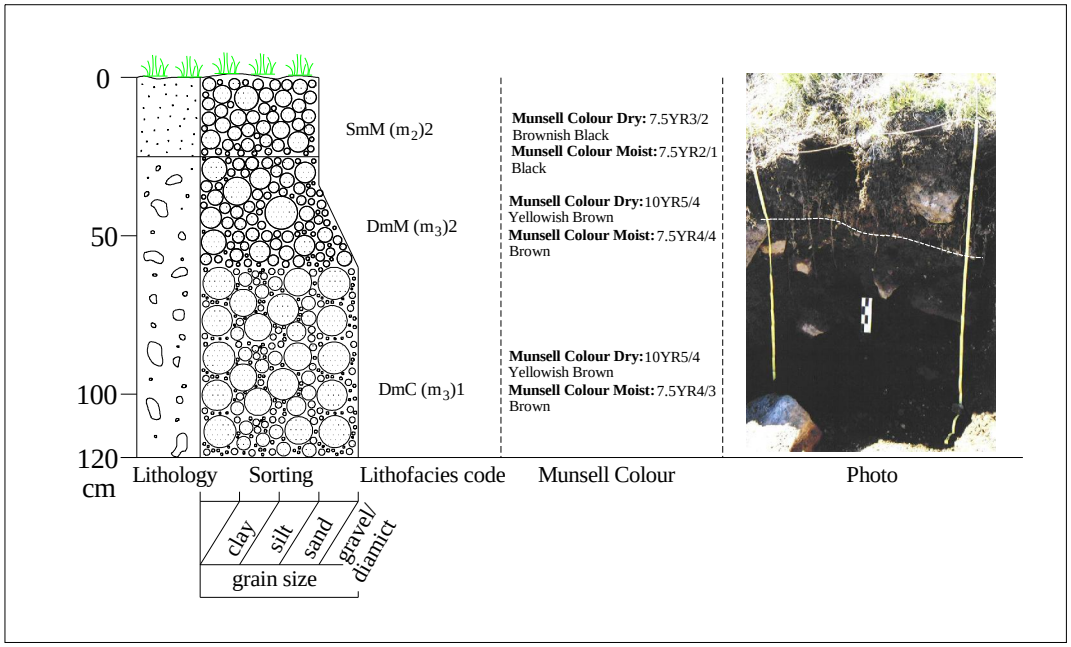



**Figure 5.5** Sedimentological and stratigraphical data for trench 2 at Tsatsa-La-Mangaung.

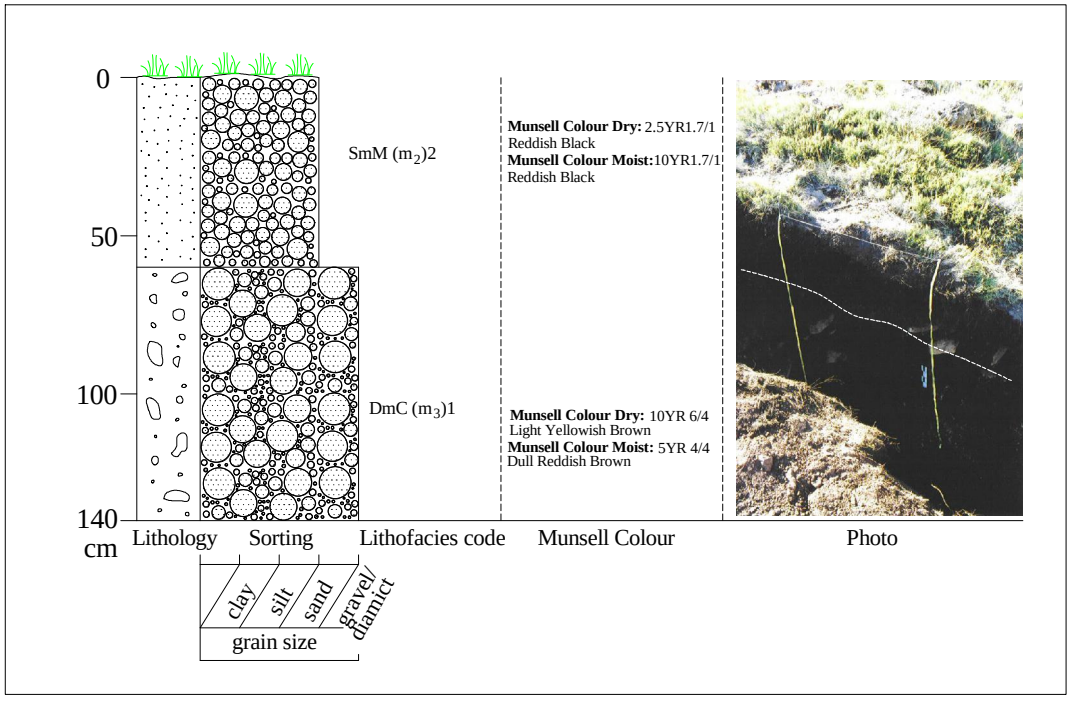



**Figure 5.6** Sedimentological and stratigraphical data for trench 3 at Tsatsa-La-Mangaung.

### 5.3.2 Tsatsa-La-Mangaung Pits

Soil profile data were collected for the five pits sampled on adjacent slopes to the slope deposit, and were reproduced as logs for each individual pit using a modified graphic data chart after Krüger and Kjær (1999) (Figures 5.7 to 5.11). Pit 1 (Figure 5.7) was sampled above the deposit (Figure 5.2) and consists of a very wet, almost peat-like soil down to 80 cm, without any horizonal changes. Pit 2 (Figure 5.8) is situated to the west of the slope deposit and is very different to the material found in pit 1. It consists of present-day soil overlying a pebbly layer. These pebbles range in size between 7 cm and 21 cm. They are predominantly angular, prolate in shape with a variable orientation and dips ranging between 9º and 15°. Despite the presence of the pebbly layer, being only 8 cm in thickness, it was not possible to collect sufficient data on clast shape and orientation, and will thus not be discussed further. Below this pebbly layer there is a coarse grained diamict unit.

Pit 3 (Figure 5.9) is located on the eastern side of the slope deposit and is once again very different to the other two pits discussed above. This pit consists of a typical soil profile which contains an A, B and C horizon. Pit 4 (Figure 5.10) is located below the slope deposit and consists of a present-day soil horizon overlying a silty horizon. Pit 5 (Figure 5.11) is once again located on the western side of the slope deposit, approximately 20 m below pit 1 in elevation. This pit is very similar to pit 1 in terms of the absence of a present-day soil horizon. The a-axis for clasts within this pit average 32 cm in length. Given that the clasts are well rounded in shape, it was not possible to undertake orientation measurements.

The sediment within the pits, excluding pit 2, varies considerably in comparison to the sediment present in the three trenches. The pits contain much finer sediment and there is an absence of clasts within the vertical profile. Pits 3 and 4 display typical soil horizons, whereas the sediment in the trenches consists of a massive diamict. The exception to this is in the case of pit 2, where there is a massive diamict present below the present-day soil horizon and also the presence of clasts within the profile.

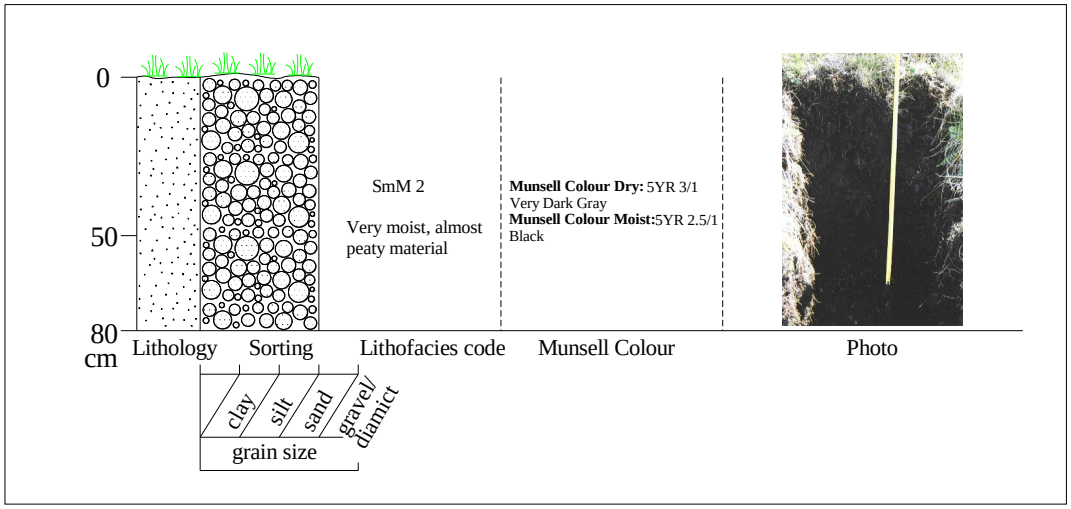



**Figure 5.7** Sedimentological and stratigraphical data for Pit 1 at Tsatsa-La-Mangaung.

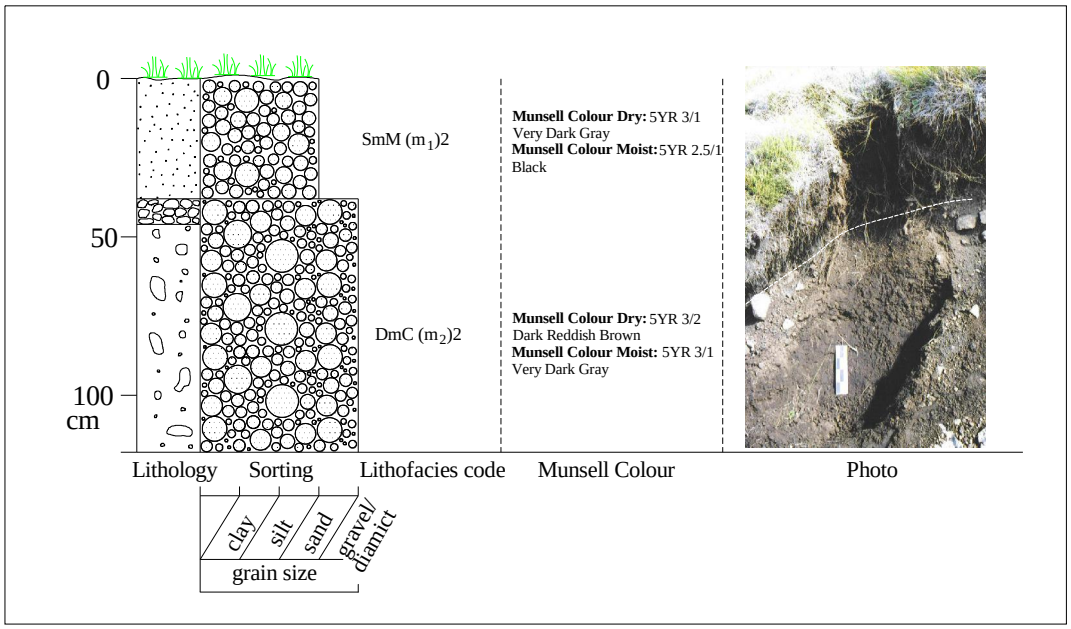



**Figure 5.8** Sedimentological and stratigraphical data for Pit 2 at Tsatsa-La-Mangaung.

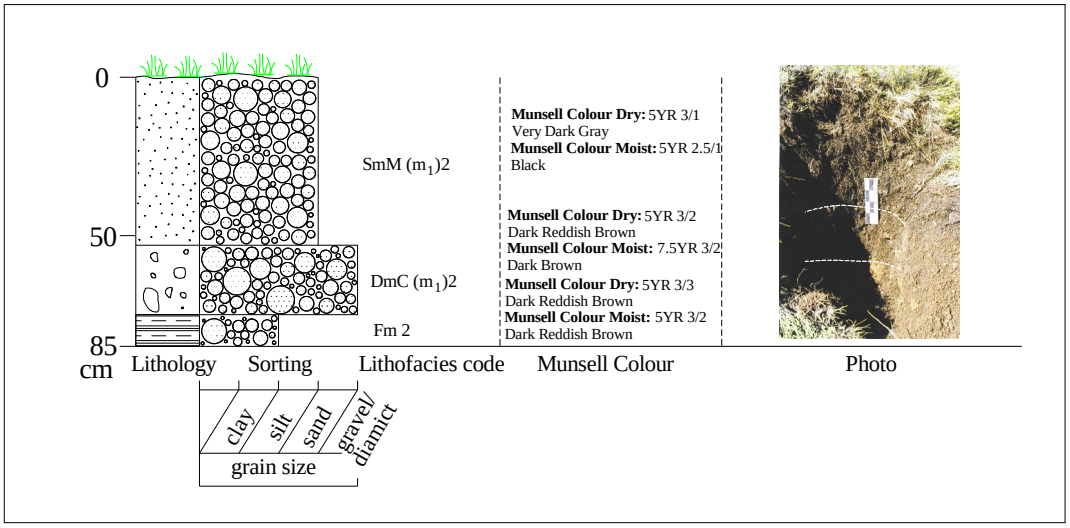



**Figure 5.9** Sedimentological and stratigraphical data for Pit 3 at Tsatsa-La-Mangaung.

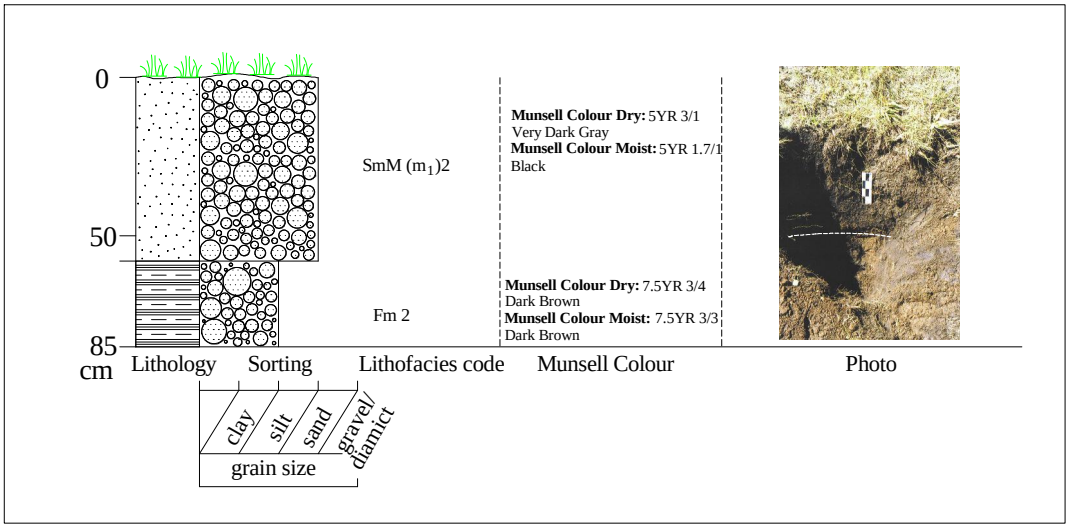



**Figure 5.10** Sedimentological and stratigraphical data for Pit 4 at Tsatsa-La-Mangaung.

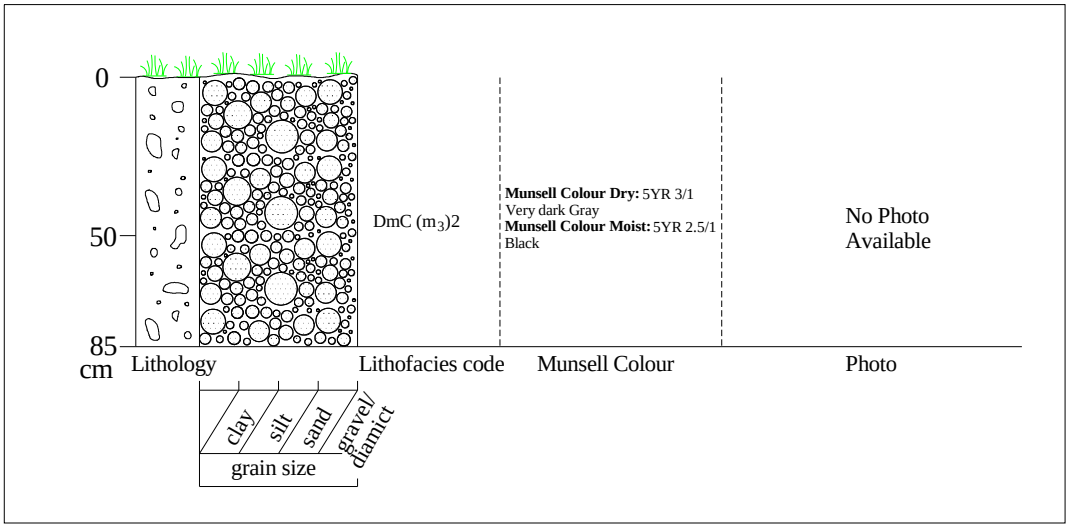



**Figure 5.11** Sedimentological and stratigraphical data for Pit 5 at Tsatsa-La-Mangaung.

## 5.4 PARTICLE SIZE ANALYSIS

### 5.4.1 Tsatsa-La-Mangaung slope deposit

The particle size distributions are very similar for the three trenches (Figures 5.12 to 5.14 and Table 5.1). Gravel is clearly the main constituent in all three trenches and constitutes >50% for all the samples, with the exception of trench 1 at 40 cm depth, which still represents part of the present-day soil horizon. The highest percentage of gravel occurs at trench 3 at 120 cm depth, where it constitutes 93% of the sample. There is a slight secondary peak at 4 phi in the case of all the trenches at 80 cm depth, however this is not indicative of a bimodal distribution, as indicated by the bimodality index in Table 5.1.

The graphic mean (Table 5.1) indicates that variation occurs in the mean values for the trenches, ranging between the -1 phi and +1 phi size classes. Thus, the samples range from fine/medium sand to gravel. Because the samples are primarily very negatively skewed, the mean is not a true representation of the sample, so in this case the mode is a better indication of the sample size. The mode for all sediment in the trenches is -1 phi, which means that the sediment is primarily of gravel size.

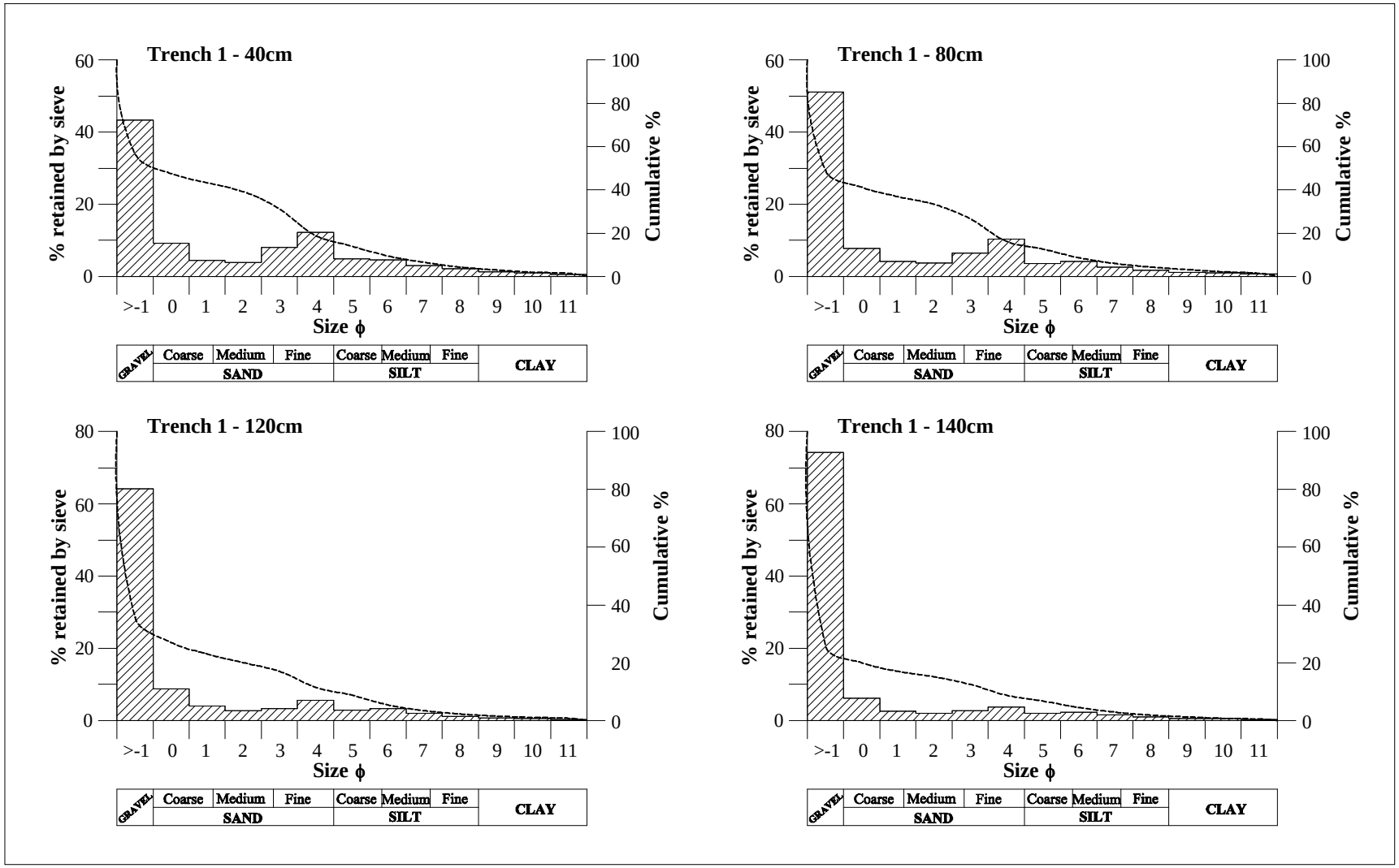



**Figure 5.12** Grain size distributions for the sediment from trench 1 at the Tsatsa-La-Mangaung Site.

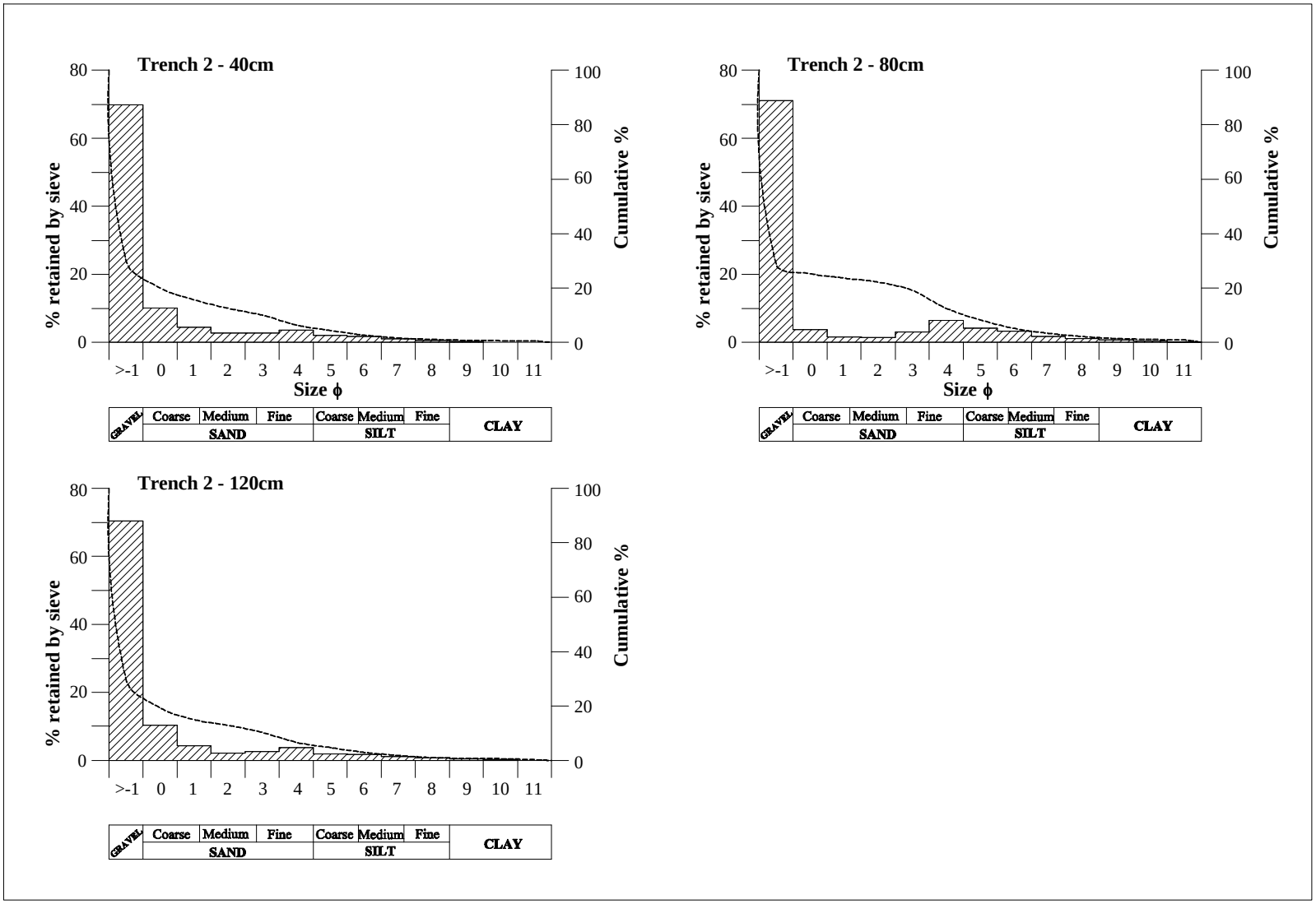



**Figure 5.13** Grain size distributions for the sediment from trench 2 at the Tsatsa-La-Mangaung Site.

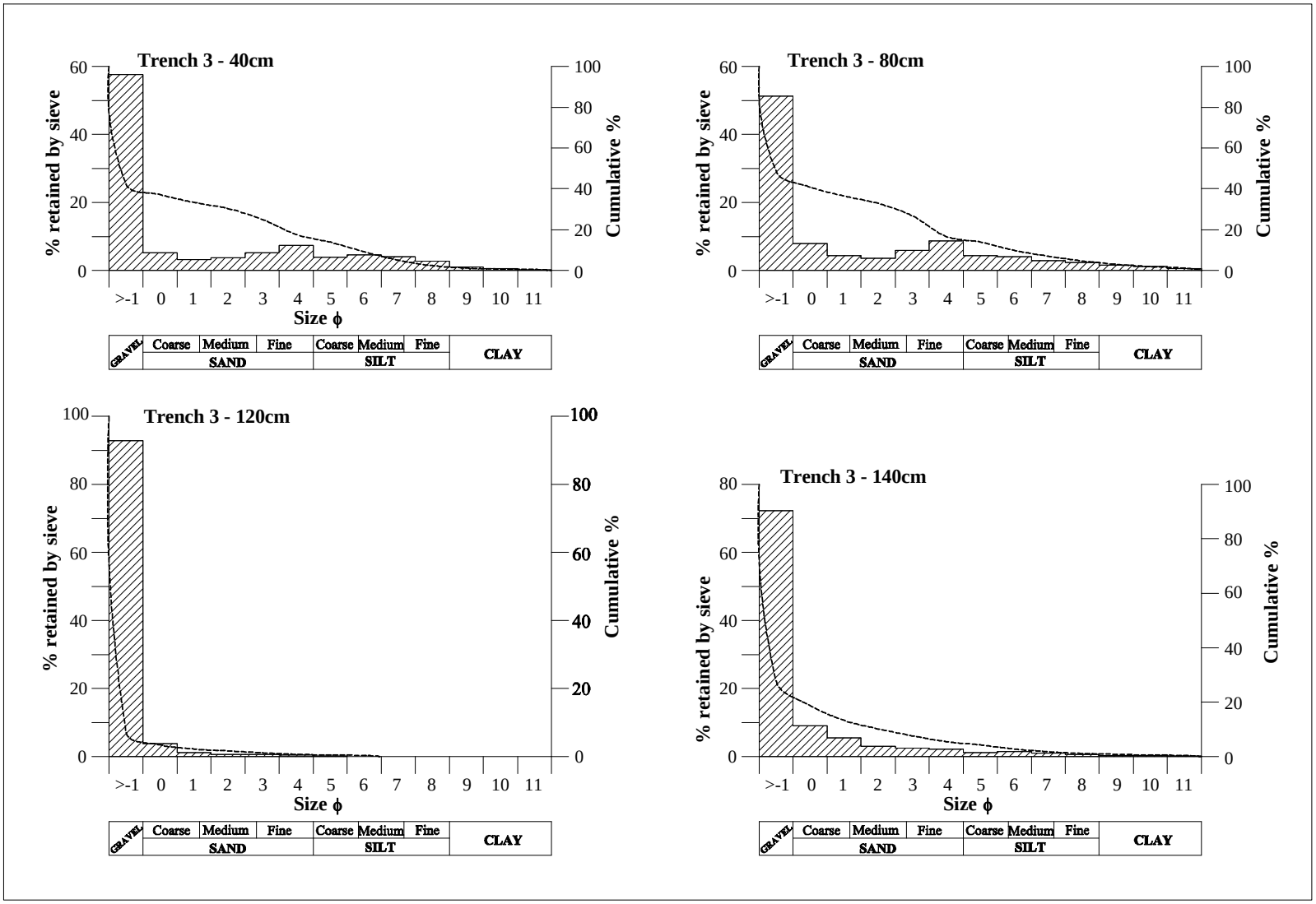



**Figure 5.14** Grain size distributions for the sediment from trench 3 at the Tsatsa-La-Mangaung Site.

**Table 5.1** Particle size statistical values for the Tsatsa-La-Mangaung slope deposit.

| Sample | Depth | Gravel (%) | Sand (%) | Silt (%) | Clay (%) | Mean (phi) | Mode (phi) | Peaks (phi) | Bimodality Index (B*) |
|---|---|---|---|---|---|---|---|---|---|
| Trench 1 | 40 cm | 43 | 38 | 16 | 3 | 1.08 | -1 | -1, 4 | 1.40 |
| | 80 cm | 51 | 33 | 13 | 3 | 0.69 | -1 | -1, 4 | 1.00 |
| | 120 cm | 64 | 24 | 10 | 2 | 0.40 | -1 | -1 | 0.45 |
| | 140 cm | 74 | 17 | 8 | 1 | -0.15 | -1 | -1 | 0.25 |
| Trench 2 | 40 cm | 70 | 24 | 5 | 1 | -0.37 | -1 | -1 | 0.25 |
| | 80 cm | 71 | 16 | 11 | 2 | 0.49 | -1 | -1 | 0.45 |
| | 120 cm | 70 | 23 | 6 | 1 | -0.43 | -1 | -1 | 0.25 |
| Trench 3 | 40 cm | 58 | 25 | 16 | 1 | 0.84 | -1 | -1 | 0.65 |
| | 80 cm | 51 | 31 | 15 | 3 | 0.85 | -1 | -1, 4 | 0.85 |
| | 120 cm | 93 | 6 | 1 | 0 | -1 | -1 | -1 | - |
| | 140 cm | 72 | 22 | 5 | 1 | -0.52 | -1 | -1 | 0.14 |

Further statistical analyses have been undertaken in the form of sorting, skewness and kurtosis and are summarised in Tables 5.2 and 5.3. The sediment is generally poorly sorted, very negatively skewed and leptokurtic (Table 5.4). The standard deviation indicates that the mean results for the particle size statistical analysis are typical of the sample distribution given that they fall within two standard deviations of the mean.

**Table 5.2** Further particle size statistical values for the Tsatsa-La-Mangaung slope deposit.

| Sample | | Sorting | Skewness | Kurtosis |
|---|---|---|---|---|
| Trench 1 | 40 cm | 2.72 | -0.82 | 0.80 |
| | 80 cm | 2.57 | -1.00 | 0.83 |
| | 120 cm | 2.13 | -1.00 | 2.02 |
| | 140 cm | 1.66 | -1.00 | >3.00 |
| Trench 2 | 40 cm | 1.33 | -1.00 | >3.00 |
| | 80 cm | 2.18 | -1.00 | 2.57 |
| | 120 cm | 1.31 | -1.00 | >3.00 |
| Trench 3 | 40 cm | 2.60 | -1.00 | 0.82 |
| | 80 cm | 2.73 | -1.00 | 0.85 |
| | 120 cm | 0.06 | -1.00 | >3.00 |
| | 140 cm | 1.17 | -1.00 | >3.00 |

### 5.4.2 Tsatsa-La-Mangaung pits

The particle size distributions vary considerably between the five pits (Figure 5.15 and Table 5.5). The particle size results for pits 1 and 5 are almost identical, with gravel constituting 42% and secondary peaks occurring between 4 phi and 8 phi. Despite the presence of several secondary peaks, the bimodality index falls between 0.9 and 1.05, which indicates that the sediment in pits 1 and 5 is unimodal. The sediment in pit 2 is very similar to that of trench 1 at 120 cm depth, where gravel is once again the main constituent, comprising 61% of the sample. The sediment within pit 3 varies with depth, as would be expected given the change in horizons. Gravel is the main constituent (64%) at 40 cm depth but decreases to 6% at 90 cm depth, where sand (48%) and silt (42%) dominate. The sediment within pit 4 is uniform with sand being the primary constituent. The sediment in both pit 4 samples is bimodal, with a bimodality index that increases with depth. The graphic mean (Table 5.5) once again indicates that the sediment in pits 1 and 5 are similar, with values falling between 1.84

**Table 5.3** Verbal scale for standard deviation (sorting), Skewness and Kurtosis (Folk and Ward, 1957).

| Standard deviation (phi units) | Category |
|---|---|
| <0.35 | Very well-sorted |
| 0.35 to 0.49 | Well-sorted |
| 0.50 to 0.99 | Moderately-sorted |
| 1.00 to 1.99 | Poorly-sorted |
| 2.00 to 3.99 | Very poorly-sorted |
| ≥ 4.00 | Extremely poorly-sorted |

| Skewness (phi units) | Category |
|---|---|
| -1.00 to -0.31 | Very negatively (coarse)-skewed |
| -0.3 to -0.11 | Negative (coarse)-skewed |
| -0.10 to 0.09 | Nearly symmetrical |
| 0.10 to 0.29 | Positive (fine)-skewed |
| 0.30 to 0.99 | Very positive (fine)-skewed |

| Kurtosis (phi units) | Category |
|---|---|
| <0.67 | Very platykurtic |
| 0.67 to 0.89 | Platykurtic |
| 0.90 to 1.10 | Mesokurtic |
| 1.11 to 1.49 | Leptokurtic |
| 1.50 to 2.99 | Very leptokurtic |
| ≥3.00 | Extremely leptokurtic |

**Table 5.4** Mean and Standard deviation for the particle size statistical analysis at the Tsatsa-La-Mangaung slope deposit.

| Trench | Mean | | Mode | | Sorting | | Skewness | | Kurtosis | |
|---|---|---|---|---|---|---|---|---|---|---|
| | *x* | *s* | | | *x* | *s* | *x* | *s* | *x* | *s* |
| Trench 1 | 0.50 | 0.52 | -1 | 0 | 2.27 | 0.48 | -0.96 | 0.09 | 1.66 | 1.06 |
| Trench 2 | -0.11 | 0.52 | -1 | 0 | 1.61 | 0.50 | -1 | 0 | 2.86 | 0.25 |
| Trench 3 | 0.04 | 0.95 | -1 | 0 | 1.64 | 1.27 | -1 | 0 | 1.92 | 1.25 |

phi at pit 1 and 1.98 phi at pit 5, which places these results in the medium sand category (Table 4.3). The sediment in pit 2 has a mean value of 0.93 phi, which corresponds well with the results of the present-day soil horizon within the slope deposit, rather than the underlying diamict sampled in the trenches (Table 5.1). The sediment in pits 3

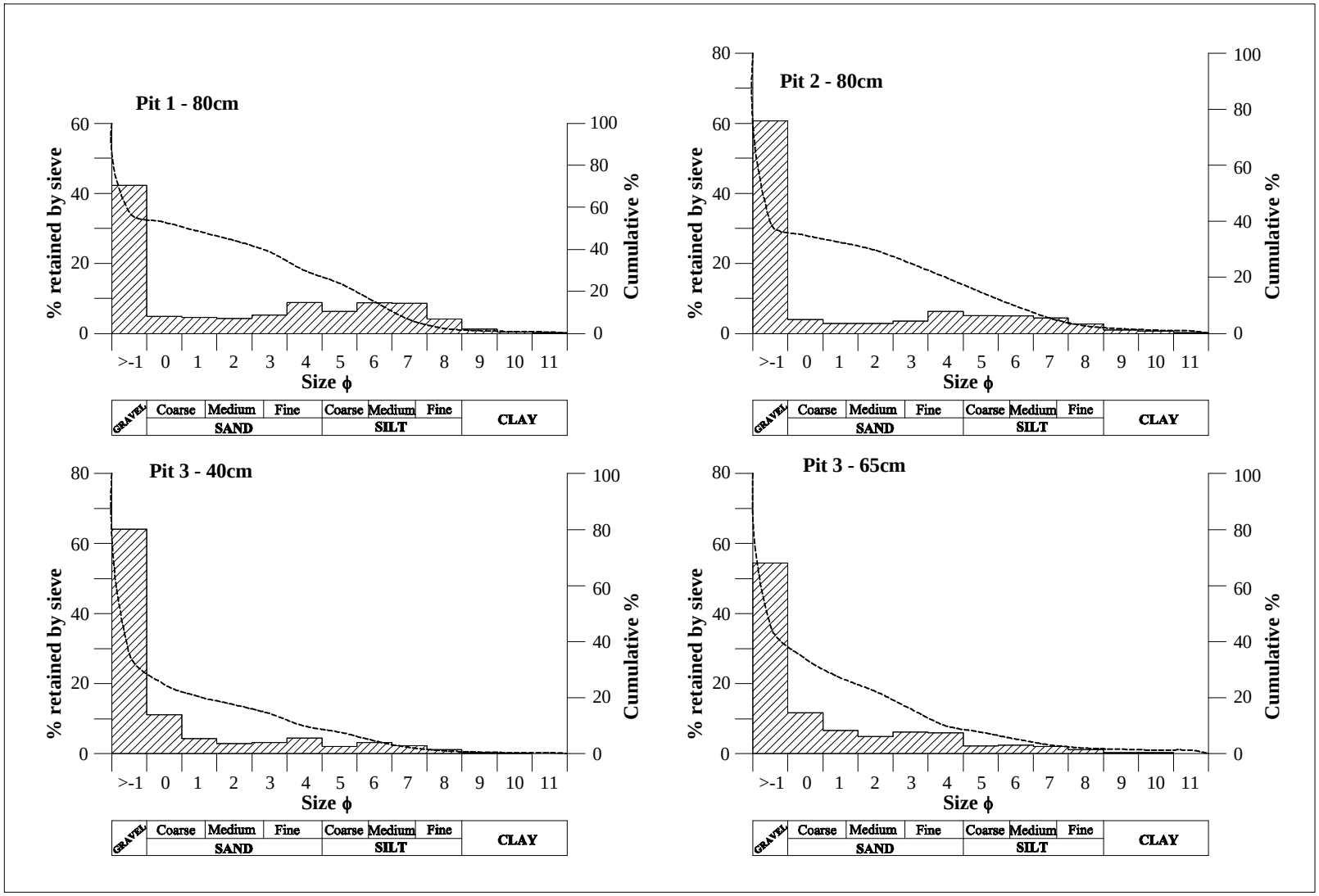



**Figure 5.15** Grain size distributions for the sediment from the pits at the Tsatsa-La-Mangaung site.

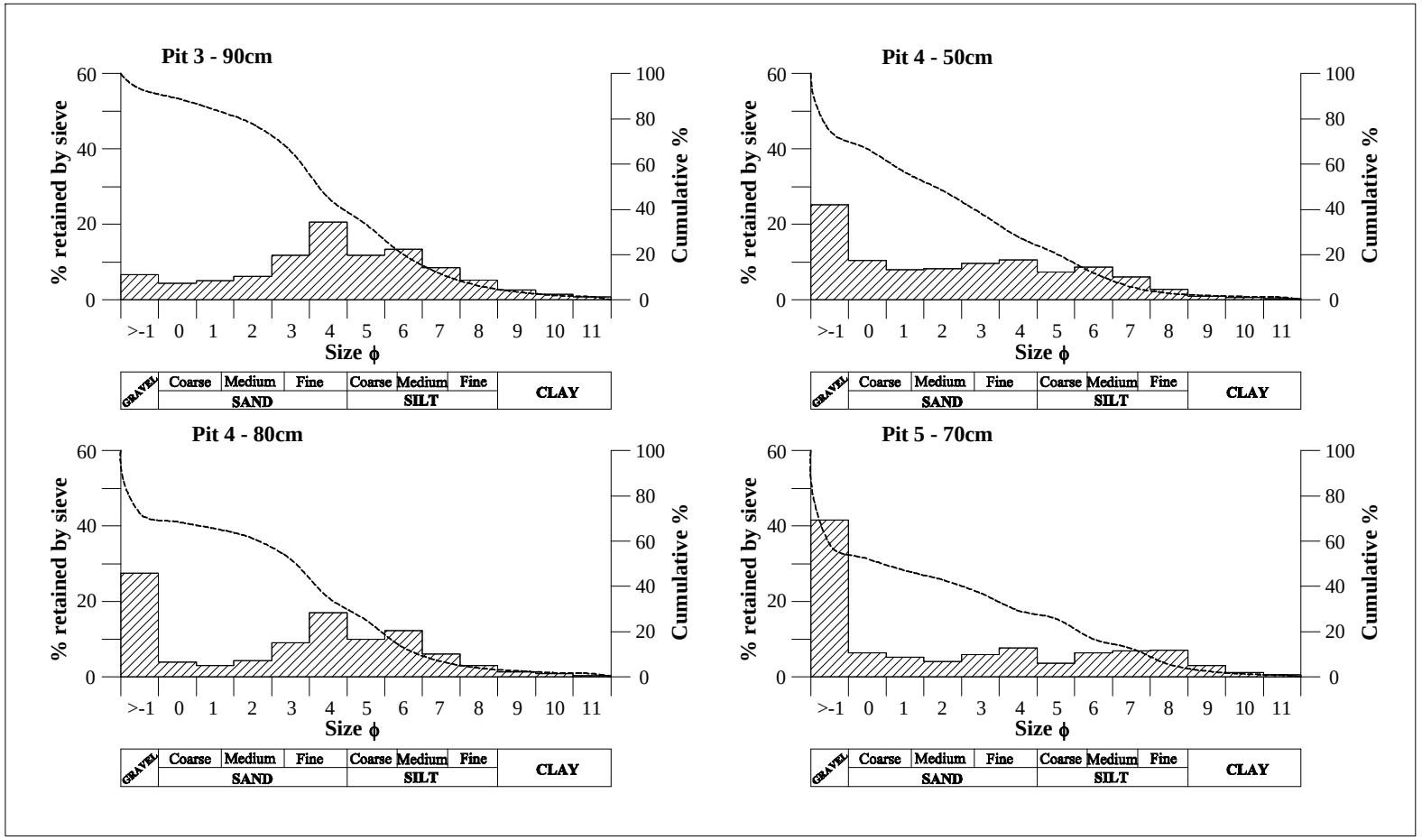



**Figure 5.15** Cont…

**Table 5.5** Particle size statistical values for the Tsatsa-La-Mangaung pits.

| Sample | Depth | Gravel (%) | Sand (%) | Silt (%) | Clay (%) | Mean (phi) | Mode (phi) | Peaks (phi) | Bimodality Index ($B^*$) |
|---|---|---|---|---|---|---|---|---|---|
| Pit 1 | 80 cm | 42 | 28 | 29 | 1 | 1.84 | -1 | -1, 4, 6, 7 | 1.05 |
| Pit 2 | 80 cm | 61 | 19 | 18 | 2 | 0.93 | -1 | -1, 4 | 0.5 |
| Pit 3 | 40 cm | 64 | 26 | 9 | 1 | 0.17 | -1 | -1 | 0.35 |
| | 65 cm | 54 | 36 | 8 | 2 | 0.33 | -1 | -1, 3 | 0.44 |
| | 90 cm | 6 | 48 | 42 | 4 | 2.73 | 4 | - | - |
| Pit 4 | 50 cm | 25 | 47 | 26 | 2 | 2.10 | -1 | -1, 4 | 2.1 |
| | 80 cm | 28 | 37 | 32 | 3 | 2.63 | -1 | -1, 4, 6 | 3.05, 1.44 |
| Pit 5 | 70 cm | 42 | 29 | 27 | 2 | 1.98 | -1 | -1, 4, 8 | 0.9 |

and 4 becomes finer with depth. The mode for all sediment in the pits is -1 phi, which means that the sediment is primarily of gravel size, with the exception of pit 3 at 90 cm depth which has a mode of 4 phi, indicating that the sample is primarily comprised of very fine sand.

Further statistical analyses have been undertaken in the form of sorting, skewness and kurtosis (Table 5.6, 5.3). In terms of sediment sorting, all samples are very poorly sorted. Pit 3 at 90 cm depth is very finely skewed as is the sediment in pit 4 at 80 cm. Sediment characteristics for pits 1 and 5 are once again very similar, with the sediment in both these pits being very coarse skewed. With regards to kurtosis, pits 1, 2, 4 and 5 are very similar, with the sediment being either platykurtic or very platykurtic. In contrast, the sediment in pit 3 is very leptokurtic at 40 cm depth and becomes less leptokurtic with depth.

**Table 5.6** Further particle size statistical values for the Tsatsa-La-Mangaung pits.

| Sample | Sorting | Skewness | Kurtosis |
|---|---|---|---|
| Pit 1 80 cm | 2.98 | -0.57 | 0.58 |
| Pit 2 80 cm | 2.68 | -1 | 0.78 |
| Pit 3 40 cm | 1.92 | -1 | 2.94 |
| 65 cm | 2.07 | -1 | 1.19 |
| 90 cm | 2.13 | 0.51 | 1.14 |
| Pit 4 50 cm | 2.87 | -0.24 | 0.62 |
| 80 cm | 2.97 | 0.11 | 0.59 |
| Pit 5 70 cm | 3.26 | -0.65 | 0.61 |

## 5.5 CLAST FABRIC AND EIGENVALUES

Clast a-axis orientation and dip were plotted as an equal-area stereographic scatter plot and an equal-area stereographic contour plot (Figure 5.16). Orientation of the clasts measured within trenches 1 and 3 indicates preferred orientation down-slope in the direction of the ridge crest. Clasts in trench 2 display orientations that are transverse to the ridge. Most clasts dip between 10º to 40°. The chi-square test was used in order to determine whether clast orientation is statistically significant. Clasts in trenches 1 and 3 have a statistically significant orientation (<0.05%), whilst clasts in trench 2 have a probability of being randomly distributed at a level >0.05%.

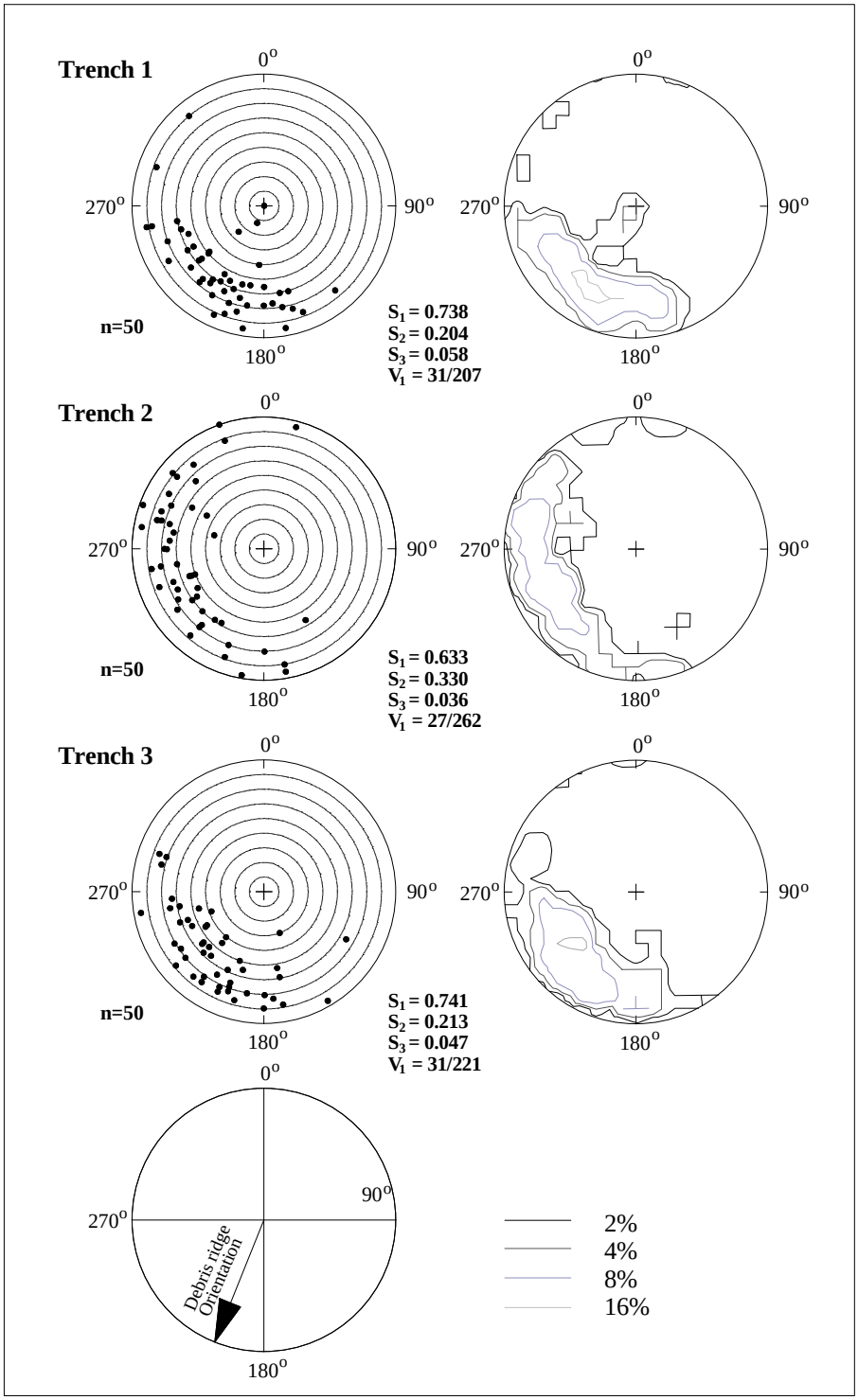



**Figure 5.16** Clast orientation, dip and contouring at trenches 1, 2 and 3 at Tsatsa-La-Mangaung (n = 50).

Eigenvalues were calculated from the dip and orientation of the clasts within the Tsatsa-La-Mangaung deposit. The $V_1$ value represents the principal eigenvector which parallels the axis of maximum clustering (Mark, 1973; Benn and Ringrose, 2001), which ties in with the preferred orientations of the clasts in the three trenches. The $S_1$, $S_2$ and $S_3$ values represent the normalised eigenvalues where $S_1 > S_2 > S_3$, and where $S_1 + S_2 + S_3 = 1$ (Mark, 1973; Benn and Ringrose, 2001). $S_1$ values, which measure the strength of clustering about the mean axis for the three sites are fairly high whilst $S_2$ and $S_3$ values are much lower, which indicates that the clast fabrics represent linear clusters, whereby all observations are approximately parallel and $S_1 \gg S_2 \approx S_3$.

The normalised eigenvalues were then plotted onto a general shape diagram (Figure 5.17), and indicate that the sediment in all three trenches have low isotropy and relatively high elongation values. Fabric shape ellipsoids are compared with plotted data from various published sources (Figure 5.17C), which indicate that sediment from all three trenches falls within the undeformed lodgement till envelope. The sediment in trenches 1 and 2 also falls within the limit of the basal ice envelope, the sediment in trench 2 within the gelifluction deposits envelope and the sediment in trench 1 also falls within the melt- out till envelope. When compared with Figure 5.17D, the sediment in all three trenches falls within the boundaries of lodgement till. A Triangular plot of normalised eigenvalues was also generated in order to further compare the Tsatsa-La-Mangaung eigenvalues to envelopes produced by previous authors for various deposits (Figure 5.18). The sediment in trench 3 falls within the melt-out till envelope and the sediment in trench 2 falls just outside it. However, the sediment in all three trenches falls within the internal fabric envelope for rock glaciers.

## 5.6 PARTICLE SHAPE

The method used to represent particle shape employs a triangular diagram after Benn and Ballantyne (1993), in which ratios of the three orthogonal axes of the particles are plotted, and which was first proposed by Sneed and Folk (1958). Particle form was plotted onto triangular diagrams using Tri-plot v1.3 (Graham and Midgley, 2000) and

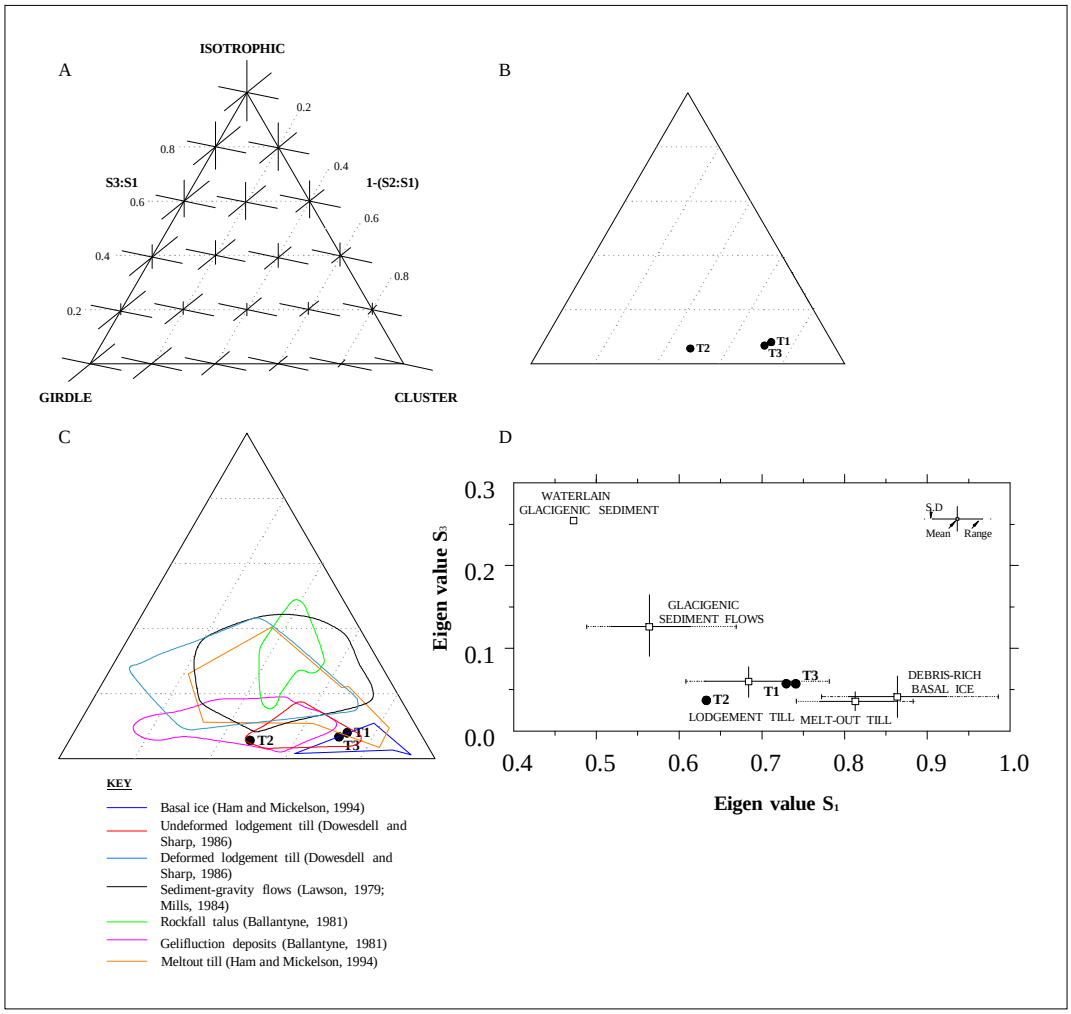



**Figure 5.17** Till fabric using eigenvalue data for the Tsatsa-La-Mangaung deposit. (A) The range of orthorhombic fabric shapes. (B) Fabric data from the three trenches. (C) Comparison with envelopes from a range of deposits. (D) Comparison with modern data fabrics from various environments (Dowdeswell *et al.*, 1985).

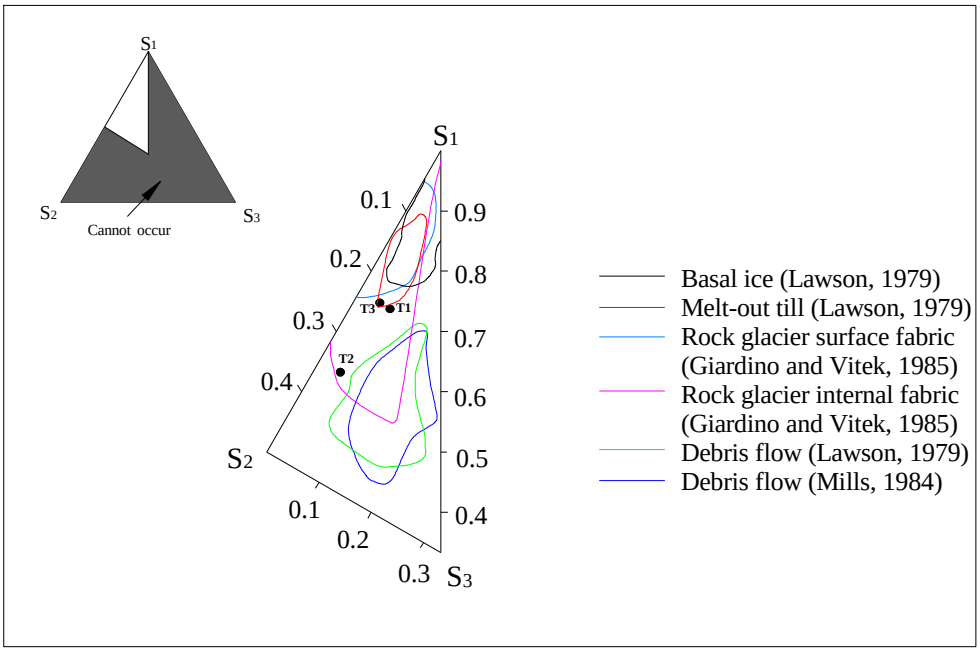



**Figure 5.18** Triangular plot of normalised eigenvalues for the Tsatsa-La-Mangaung deposit, showing envelopes suggested by various authors. The usable field diagram occupies one sixth of the diagram because $S_1 > S_2 > S_3$.

represents the descriptive classes defined by Sneed and Folk (1958) (Figure 5.19) and the isolines of the Oblate-prolate (OP) index of Dobkins and Folk (1970) (Figure 5.20).

All three trenches tend to contain a majority of bladed clasts (Figure 5.19 and Table 5.7), with mean values representing almost a perfect blade (0) (Table 5.8). Trenches 1 and 2 contain just above 50% of bladed clasts whereas trench 3 contains 46%. Rod-like (elongate) clasts are the second most common clast shape ranging from 28% in trench 2 to 34% in trench 3. The large number of bladed clasts is also reflected in Figure 5.20 which displays the Oblate-prolate Index. The majority of clasts fall within the -5 and +5 boundaries of the blade category, whilst relatively few fall within the disc (platy) category. The maximum projection sphericity is represented in Figure 5.21, which indicates varied results, with the clasts in all three trenches falling between 0.3 and 0.9. A further indication of the varied nature of the clasts in terms of maximum projection sphericity is indicated in Table 5.8, where the mean value ranges from 0.61 in trench 2 to 0.64 in trench 1. A sphere has a value of 1, whilst

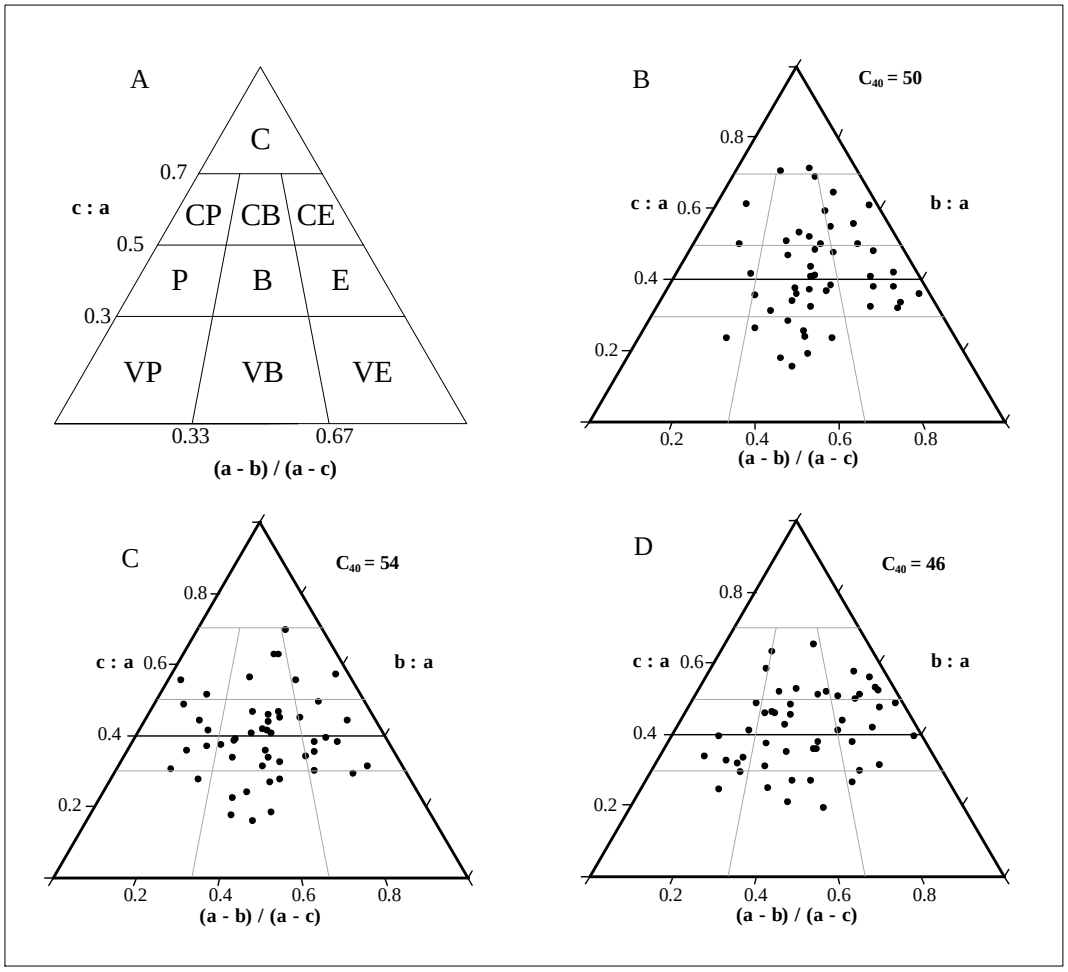



**Figure 5.19** Triangular diagrams after Sneed and Folk (1958). (A) The descriptive classes according to Sneed and Folk (1958) where C = compact, P = platy, B = bladed, E = elongate and V = very. (B-D) Triangular diagrams for clasts in trenches 1, 2 and 3 respectively at Tsatsa-La-Mangaung. $C_{40}$ is the percentage of sample with c:a ≤ 0.4 (Benn and Ballantyne, 1993) (n = 50).

**Table 5.7** The percentage of clasts falling within the various shape categories at Tsatsa-La-Mangaung.

| Shape | Trench 1 (%) | Trench 2 (%) | Trench 3 (%) |
|---|---|---|---|
| Compact | 2 | - | - |
| Platy | 8 | 18 | 20 |
| Bladed | 56 | 54 | 46 |
| Elongate | 32 | 28 | 34 |

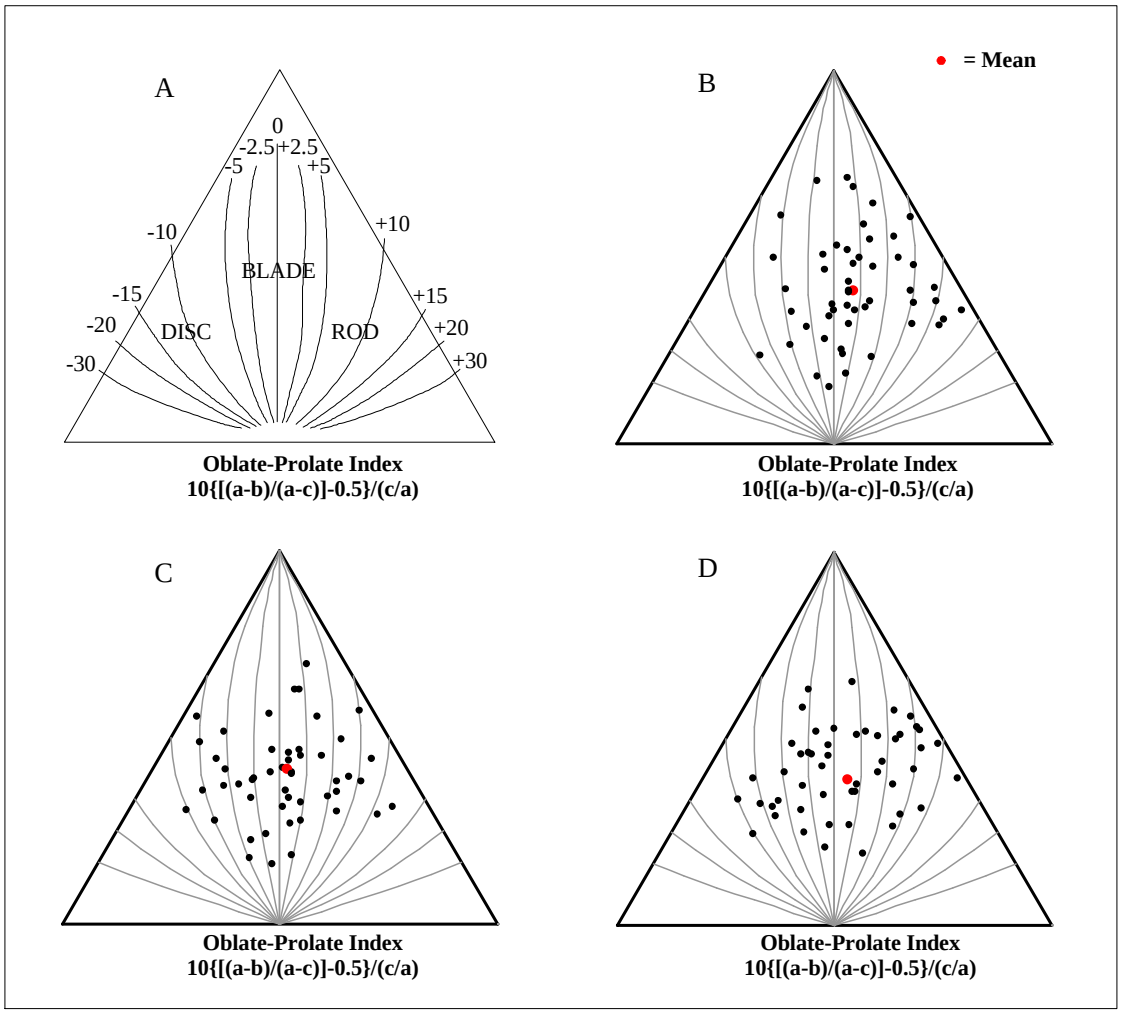



**Figure 5.20** Triangular diagrams after Sneed and Folk (1958). (A) Isolines of the Oblate-prolate index according to Dobkins and Folk (1970). Triangular diagrams for trenches 1, 2 and 3 respectively at Tsatsa-La-Mangaung (n = 50).

**Table 5.8** The shape of clasts measured at the Tsatsa-La-Mangaung slope deposit ($x$ = mean, $s$ = standard deviation).

| | Number in Sample | Oblate-prolate Index | | Maximum Projection Sphericity ($\chi_P$) | | Visual Roundness (Powers, 1953) | |
|---|---|---|---|---|---|---|---|
| | | $x$ | $s$ | $x$ | $s$ | $x$ | $s$ |
| Trench 1 | 50 | 2.05 | 4.74 | 0.64 | 0.13 | 1.4 | 0.93 |
| Trench 2 | 50 | 0.56 | 5.29 | 0.61 | 0.11 | 1.5 | 0.68 |
| Trench 3 | 50 | 0.81 | 5.46 | 0.63 | 0.11 | 1.6 | 0.73 |

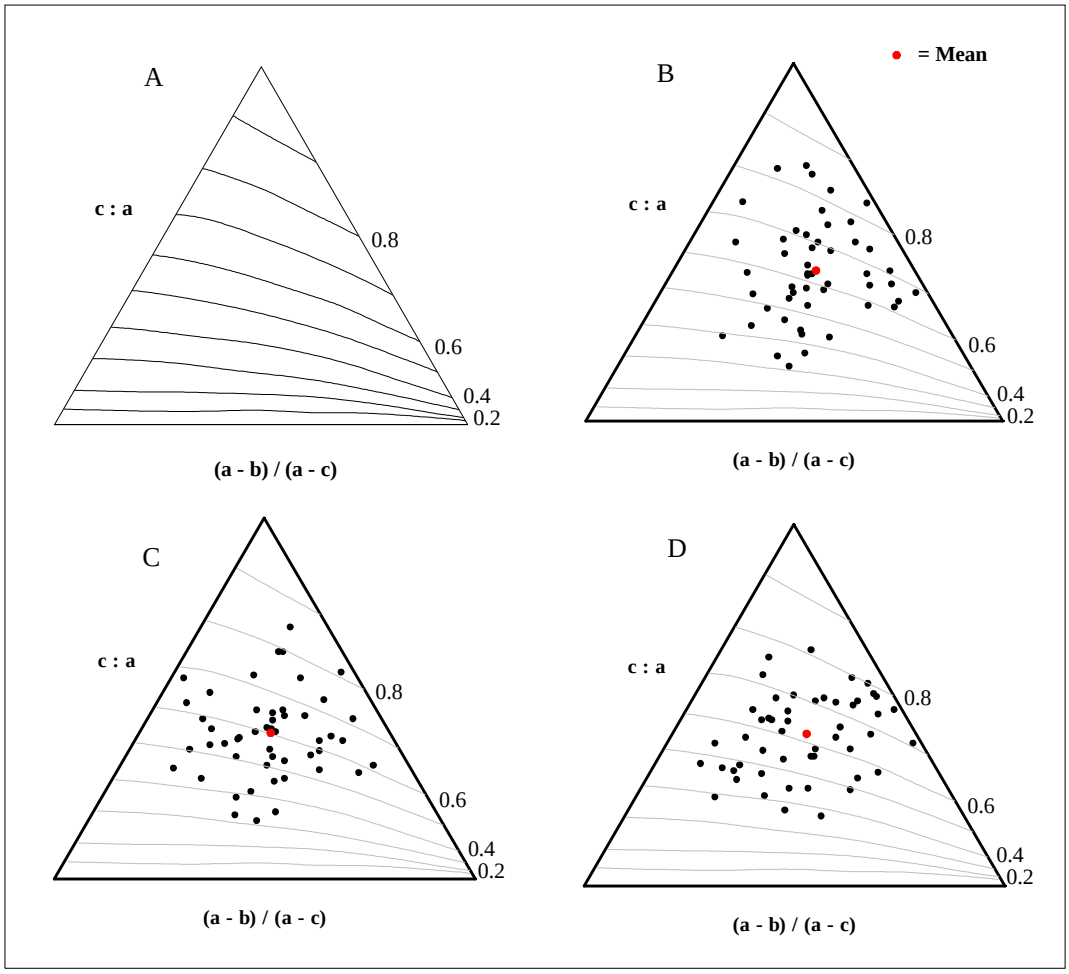



**Figure 5.21** Triangular diagrams after Sneed and Folk (1958). (A) Isolines of the maximum projection sphericity according to Sneed and Folk (1958). Triangular diagrams for trenches 1, 2 and 3 respectively at Tsatsa-La-Mangaung (n = 50).

the more discoid a particle becomes, the more the maximum projection sphericity tends towards 0.

Clast roundness is represented in Figure 5.22 and Tables 5.8 and 5.9. The majority of clasts from the three trenches fall within the angular and subangular categories of roundness. Trench 3 contains the highest percentage (18%) of very angular clasts, whilst trench 1 contains 12% very angular clasts. The subangular category contains the next highest percentage of clasts, whilst subrounded and rounded clasts form the minority of the results. It should also be noted that there is a slight increase in roundness towards the lower end of the deposit in trench 3.

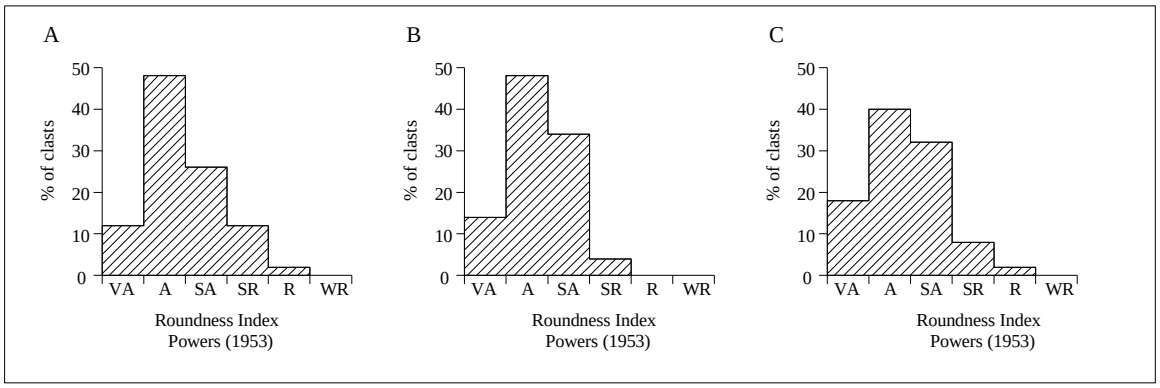



**Figure 5.22** Graphs representing visual roundness of clasts (after Powers 1953) in trenches 1 (A), 2 (B) and 3 (C) at Tsatsa-La-Mangaung. VA = Very Angular, A = Angular, SA = Sub Angular, SR = Sub Rounded, R = Rounded, WR = Well Rounded (n = 50).

**Table 5.9** The percentage of clasts falling in the roundness categories at Tsatsa-La-Mangaung.

| | VA (%) | A (%) | SA (%) | SR (%) | R (%) | WR (%) |
|---|---|---|---|---|---|---|
| Trench 1 | 12 | 48 | 26 | 12 | 2 | - |
| Trench 2 | 14 | 48 | 34 | 4 | - | - |
| Trench 3 | 18 | 40 | 32 | 8 | 2 | - |

The t-test was performed to determine whether the sediment sampled in the three trenches for form, sphericity and roundness was statistically significant (<0.05%), and whether there was a relationship between the sediment in the trenches (Table 5.10). It

**Table 5.10** The statistical significance calculated by the t-test of the shape of clasts sampled in the three trenches in the Tsatsa-La-Mangaung deposit (SS = Statistically significant).

| Trenches | Oblate Prolate Index | Maximum Projection Sphericity | Visual Roundness |
|---|---|---|---|
| T1-T2 | **SS** | **SS** | **SS** |
| T1-T3 | **SS** | **SS** | **SS** |
| T2-T3 | **SS** | **SS** | **SS** |

is clear from Table 5.10 that the results for clast shape in the three trenches are statistically significant in all cases.

## 5.7 MICROMORPHOLOGY

Although nine thin sections were collected at the Tsatsa-La-Mangaung deposit (three from each trench), these will be discussed collectively in terms of the deposit as a whole, given the similarities between the thin sections (Table 5.11). The fabric of the Tsatsa-La-Mangaung deposit is random, which means that the distribution of the individual particles is statistically random. The degree of parallelism of particles has a broad angle, which means that individual particles are oriented with their principle axes within 90º of each other and the quantity of oriented particles is <33% (Stoops, 2003).

The c/f related distribution described in section 4.3.2.2 shows the distribution of individual fabric units compared to smaller fabric units and associated pores (Stoops and Jongerius, 1975), and in the case of the Tsatsa-La-Mangaung deposit it is either single spaced or double spaced porphyric, which means that the larger fabric units occur in a dense groundmass of smaller units (Stoops, 2003). The size of the fabric is coarse sand, which is poorly sorted or unsorted with platy and blocky shapes, and which are subangular and have an undulating surface roughness (Figure 5.23). This corresponds to the sedimentological results obtained in the previous sections (5.4.1 and 5.6).

The aggregates in the thin sections are spheroidal peds, which means that the particles are arranged in more or less equant peds that are bounded by rounded faces and are not accommodated to the adjoining peds. These are weakly separated which means

**Table 5.11** Micromorphological description of the Tsatsa-La-Mangaung samples.

| Micromorphological features → / Sample No. ↓ | Skeleton: Fabric: Pattern | Skeleton: Fabric: Degree of parallelism | Skeleton: Fabric: Quantity of oriented particles | Skeleton: Fabric: C/F related distribution | Skeleton: Fabric: Dominant size fraction | Skeleton: Fabric: sorting | Skeleton: Shape: Shape | Skeleton: Shape: Degree of roundness | Skeleton: Shape: surface roughness | Aggregates: peds | Aggregates: ped seperation and pedality | Voids: Void type | Voids: Microstructure | Voids: % total area occupied by voids | Parent Material: Rock type | Parent Material: Average size um | Parent Material: Fine: Colour | Parent Material: Fine: Limpidity | Groundmass: C/F 2mm | Groundmass: C/F 10um | Groundmass: C/F related distribution | Groundmass: Cappings | Pedofeatures: Texture | Pedofeatures: laminated | Pedofeatures: Infillings: Classification | Pedofeatures: Infillings: Descriptive criteria | Pedofeatures: Crystals: Crystals | Pedofeatures: Crystals: Crystal intergrowth |
|---|---|---|---|---|---|---|---|---|---|---|---|---|---|---|---|---|---|---|---|---|---|---|---|---|---|---|---|---|
| T1 90 | R | BA | W-E | DSP | CS | P/U | P&B | SA | U | S | WS | V&C | CM | 20 | B | 4600 | YB | SP | 3:2 | 4:1 | DSP | ● | SL | NL | LD | PF | ●● | P |
| T1 115 | R | BA | W-E | DSP | CS | P/U | P&B | SA | U | S | WS | V | VM | 10 | B | 5200 | YB | SP | 4:1 | 9:1 | DSP | ● | SL | NL | LD | PF | ● | P |
| T1 135 | R | BA | W-E | SSP | CS | P/U | P&B | SA | U | S | WS | VCM | VM | 25 | B | 5000 | YB | SP | 3:2 | 4:1 | CP | ● | SL | NL | - | - | ● | P |
| T2 80 | R | BA | W-E | SSP | CS | P/U | P&B | SA | U | S | WS | V&C | CM | 15 | B | 6400 | YB | SP | 4:1 | 9:1 | SSP | ●● | SL | L | - | - | ●● | P |
| T2 110 | R | BA | W-E | SSP | CS | P/U | P&B | SA | U | S | WS | V&C | CM | 25 | B | 5800 | YB | SP | 4:1 | 9:1 | DSP | ●●● | SL | NL | LD | PF | ● | P |
| T2 130 | R | BA | W-E | SSP | CS | P/U | P&B | SA | U | S | WS | V&C | VM | 20 | B | 4500 | YB | SP | 4:1 | 9:1 | DSP | ● | SL | NL | LD | PF | ● | P |
| T3 80 | R | BA | W-E | DSP | CS | P/U | P&B | SA | U | S | WS | V&C | CM | 30 | B | 5000 | YB | SP | 4:2 | 9:1 | DSP | ●●● | SL | NL | LD | PF | ●● | P |
| T3 135 | R | BA | W-E | DSP | CS | P/U | P&B | SA | U | S | WS | V&C | CM | 20 | B | 5000 | YB | SP | 3:2 | 4:2 | SSP | ●●● | SL | L | LD | PF | ●● | P |
| T3 155 | R | BA | W-E | DSP | CS | P/U | P&B | SA | U | S | WS | V&C | CM | 20 | B | 5000 | YB | SP | 3:2 | 4:2 | SSP | ●●● | SL | L | LD | PF | ●● | P |

KEY:

**Pattern:**
R = Random

**Degree of parallelism:**
BA = Broad angle

**Quantity of oriented particles:**
WE = Weakly expressed:<33% of particles are oriented

**C/F related distribution:**
SSP = Single spaced porphyric
DSP = Double spaced porphyric

**Size:**
CS = Coarse sand

**Sorting:**
PS = Porly sorted
U = Unsorted

**Shape:**
P = Platy
B = Blocky

**Degree of roundness:**
A = Angular
SA = Subangular

**Surface roughness:**
U= Undulating

**Peds:**
S = Spheroidal Peds

**Ped seperation and pedality:**
WS = Weakly seperated

**Void type:**
C = Channels
CM = Chambers
V = Vughs
VCM = Vugh and Chamber

**Microstructure:**
VM = Vughy microstructure
CM = Channel microstructure

**Mineral type**
B = Basalt

**Colour:**
YB = Yellowish Brown

**Limpidity:**
SP = Speckled

**Cappings:**
● <10%
●● <10-20%
●●● >20%

**Texture:**
SL = Silt

**Laminated:**
NL = Nonlaminated
L = Laminated

**Infillings classification:**
LD = Loose discontinuous

**Descriptive criteria:**
PF = Passage features

**Crystals:**
● Few
●● Some
●● Many

**Crystal intergrowth:**
P = Parallel

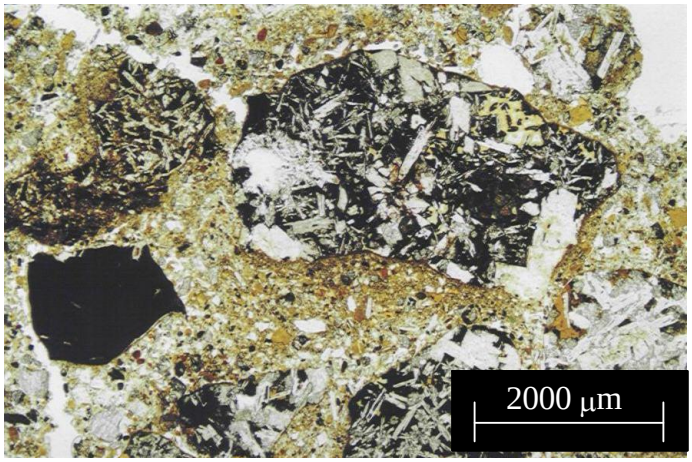



**Figure 5.23** An example of coarse, weakly oriented, platy, subangular, undulating particles taken in PPL (Plane Polarized Light).

that the material is divided into a number of units (Stoops, 2003). Void types include vughs (Figure 5.24), channels (Figure 5.25) and chambers. Vughs are almost equidimensional, irregular voids and result from the welding of aggregates, disruption of the microstructure or dissolution of components (Stoops, 2003). Channels are tubular, smooth voids and are mainly root channels or bioallergies, whereas chambers are almost equidimensional, smooth-walled pores, interconnected by channels (Stoops, 2003). The microstructure of the thin sections is either vughy, which means that the vughs are not connected and occasional channels and chambers are present, or channel, whereby channels are the dominant voids (Stoops, 2003). The total area occupied by voids averages 20% for the Tsatsa-La-Mangaung deposit.

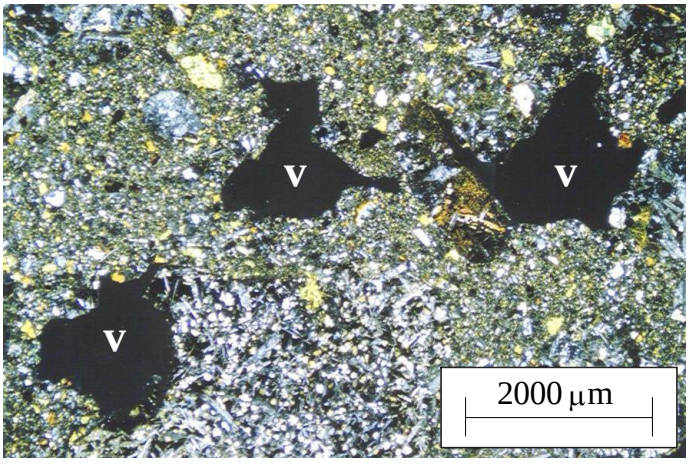



**Figure 5.24** An example of typical vugh voids taken in XPL (cross polarized light) (v =voids).

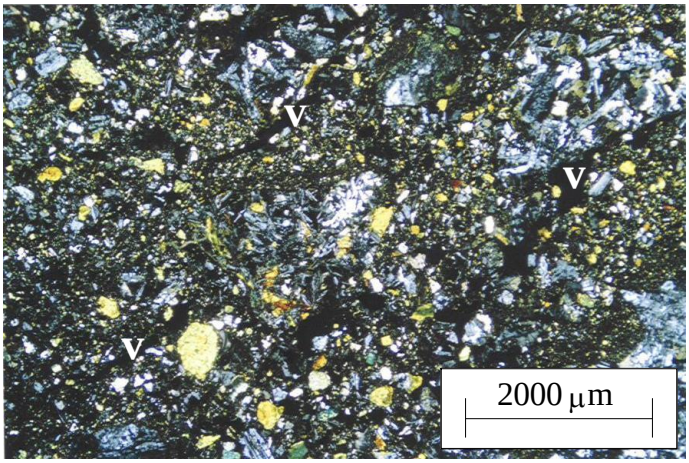



**Figure 5.25** An example of typical channel voids taken in XPL (v = voids).

The main rock type in the Tsatsa-La-Mangaung deposit is basalt, which averages approximately 5000 μm in length in thin section (Figure 5.26). This rock consists of plagioclase and olivine minerals. The plagioclase is rectangular in shape and randomly arranged. Some olivine crystals have a narrow brown rim on the crystal which is formed by hydration and oxidation of the olivine (MacKenzie *et al.,* 1982) (Figure 5.27). The colour of the fine mineral components is yellowish brown with a speckled limpidity, with clay-sized particles appearing as opaque specks (Table 5.11) (Stoops, 2003). The c/f ratio indicates that the samples are predominantly coarse with very little material under 10 μm in size. The c/f related distribution of the groundmass is similar to that of the fabric, and is single and double spaced porphyric in all but one case, where it is a close porphyric distribution.

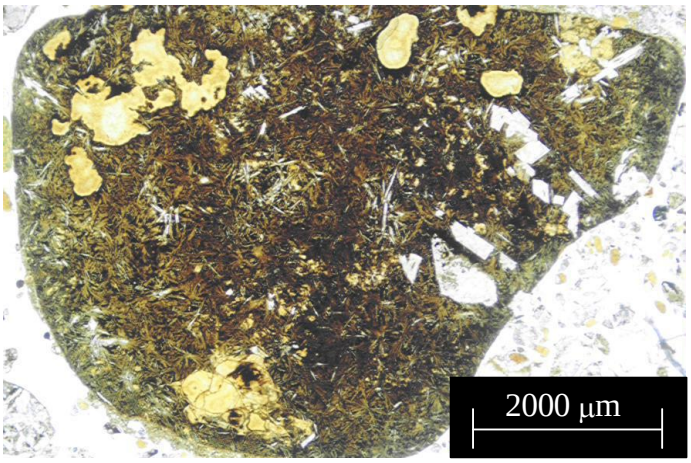



**Figure 5.26** An example of a basalt grain taken in PPL.

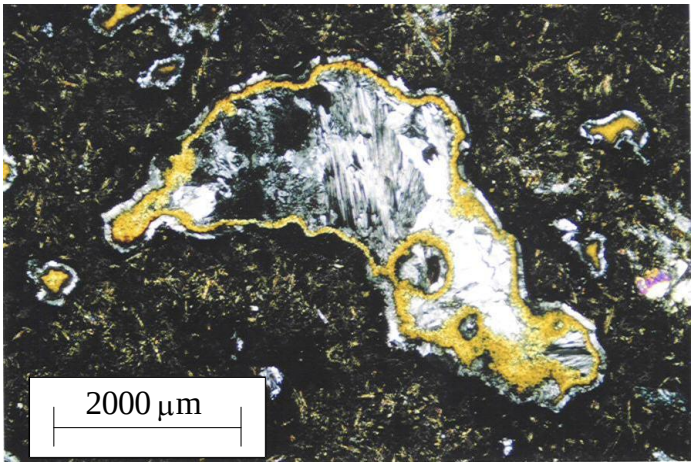



**Figure 5.27** An example of an olivine crystal with a brown rim taken in XPL.

The pedofeatures present in the thin sections are coatings, which are described as cappings as they lie on top of the grains (Stoops, 2003). These cappings are present on <10% of particles in trench 1, increasing to between 10 % and 20% in trench 2 and >20% in trench 3. These silt cappings (Figure 5.28) are composed of mainly silt-sized particles and are on occasion laminated (Figure 5.29), in which case alternating layers of silt occur with differences in colour or limpidity. Infillings are voids filled or partly filled by soil material or some fraction of it (Bullock *et al.*, 1985), and occur as loose discontinuous passage features in most of the thin sections. This means that the material is loosely packed and that the material in the void is of the same composition as the groundmass (Stoops, 2003). In addition to this, parallel crystal intergrowths are present with either few or some crystals being present in the samples.

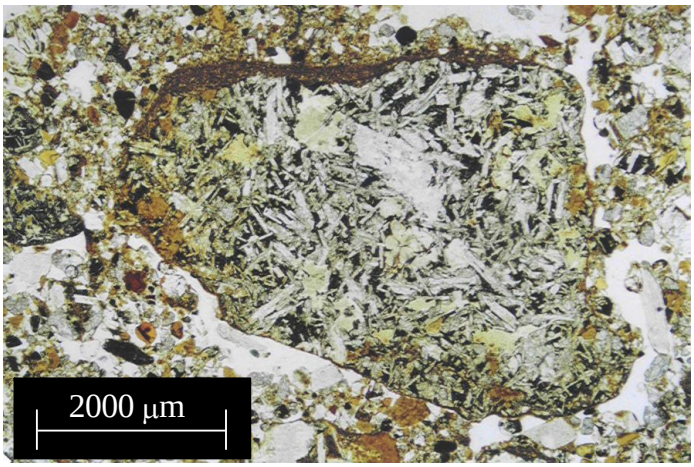



**Figure 5.28** A basalt clast with a non-laminated silt capping taken in PPL.

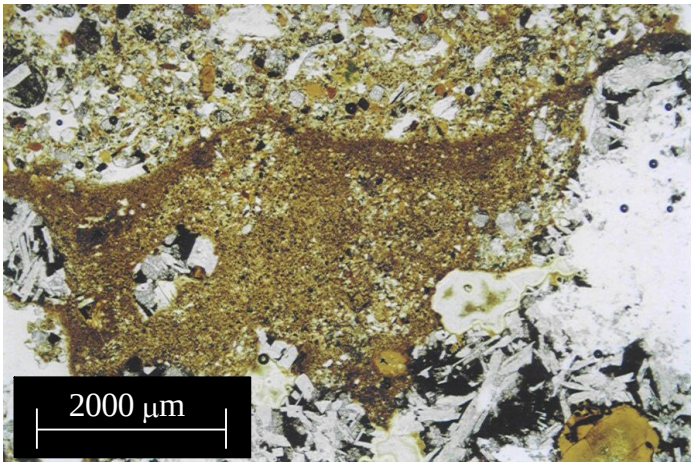



**Figure 5.29** A basalt clast with a laminated silt capping taken in PPL.

## 5.8 RADIOCARBON DATING

The AMS ages were obtained in the three trenches of the Tsatsa-La-Mangaung deposit at a depth of 1.5 m (trench 1), 1.35 m (trench 2) and 1.45 m (trench 3) (Table 5.12). These sampling depths represent the maximum depth of each trench. The ages range from 11 700 ± 70 radiocarbon yrs BP in trench 3 to 17 300 ± 100 radiocarbon yrs BP in trench 2. The calibrated ages range from 13 820 yrs BP in trench 3 to 20 530 yrs BP in trench 2. Details of the methodologies used have already been discussed in section 4.2.1.8.

## 5.9 SUMMARY

A site summary of the sedimentary characteristics of the Tsatsa-La-Mangaung deposit is presented in Table 5.13. The three trenches contain very similar sedimentary characteristics and are all composed of present-day soil overlying a gravely, poorly sorted diamict. The sediment within this diamict unit tends to become coarser and more unconsolidated with depth. Gravel is the primary constituent in all samples and the sediment is unimodal. Fabric orientation is downslope in trenches 1 and 3 and transverse to the ridge crest in trench 2 and mean dip is between 20° and 25°. Clasts are predominantly bladed, with elongate shapes being the second most common clast shape. Although clast roundness is predominantly angular, there is also the presence of a significant amount of subangular clasts. The thin sections once again reflect the coarse grained nature of the sediment and pedofeatures present include silt cappings. These increase in frequency downslope towards trench 3. The calibrated AMS ages

**Table 5.12** AMS and calibrated ages for the Tsatsa-La-Mangaung deposit (sampling depths: T1 = 1.5 m, T2 = 1.35 m, T3 = 1.45 m).

| Anal. No. [1] Gr-A | Sample designation | $\delta^{13}C$ (‰ PDB) | Radiocarbon Age yrs BP | 1σ yrs BC | 2σ yrs BC | Calibrated yrs BP |
|---|---|---|---|---|---|---|
| 21456 | Sani Top T1 | -20.8 | 13 790 ± 110 | 14 670 – 14 417 | 14 797 – 14 291 | 16 500 |
| 21459 | Sani Top T2 | -21.3 | 17 300 ± 100 | 18 695 – 18 465 | 18 810 – 18 350 | 20 530 |
| 21457 | Sani Top T3 | -16.1 | 11 700 ± 70 | 11 965 – 11 781 | 12 057 – 11 689 | 13 820 |

**Table 5.13** A summary of the sedimentary characteristics at Tsatsa-La-Mangaung.

| | Trench 1 | Trench 2 | Trench 3 |
|---|---|---|---|
| **Lithofacies** | Soil overlying gravely diamict | Soil overlying gravely diamict | Soil overlying gravely diamict |
| **Particle Size** | -1 Phi (Gravel) | -1 Phi (Gravel) | -1 Phi (Gravel) |
| **Sorting** | Poorly – very poorly sorted | Poorly – very poorly sorted | Very well - very poorly sorted |
| **Fabric** | Downslope | Transverse to the slope | Downslope |
| **Dip** | 20° - 30° | 10° - 30° | 10° - 40° |
| **Shape** | Bladed | Bladed | Bladed |
| **Roundness** | Angular | Angular | Angular |
| **Micromorphology** | Few cappings | Few to many cappings | Many cappings |
| **AMS dating** | 16 500 yrs BP | 20 530 yrs BP | 13 820 yrs BP |

for the deposit range between 13 820 yrs BP and 20 530 yrs BP, which indicates that the deposit is pre-Holocene.

# CHAPTER 6

# Sekhokong results

## 6.1 INTRODUCTION

A number of linear deposits with varying morphologies occur along the Sekhokong mountain range and two have been selected for analysis in this research. These occur on the upper portions of the south-facing slopes of this mountain range, within 2 km of each other and within 4 km of the Great Escarpment. This chapter will consist of two sections. The first section will describe the morphological, sedimentological and micromorphological results at the first site and the second section will describe these same points for the second site.

## 6.2 SITE 1

### 6.2.1 Morphology

The Sekhokong Site 1 ridge (Figures 6.1 and 6.2) is 170 m in length, varies in width between 17 m and 47 m and reaches a maximum height of 13 m. The altitudinal range of the deposit varies from 3010 m a.s.l. to 3074 m a.s.l. The slope gradient on the western aspect of the deposit ranges from 13º (cross section D-D; Figure 6.2) to 29° (cross sections and C-C; Figure 6.2), whereas the slope angle on the eastern aspect is gentler, ranging from 11° (cross sections B-B and D-D; Figure 6.2) to 17° (cross section C-C; Figure 6.2). The longitudinal profile indicates that the average gradient of the deposit is 19º. There are two smaller ridges on the eastern side of the deposit. The largest one of the two is 92 m long, 13 m wide and 4 m high. Cross section E-E represents the slope profile containing a range of units related to various types of processes. The slope profile begins with an interfluve unit, with a slope angle of 0º. This unit then merges into the convex slope unit which has a slope angle of 20º, increasing to 36º downslope. On the transportational midslope, the slope angle averages 27º and becomes gentler on the colluvial footslope where the slope angle ranges from 10º to 6º. The slope gradient becomes even gentler on the alluvial toeslope where it averages 4º and then increases to 20º on the channel wall. The deposit occurs at the boundary of the transportational midslope and colluvial footslope and the total slope length is 2.2 km down to the river.

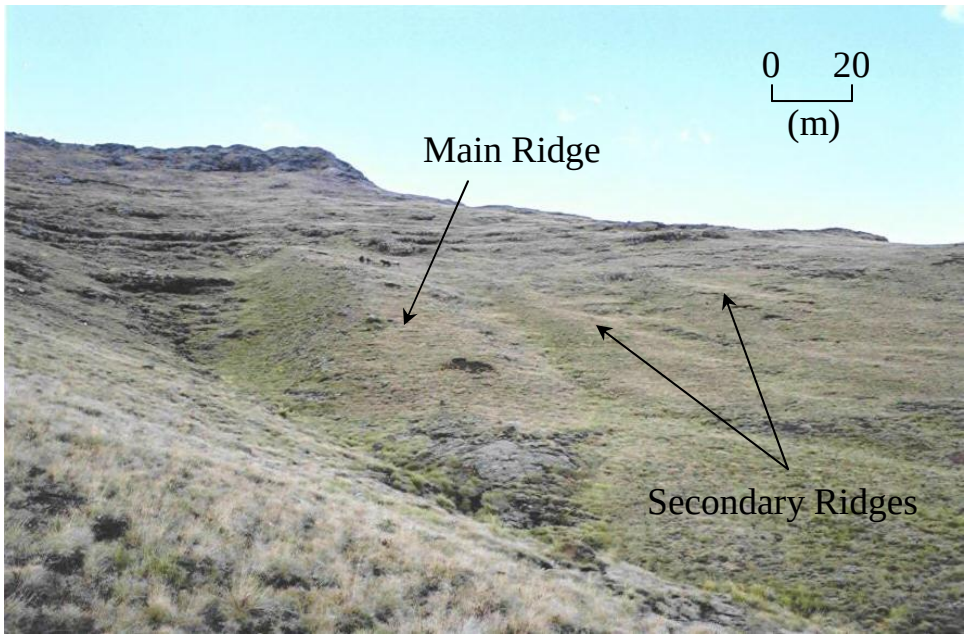



**Figure 6.1** The Sekhokong Site 1 slope deposit (photo by S. Mills).

### 6.2.2 Field observations

The lithofacies at the three trenches consist of a present-day soil approximately 60 cm in depth, underlain by a gravelly diamict (Figures 6.3 to 6.5). Although the excavation was to a depth between 140 cm and 160 cm, this is not the depth at which bedrock was reached but the depth at which it became increasingly difficult to excavate boulders. Within this diamict, a variety of different sized boulders are present, ranging in size from 2 cm to over 100 cm, and which are held together by a sandy matrix. Although the boulders fall within the same size range as those found within the Tsatsa-La-Mangaung deposit, there were fewer large boulders that were excavated.

The diamict unit in trench 1 consists of two horizons defined by a change in colour and texture. The lower unit is slightly coarser; however both are moderately sorted, friable, with abundant clasts. Trenches 2 and 3 consist of a single diamict unit which becomes coarser with depth, however sorting remains moderately sorted throughout. The soil is yellowish brown when dry in the upper part of the unit and brownish yellow in the lower part.

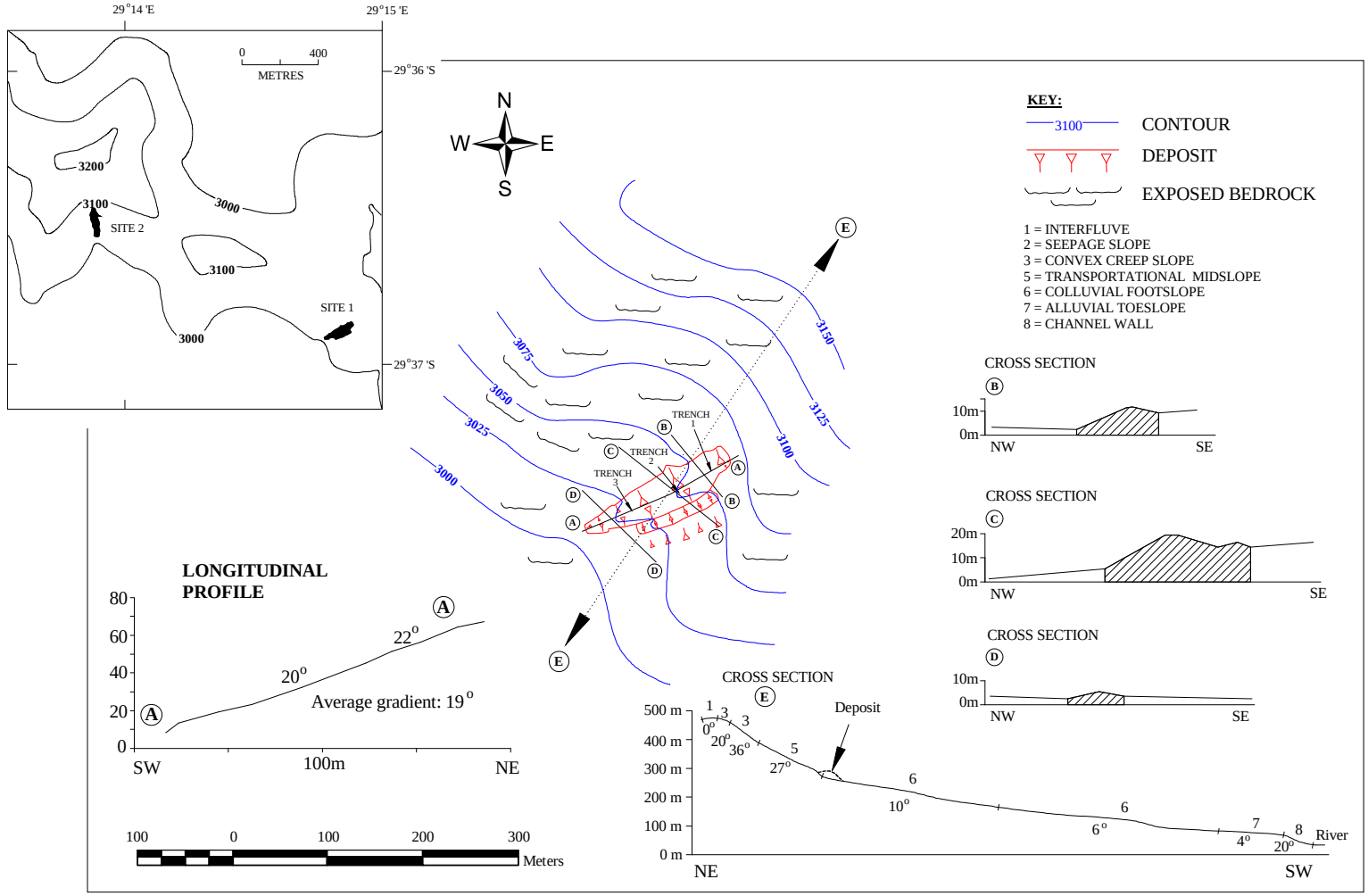



**Figure 6.2** Morphological map of the Sekhokong Site 1 deposit.

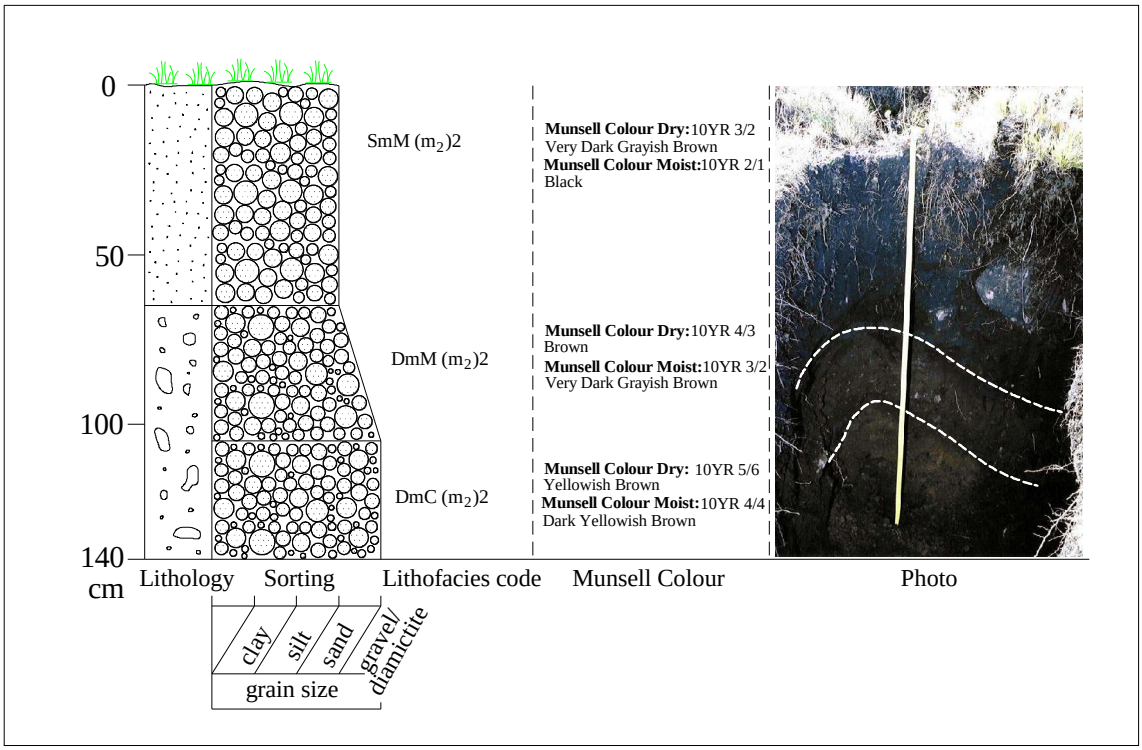



**Figure 6.3** Sedimentological and stratigraphical data for trench 1 at Sekhokong Site 1.

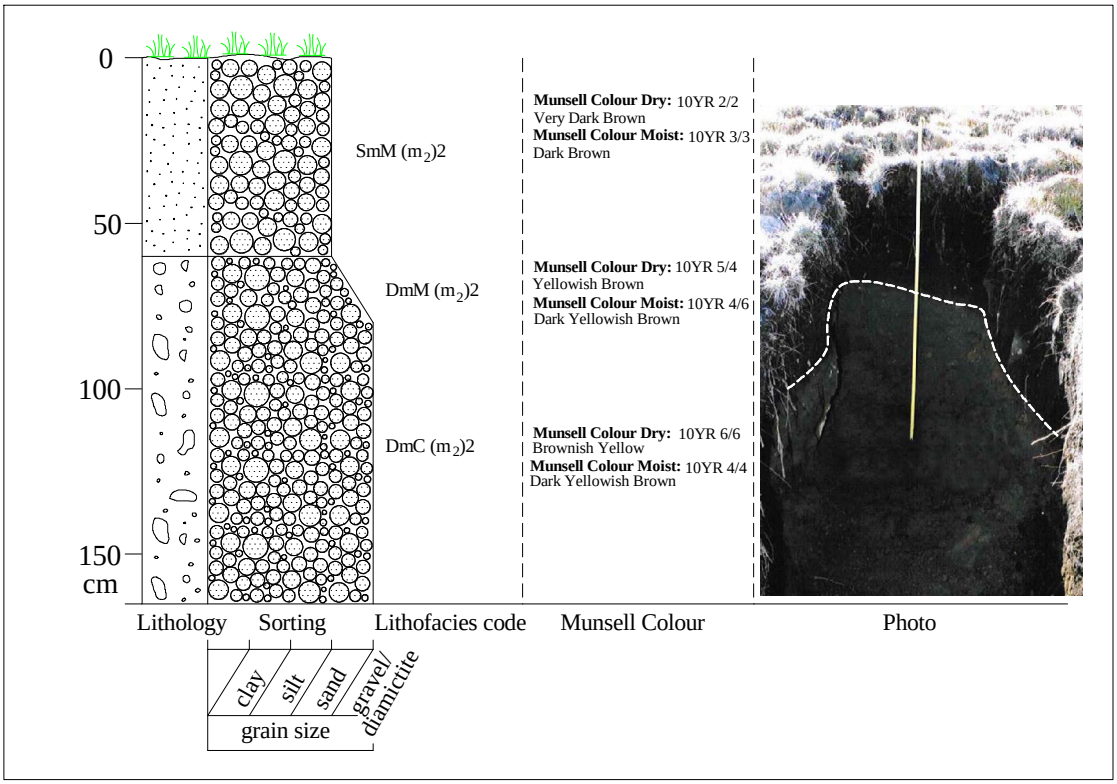



**Figure 6.4** Sedimentological and stratigraphical data for trench 2 at Sekhokong Site 1.

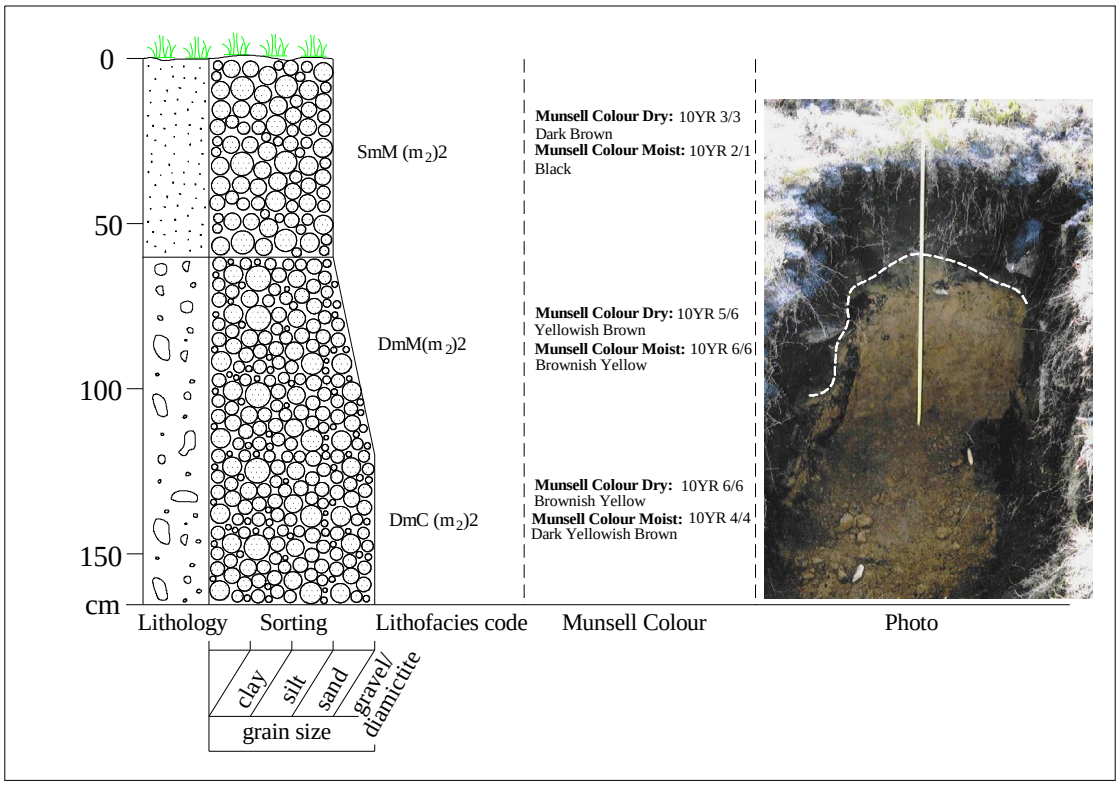



**Figure 6.5** Sedimentological and stratigraphical data for trench 3 at Sekhokong Site 1.

### 6.2.3 Particle size analysis

Particle size analysis results (Figures 6.6 to 6.8 and Table 6.1) indicate that the sediment in trenches 1 and 3 is similar and consists of <52% gravel. Sand and silt are the main constituents in several samples within these trenches, with values ranging from 28% to 43% sand and 17% to 42% silt. Both trenches contain <7% clay. The sediment collected at 40 cm in the three trenches is polymodal in trench 1 and bimodal in trenches 2 and 3 where peaks occur at -1, 4 and 6 phi (Table 6.1). The sediment sampled within the diamict at trench 1 is also bimodal down to 120 cm where it becomes unimodal, with a bimodality index of 1. Sediment in trench 2 is unimodal throughout, whilst sediment in trench 3 becomes bimodal at 140 cm, then transitional at 160 cm. Although there are secondary peaks at 4 and 8 phi within trench 3 at 120 cm depth, the sediment is not polymodal, as the bimodality index falls within the transitional range (Hoey, 2004).

The graphic mean indicates that the sediment in trench 2 is coarser than the sediment in trenches 1 and 3, and falls in the very coarse sand to coarse sand categories (Table 6.1).

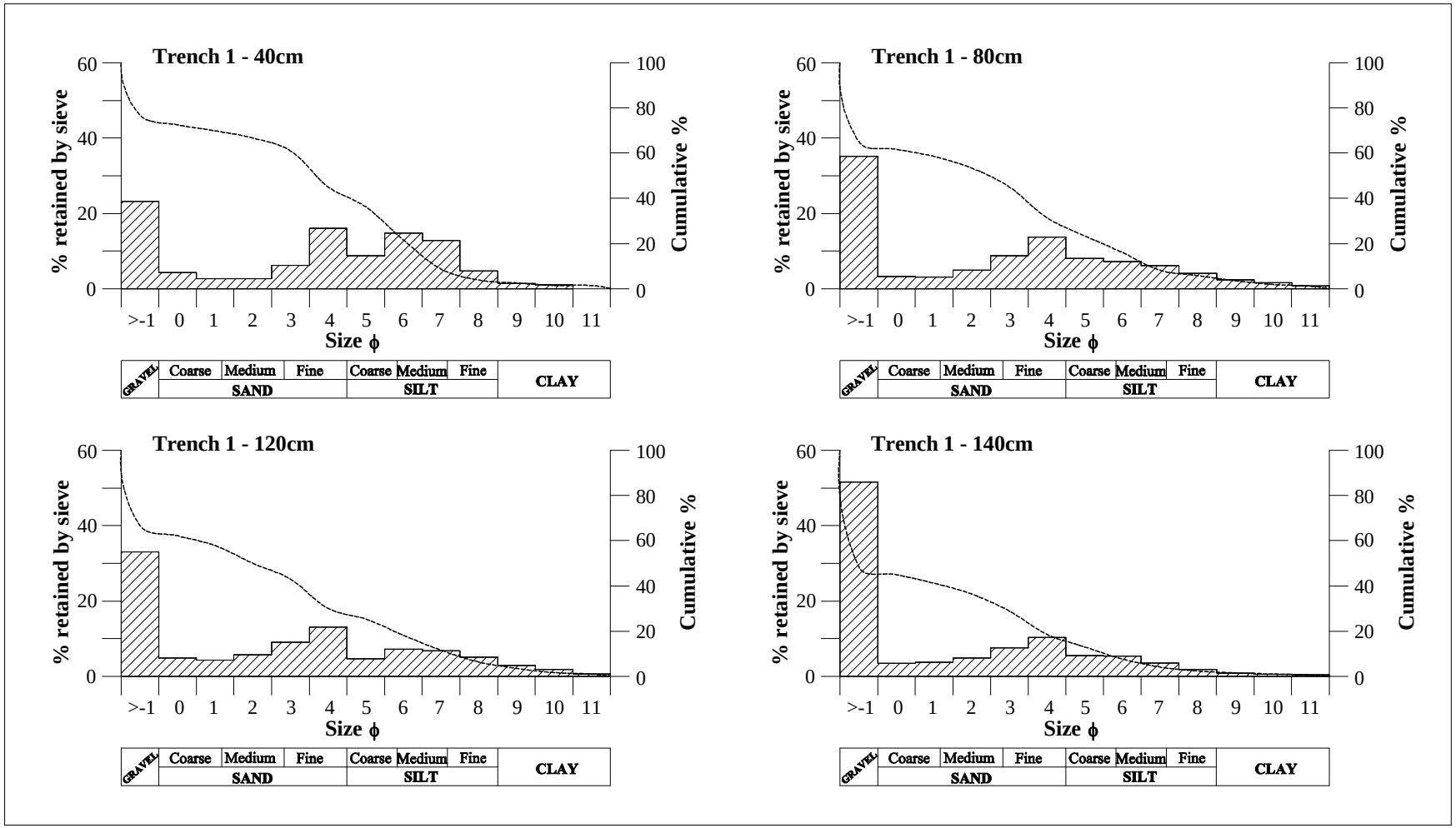



**Figure 6.6** Grain size distributions for the sediment from trench 1 at Sekhokong Site 1.

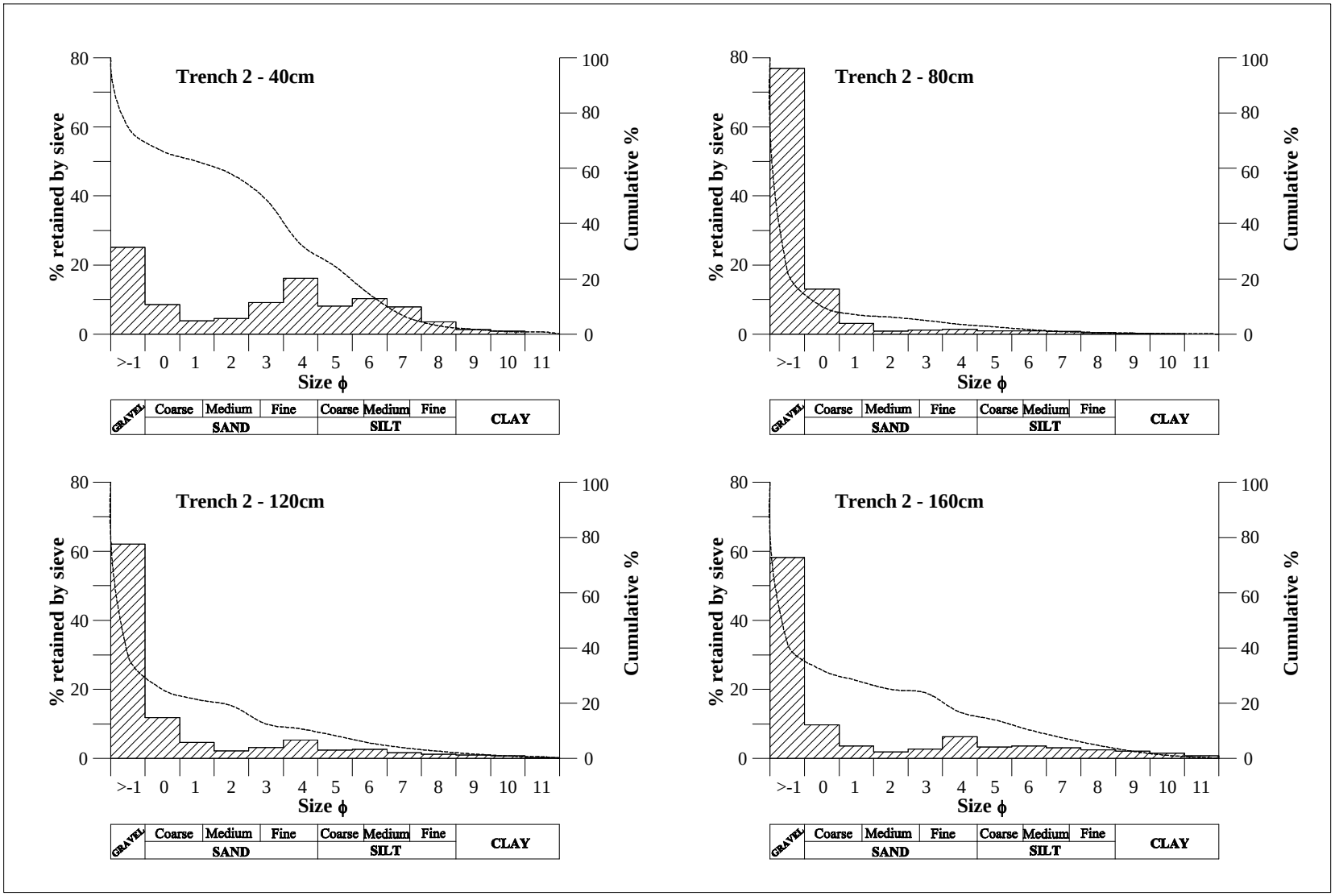



**Figure 6.7** Grain size distributions for the sediment from trench 2 at Sekhokong Site 1.

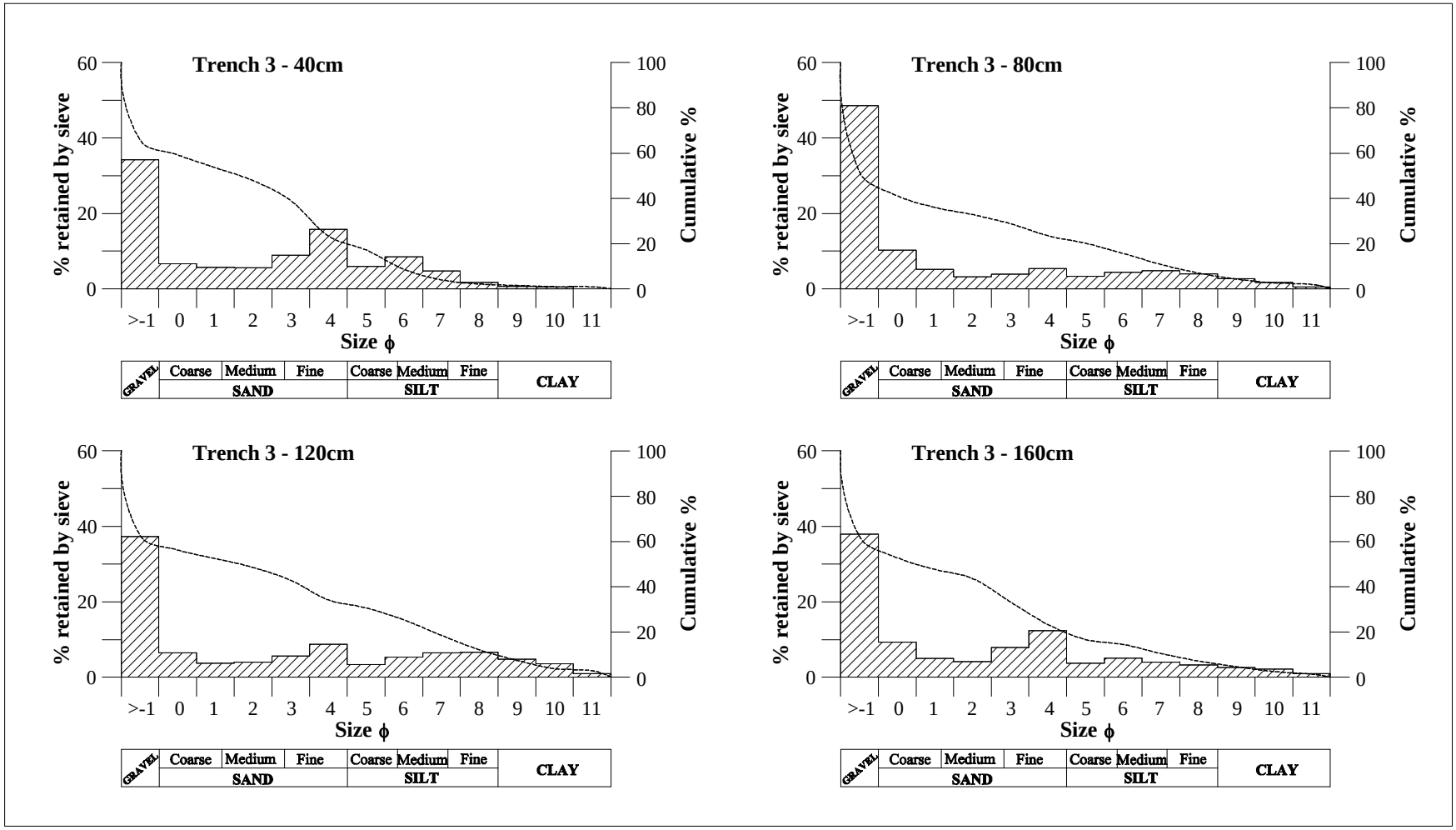



**Figure 6.8** Grain size distributions for the sediment from trench 3 at Sekhokong Site 1.

**Table 6.1** Particle size statistical analysis for the Sekhokong Site 1 deposit.

| Sample | Depth | Gravel (%) | Sand (%) | Silt (%) | Clay (%) | Mean (phi) | Mode (phi) | Peaks (phi) | Bimodality Index ($B^*$) |
|---|---|---|---|---|---|---|---|---|---|
| Trench 1 | 40 cm | 23 | 32 | 42 | 3 | 3.01 | -1 | -1, 4, 6 | 3.5, 1.8 |
| | 80 cm | 35 | 34 | 28 | 3 | 2.37 | -1 | -1, 4 | 1.9 |
| | 120 cm | 33 | 37 | 27 | 3 | 2.51 | -1 | -1, 4 | 2.0 |
| | 140 cm | 52 | 30 | 17 | 1 | 0.75 | -1 | -1, 4 | 1 |
| Trench 2 | 40 cm | 25 | 42 | 31 | 2 | 2.48 | -1 | -1, 4, 6 | 3.2, 1.3 |
| | 80 cm | 77 | 20 | 3 | 0 | -0.87 | -1 | -1 | 0.09 |
| | 120 cm | 62 | 27 | 9 | 2 | 0.35 | -1 | -1 | 0.43 |
| | 160 cm | 58 | 24 | 15 | 3 | 0.82 | -1 | -1 | 0.54 |
| Trench 3 | 40 cm | 34 | 43 | 22 | 1 | 1.92 | -1 | -1, 4, 6 | 2.3, 1.1 |
| | 80 cm | 49 | 28 | 19 | 4 | 1.36 | -1 | -1 | 0.60 |
| | 120 cm | 37 | 29 | 27 | 7 | 2.68 | -1 | -1, 4, 8 | 1.2, 3.0 |
| | 160 cm | 38 | 39 | 19 | 4 | 1.73 | -1 | -1, 4 | 1.6 |

The mean for trench 1 falls in the coarse sand to fine sand categories and the mean for trench 3 in the medium sand to fine sand categories. The sediment in trench 1 appears to become finer with depth and there is also a clear difference in mean values at 120 cm in trench 3 (2.68 phi), where this sample is considerably finer. Although the mean correctly identifies that trench 3 contains finer particles than the other two trenches, these samples are negatively skewed (Table 6.2). The mode thus gives a better indication of sample size and in this case indicates that most of the sample for all three trenches falls in the -1 phi category, which indicates a predominantly gravelly sample.

**Table 6.2** Further particle size statistical values for Sekhokong Site 1.

| Sample | | Sorting | Skewness | Kurtosis |
|---|---|---|---|---|
| Trench 1 | 40 cm | 3.15 | 0.18 | 0.56 |
| | 80 cm | 3.16 | -0.22 | 0.63 |
| | 120 cm | 3.24 | -0.21 | 0.63 |
| | 140 cm | 2.48 | -1 | 0.72 |
| Trench 2 | 40 cm | 2.91 | 0.05 | 0.57 |
| | 80 cm | 0.90 | -1 | >3 |
| | 120 cm | 2.12 | -1 | 2.44 |
| | 160 cm | 2.72 | -1 | 1.04 |
| Trench 3 | 40 cm | 2.70 | -0.23 | 0.65 |
| | 80 cm | 3.20 | -0.97 | 0.84 |
| | 120 cm | 3.72 | -0.44 | 0.62 |
| | 160 cm | 3.16 | -0.62 | 0.83 |

Further statistical analyses have been undertaken in the form of sorting, skewness and kurtosis (Table 6.2). The sediment sorting in the three trenches tends to be very poorly sorted, whilst all values are negatively skewed with the exception of trenches 1 and 2 at 40 cm depth, which represents the present-day soil (Table 6.2). Kurtosis ranges from very platykurtic to platykurtic in trenches 1 and 3, whilst the diamict unit in trench 2 ranges from mesokurtic to extremely leptokurtic. The mean values in Table 6.3 indicate that the sediment within the Sekhokong Site 1 deposit is similar in the case of trenches 1 and 3. The mean indicates that the sediment within these trenches is fine sand, however the mode suggests the sediment is predominantly coarse grained. Both trenches are very poorly sorted, negatively or very negatively skewed and platykurtic. On the other hand,

**Table 6.3** Mean and Standard deviation for the particle size statistical analysis at Sekhokong Site 1.

| Trench | Mean | | Mode | | Sorting | | Skewness | | Kurtosis | |
|---|---|---|---|---|---|---|---|---|---|---|
| | *x* | *s* | *x* | *s* | *x* | *s* | *x* | *s* | *x* | *s* |
| Trench 1 | 2.16 | 0.98 | -1 | 0 | 3.01 | 0.36 | -0.31 | 0.49 | 0.63 | 0.07 |
| Trench 2 | 0.70 | 1.39 | -1 | 0 | 2.11 | 1.00 | -0.74 | 0.53 | 1.78 | 1.17 |
| Trench 3 | 1.92 | 0.56 | -1 | 0 | 3.19 | 0.41 | -0.57 | 0.31 | 0.73 | 0.12 |

trench 2 is predominantly composed of coarse sand, is very poorly sorted, very negatively skewed and very leptokurtic.

### 6.2.4 Clast fabric and fabric eigenvalues

Clast a-axis orientation and dip were plotted as an equal-area stereographic scatter plot and an equal-area stereographic contour plot (Figure 6.9). Orientation of the clasts measured at trench 1 is fairly varied; however the mean orientation tends to be in the direction of the ridge crest. Clast orientation in trench 2 is once again varied, whilst clasts in trench 3 display orientations transverse to the ridge crest. Clast dip tends to be between 0º and 40º; however there is also a concentration of clasts that dip at 60º in trench 2. The chi-square test was used in order to determine whether clast orientation is statistically significant. Clasts within all three trenches have a probability of being randomly distributed at a level >0.05%. However clasts within trench 1 show more preferred orientations and have a statistically significant orientation (<0.10%). $S_1$ values, which measure the strength of clustering about the mean axis for the three sites, are fairly high and range from 0.606 at trench 2 to 0.710 at trench 1. $S_2$ and $S_3$ values are much lower which indicates that the clast fabrics represent linear clusters, where all observations are approximately parallel and $S_1 \gg S_2 \approx S_3$.

The normalised eigenvalues were then plotted onto a general shape diagram (Figure 6.10) and indicate that the sediment in all three trenches has low isotropy values and moderate elongation values, with the exception of trench 1 which has a relatively high elongation value. Fabric shape ellipsoids are compared with plotted data from various published sources (Figure 6.10C), which indicate that the clasts in the three trenches fall within a variety of envelopes. Clasts in trenches 1 and 3 fall within the undeformed lodgement till

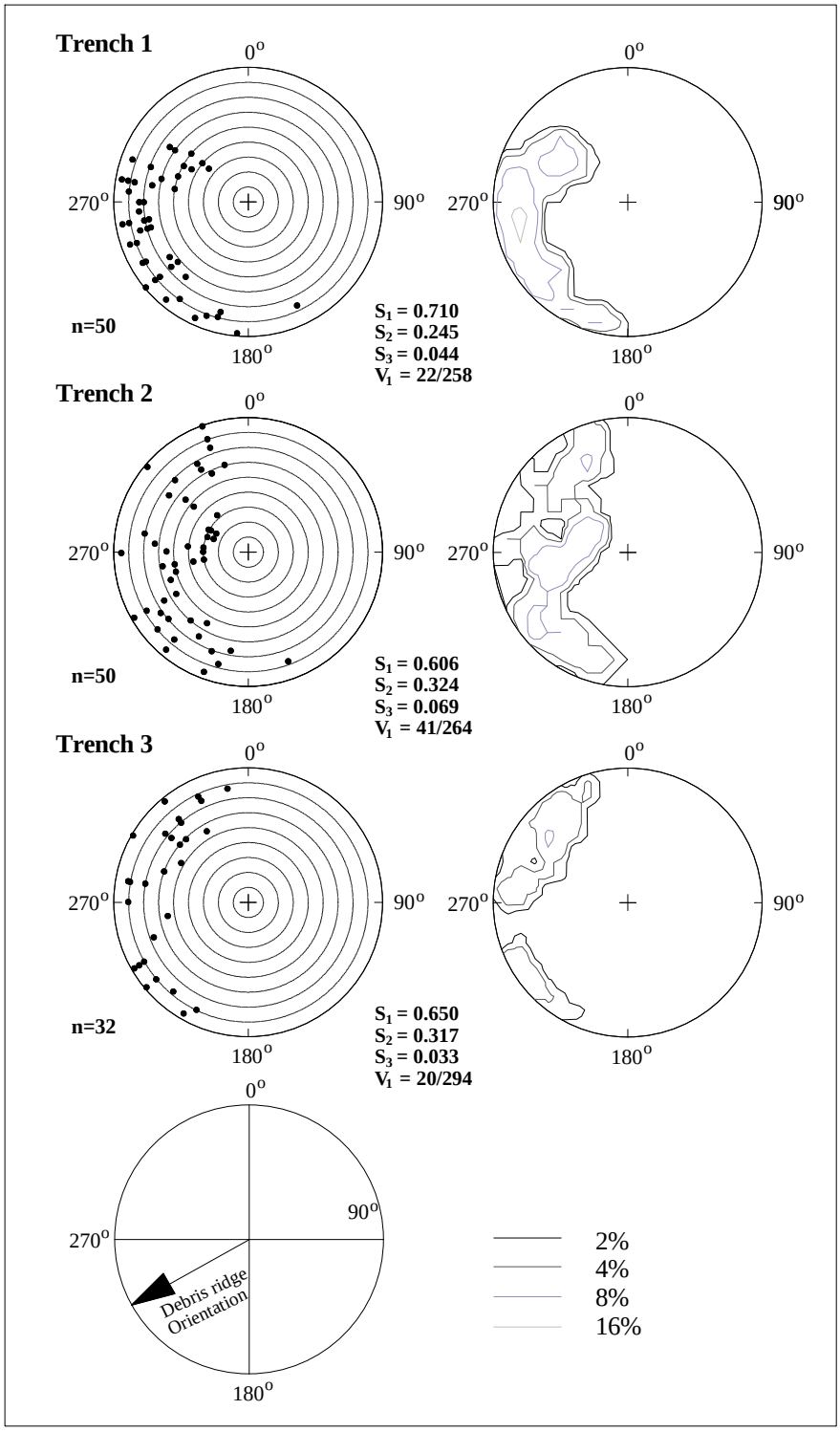



**Figure 6.9** Clast orientation, dip and contouring at trenches 1, 2 and 3 at Sekhokong Site 1.

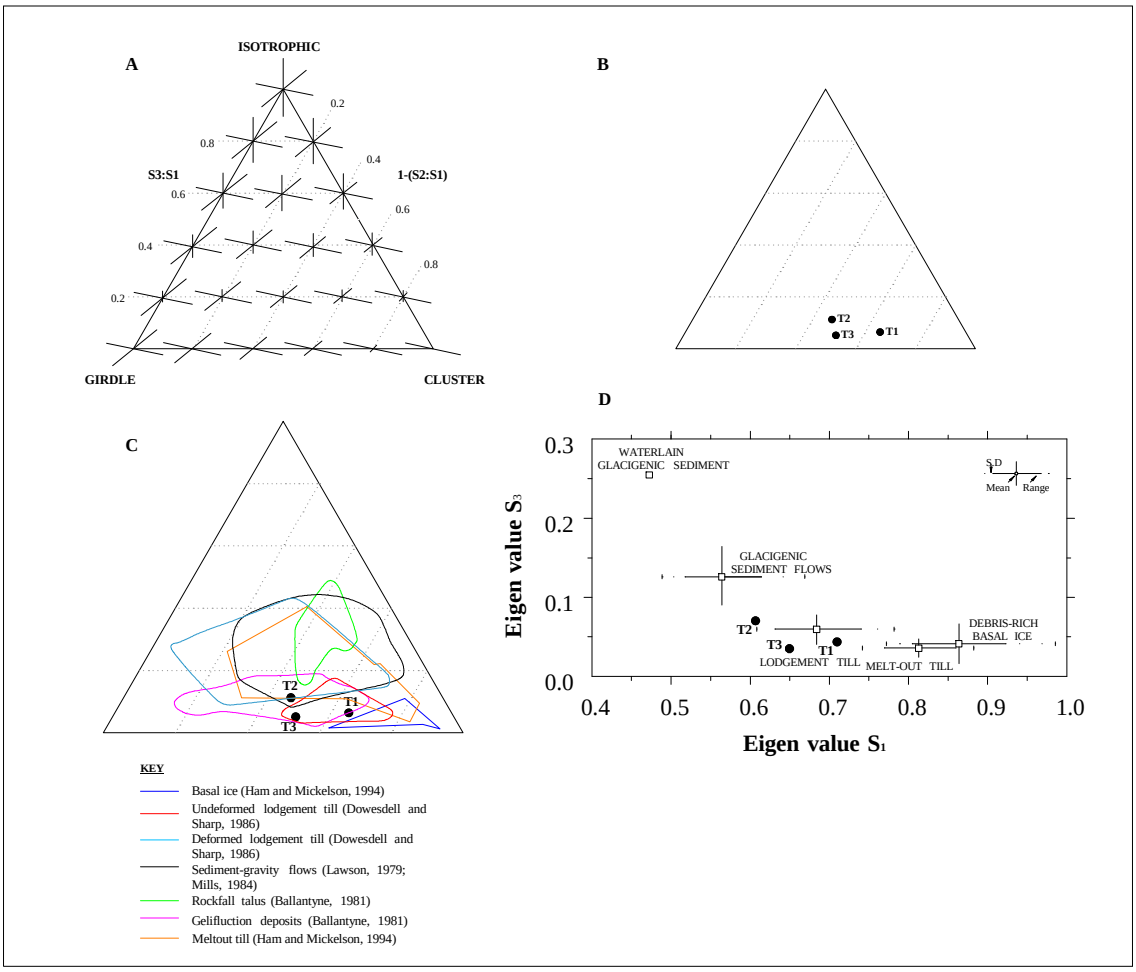



**Figure 6.10** Till fabric using eigenvalue data for the Sekhokong Site 1 deposit. (A) The range of orthorhombic fabric shapes. (B) Fabric data from the three trenches. (C) Comparison with envelopes from a range of deposits. (D) Comparison with modern data fabrics from various environments (Dowdeswell *et al.*, 1985).

envelope, and all clasts within all three trenches fall within the gelifluction deposit envelope. Clasts within trench 2 fall on the boundary of the deformed lodgement till and melt-out till envelopes and within the sediment gravity flow envelope. A triangular plot of normalised eigenvalues was also generated in order to further compare the Sekhokong Site 1 eigenvalues to envelopes produced by previous authors for various deposits (Figure 6.11). The sediment in trench 2 falls just within the debris flow envelope, whilst the sediment in all three trenches falls within the envelope for the internal fabric of rock glaciers.

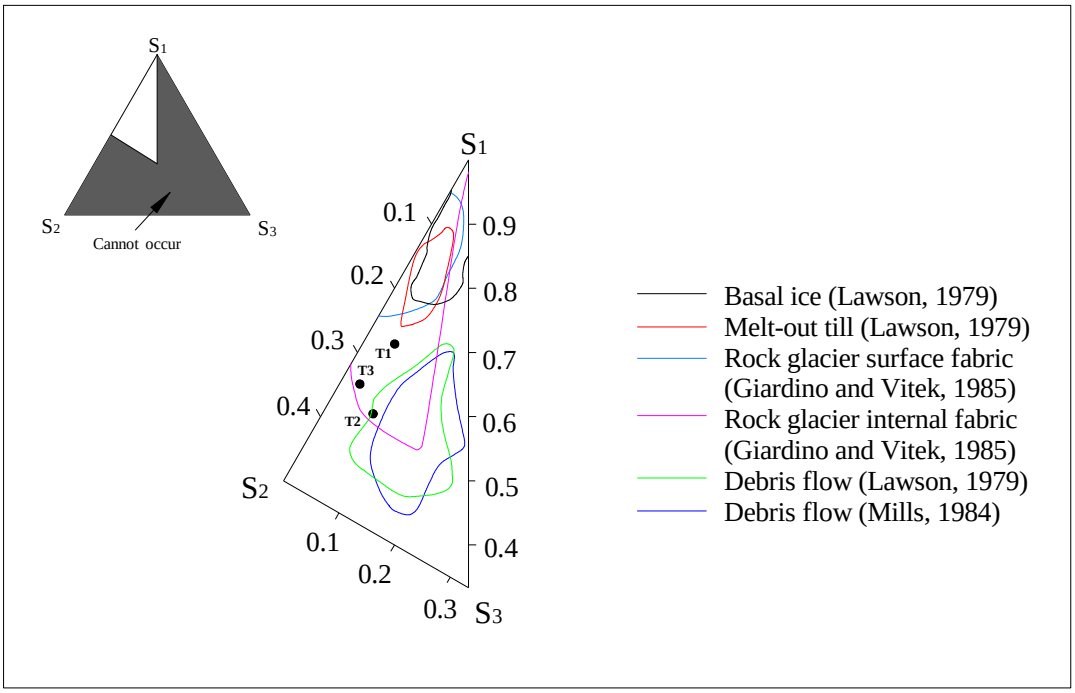



**Figure 6.11** Triangular plot of normalised eigenvalues for the Sekhokong Site 1 deposit, showing envelopes suggested by various authors. The usable field diagram occupies one sixth of the diagram because $S_1 > S_2 > S_3$.

### 6.2.5 Particle shape

Particle form was plotted onto triangular diagrams using Tri-plot v1.3 (Graham and Midgley, 2000) and representing the descriptive classes defined by Sneed and Folk (1958) (Figure 6.12) and the isolines of the Oblate-prolate (OP) index of Dobkins and Folk (1970) (Figure 6.13). All three trenches tend to contain a majority of bladed clasts (Figure 6.12 and Table 6.4), with clasts in trenches 2 and 3 displaying mean values of 0,

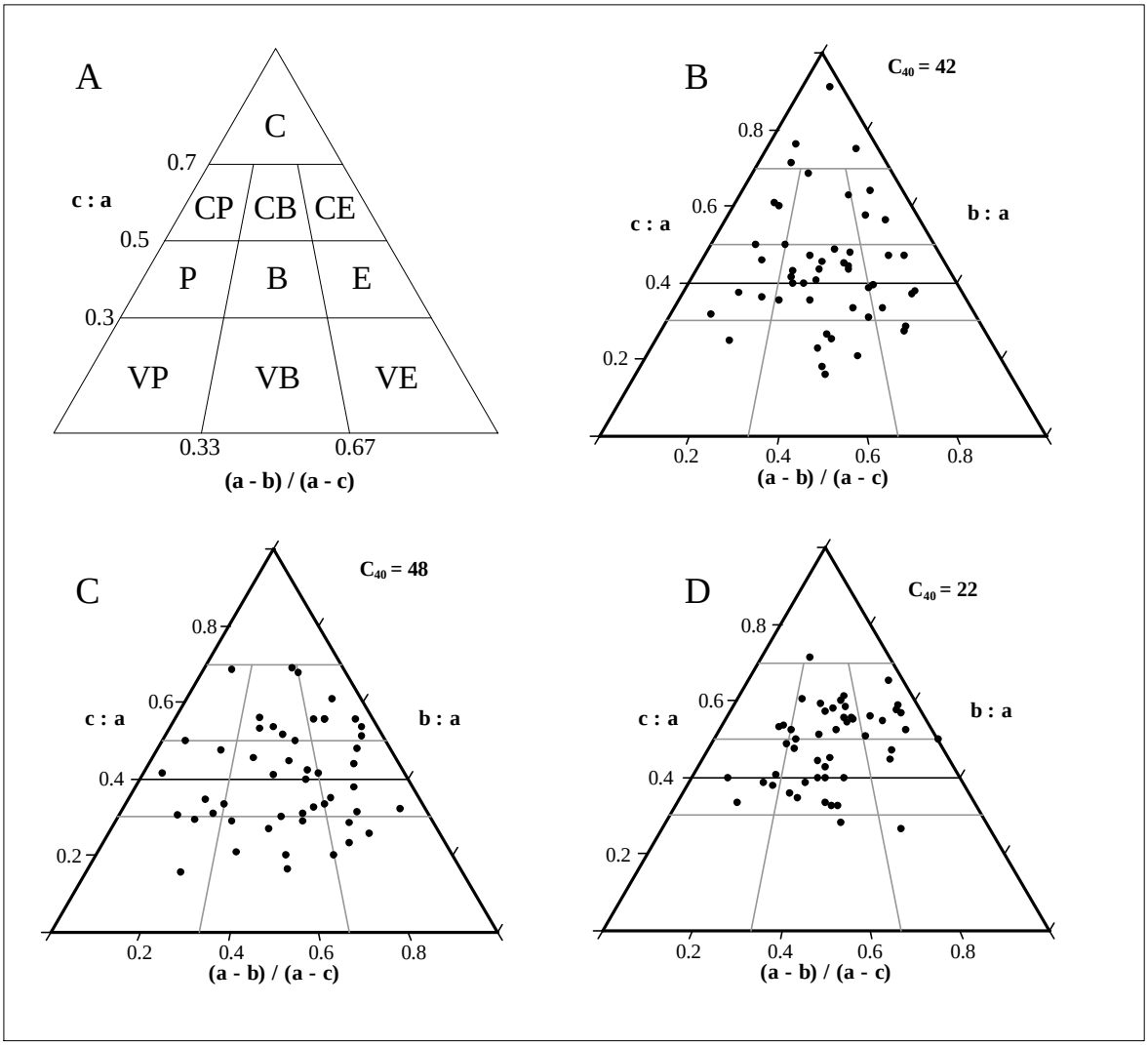



**Figure 6.12** Triangular diagrams after Sneed and Folk (1958). (A) The descriptive classes according to Sneed and Folk (1958) where C = compact, P = platy, B = bladed, E = elongate and V = very. (B-D) Triangular diagrams for trenches 1, 2 and 3 respectively at Sekhokong Site 1. $C_{40}$ is the percentage of sample with c:a ≤ 0.4 (Benn and Ballantyne, 1993) (n = 50).

**Table 6.4** The percentage of clasts falling within the various shape categories at Sekhokong Site 1.

| Shape | Trench 1 (%) | Trench 2 (%) | Trench 3 (%) |
|---|---|---|---|
| Compact | 8 | - | 2 |
| Platy | 18 | 20 | 18 |
| Bladed | 50 | 50 | 56 |
| Elongate | 24 | 30 | 24 |

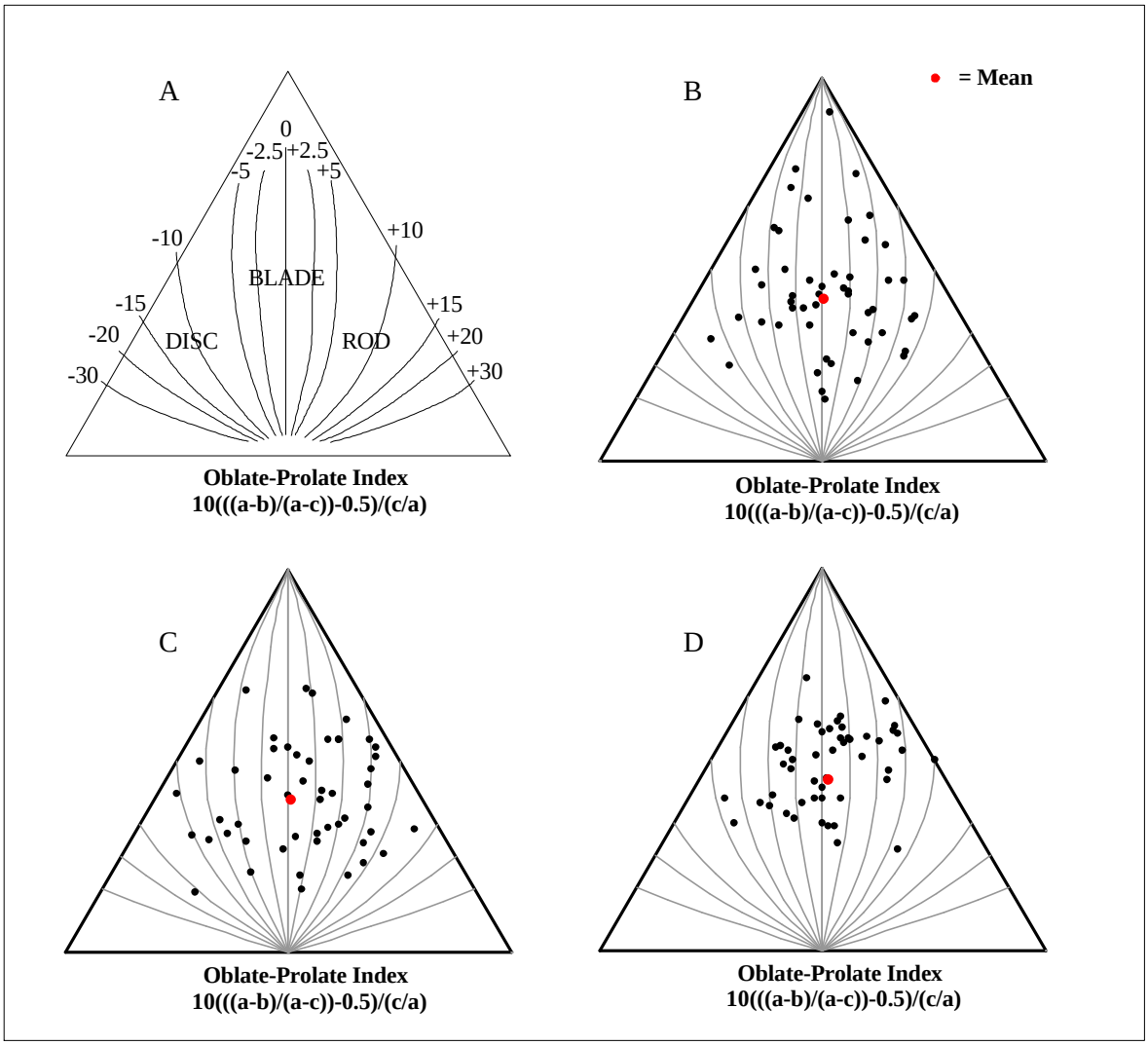



**Figure 6.13** Triangular diagrams after Sneed and Folk (1958). (A) Isolines of the Oblate-prolate index according to Dobkins and Folk (1970). Triangular diagrams for Trenches 1, 2 and 3 respectively at Sekhokong Site 1 (n = 50).

which represents a perfect blade (Table 6.5). Bladed clasts constitute the modal clast shape, with 50% of blades in trenches 1 and 2, and 56% blades in trench 3. Elongate clasts are the second most common clast shape, ranging from 24% in trenches 1 and 3 to 30% in trench 2, whilst platy clasts range from18% in trenches 1 and 3 to 20% in trench 3. Compact clasts are relatively few, with trench 2 containing no compact clasts, trench 3 containing 2% and trench 1 containing 8%. The large amount of bladed clasts is also represented in Figure 6.13, which displays the Oblate-prolate Index. The majority of clasts fall within the -5 and +5 boundaries of the blade category.

**Table 6.5** The shape of clasts measured at the Sekhokong Site 1 slope deposit. *x* = mean, *s* = standard deviation.

| | **Number In Sample** | **Oblate-prolate Index** | | **Maximum Projection Sphericity** | | **Visual Roundness (Powers, 1953)** | |
|---|---|---|---|---|---|---|---|
| | | *x* | *s* | *x* | *s* | *x* | *s* |
| Trench 1 | 50 | -0.45 | 6.27 | 0.62 | 0.13 | 1.34 | 0.59 |
| Trench 2 | 50 | 0 | 5.71 | 0.62 | 0.11 | 1.46 | 0.99 |
| Trench 3 | 50 | 0.01 | 5.85 | 0.67 | 0.11 | 1.80 | 0.99 |

The maximum projection sphericity is represented in Figure 6.14. The results are varied with the clasts in trenches 1 and 2 falling between 0.3 and 0.9. The clasts are slightly more clustered in trench 3 and fall between 0.5 and 0.9. A further indication of the varied nature of the clasts in terms of maximum projection sphericity is indicated in Table 6.5, where the mean value ranges from 0.62 in trenches 1 and 2 to 0.67 in trench 3.

Clast Roundness is represented in Figure 6.15 and Table 6.6. The majority of clasts from the three trenches fall within the angular and subangular categories of roundness in trenches 1 and 2 and subangular and subrounded categories in trench 3. Trench 2 contains the highest percentage of very angular clasts which accounts for 22% of the sample, as opposed to trench 1 which contains only 8% very angular clasts. The percentage of angular clasts ranges from 24% in trenches 2 and 3 to 52% in trench 1. The subangular category contains the next highest percentage of clasts, with values ranging from 36% in trench 3 to 40% in trenches 1 and 3. Although there are no subrounded clasts within trench 1, they make up between 14% and 28% of the sample in trenches 2 and 3. Table

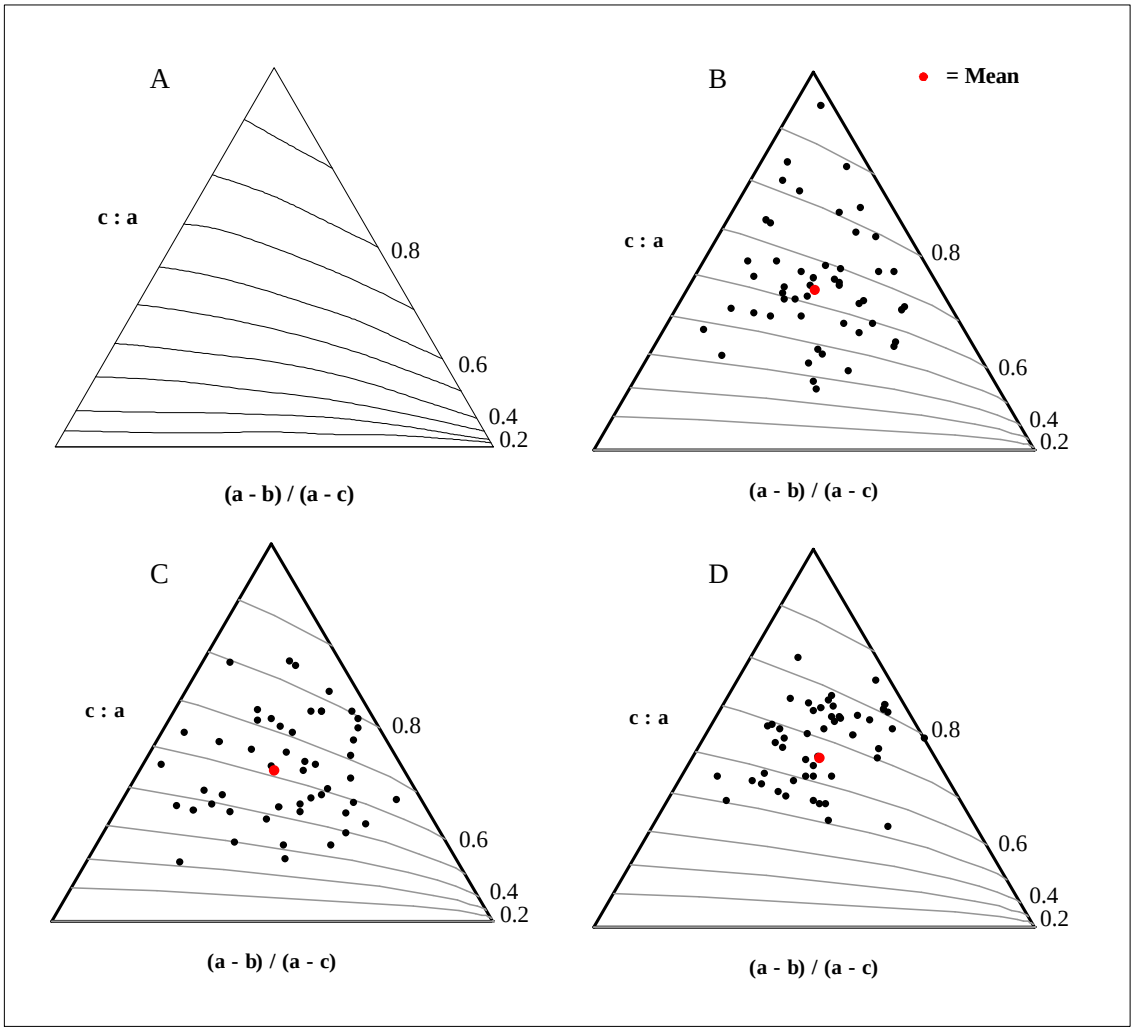



**Figure 6.14** Triangular diagrams after Sneed and Folk (1958). (A) Isolines of the maximum projection sphericity according to Sneed and Folk (1958). Triangular diagrams for trenches 1, 2 and 3 respectively at Sekhokong Site 1 (n = 50).

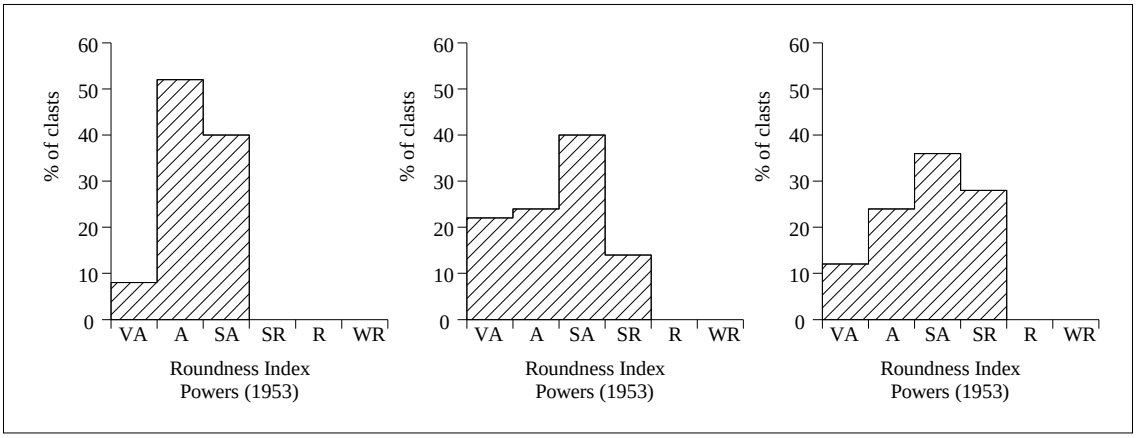



**Figure 6.15** Graphs representing Powers (1953) visual roundness in trenches 1 (A), 2 (B) and 3 (C) at Sekhokong Site 1. VA = Very Angular, A = Angular, SA = Sub Angular, SR = Sub Rounded, R = Rounded, WR = Well Rounded (n = 50).

**Table 6.6** The percentage of clasts falling in the roundness categories at Sekhokong Site 1.

| | VA (%) | A (%) | SA (%) | SR (%) | R (%) | WR (%) |
|---|---|---|---|---|---|---|
| Trench 1 | 8 | 52 | 40 | - | - | - |
| Trench 2 | 22 | 24 | 40 | 14 | - | - |
| Trench 3 | 12 | 24 | 36 | 28 | - | - |

6.5 indicates that average roundness ranges from 1.34 in trench 1 to 1.8 in trench 3, which places these results between the angular and subangular categories. There is a noticeable increase in roundness towards the lower end of the deposit in trench 3.

The t-test was performed to determine whether the sediment sampled in the three trenches for form, sphericity and roundness was statistically significant (<0.05%), and whether there was a relationship between the sediment in the trenches (Table 6.7) and between deposits (Table 6.8). It is clear from Table 6.7 that the results for clast shape in the three trenches are statistically significant in all but visual roundness where the results are not significant between trenches 1 and 3.

Table 6.8 indicates that particle shape is statistically significant between the Tsatsa-La-Mangaung deposit and the Sekhokong Site 1 deposit, with the exception of the results for the Oblate-prolate Index between trenches 1 at Tsatsa-La-Mangaung and Sekhokong Site

**Table 6.7** The statistical significance calculated by the t-test of the shape of clasts sampled in the three trenches in the Sekhokong Site 1 deposit (SS = Statistically significant, NS = Not significant).

| Trenches | Oblate Prolate Index | Maximum Projection Sphericity | Visual Roundness |
|---|---|---|---|
| T1-T2 | **SS** | **SS** | **SS** |
| T1-T3 | **SS** | **SS** | NS |
| T2-T3 | **SS** | **SS** | **SS** |

**Table 6.8** The statistical significance calculated by the t-test of the shape of clasts sampled in the three trenches in the Tsatsa-La-Mangaung and Sekhokong Site 1 deposits (SS = Statistically significant, NS = Not significant).

| Site and Trenches | Oblate Prolate Index | Maximum Projection Sphericity | Visual Roundness |
|---|---|---|---|
| TstatsaT1-Sek1T1 | NS | **SS** | **SS** |
| TsatsaT1-Sek1T2 | **SS** | **SS** | **SS** |
| TsatsaT1-Sek1T3 | **SS** | **SS** | **SS** |
| TsatsaT2-Sek1T1 | **SS** | **SS** | **SS** |
| TsatsaT2-Sek1T2 | **SS** | **SS** | **SS** |
| TsatsaT2-Sek1T3 | **SS** | NS | NS |
| TsatsaT3-Sek1T1 | **SS** | **SS** | NS |
| TsatsaT3-Sek1T2 | **SS** | **SS** | **SS** |
| TsatsaT3-Sek1T3 | **SS** | **SS** | **SS** |

1. Maximum Projection Sphericity is also not significant between trench 2 at Tsatsa-La-Mangaung and trench 3 at Sekhokong Site 1. Visual roundness is not significant between Tsatsa-La-Mangaung trench 2 and Sekhokong Site 1 trench 3 and Tsatsa-La-Mangaung trench 3 and Sekhokong Site 1 trench 1.

### 6.2.6 Micromorphology

Samples were collected at 90 cm depth in trench 2 and at 80 cm and 125 cm depth in trench 3 (Table 6.9). The fabric pattern of the three samples is random and the clasts have a broad degree of parallelism which is weakly expressed. The c/f related distribution is double-spaced porphyric and the dominant size fraction is coarse sand. Sediment sorting ranges from poorly sorted to unsorted in trench 2 and poorly sorted in trench 3. Particles are predominantly blocky in trench 2 and platy and blocky in trench 3. They are

**Table 6.9** Micromorphological description of the Sekhokong Site 1 samples.

| Micromorphological features → / Sample No. ↓ | Skeleton: Fabric: Pattern | Degree of parallelism | Quantity of oriented particles | C/F related distribution | Dominant size fraction | sorting | Skeleton: Shape: Shape | Degree of roundness | surface roughness | Aggregates: peds | ped seperation and pedality | Voids: Void type | Microstructure | % total area occupied by voids | Parent Material: Rock type | Average size um | Fine: Colour | Limpidity | Groundmass: C/F 2mm | C/F 10um | C/F related distribution | Pedofeatures: Cappings | Texture | laminated | Infillings: Classification | Descriptive criteria | Crystals |
|---|---|---|---|---|---|---|---|---|---|---|---|---|---|---|---|---|---|---|---|---|---|---|---|---|---|---|---|
| T2 90 | R | BA | W-E | DSP | CS | P/U | B | SA | U | S | WS | V&C | VM | 20 | B | 3000 | YB | SP | 3:2 | 4:1 | DSP | ● | SL | NL | LD | PF | ● |
| T3 80 | R | BA | W-E | DSP | CS | P | P&B | SA | U | S | WS | V&C | CM | 25 | B | 3100 | YB | SP | 7:3 | 7:3 | DSP | ● | SL | L | LD | PF | ●● |
| T3 125 | R | BA | W-E | DSP | CS | P | P&B | SA | U | S | WS | V&P | VM | 15 | B | 2700 | YB | SP | 2:3 | 7:3 | DSP | ● | SL | NL | LD | PF | ● |

KEY:

**Pattern:**
R = Random

**Degree of parallelism:**
BA = Broad angle

**Quantity of oriented particles:**
WE = Weakly expressed:<33% of particles are oriented

**C/F related distribution:**
SSP = Single spaced porphyric
DSP = Double spaced porphyric

**Size:**
CS = Coarse sand

**Sorting:**
PS = Poorly sorted
U = Unsorted

**Shape:**
P = Platy
B = Blocky

**Degree of roundness:**
A = Angular
SA = Subangular

**Surface roughness:**
U= Undulating

**Peds:**
S = Spheroidal Peds

**Ped seperation and pedality:**
WS = Weakly seperated

**Void type:**
C = Channels
CM = Chambers
V = Vughs
VCM = Vugh and Chamber
P = Planes

**Microstructure:**
VM = Vughy microstructure
CM = Channel microstructure

**Mineral type**
B = Basalt

**Colour:**
YB = Yellowish Brown

**Limpidity:**
SP = Speckled

**Cappings:**
● <10%
●● <10-20%
●●● >20%

**Texture:**
SL = Silt

**Laminated:**
NL = Nonlaminated
L = Laminated

**Infillings classification:**
LD = Loose discontinuous

**Descriptive criteria:**
PF = Passage features

**Crystals:**
● Few
●● Some
●● Many

**Crystal intergrowth:**
P = Parallel

subangular in shape, with an undulating surface. Peds are weakly separated in all three samples and void types are vughy and channel in trench 2 at 90 cm depth and trench 3 at 80 cm depth, and vughy and planes (Figure 6.16) in trench 3 at 125 cm depth. The microstructure is vughy in trench 2 at 90 cm depth and trench 2 at 125 cm depth, whilst trench 3 at 80 cm depth has a channel microstructure. The total area occupied by voids ranges from 15% in trench 3 at 125 cm depth to 25% in trench 2 at 80cm depth.

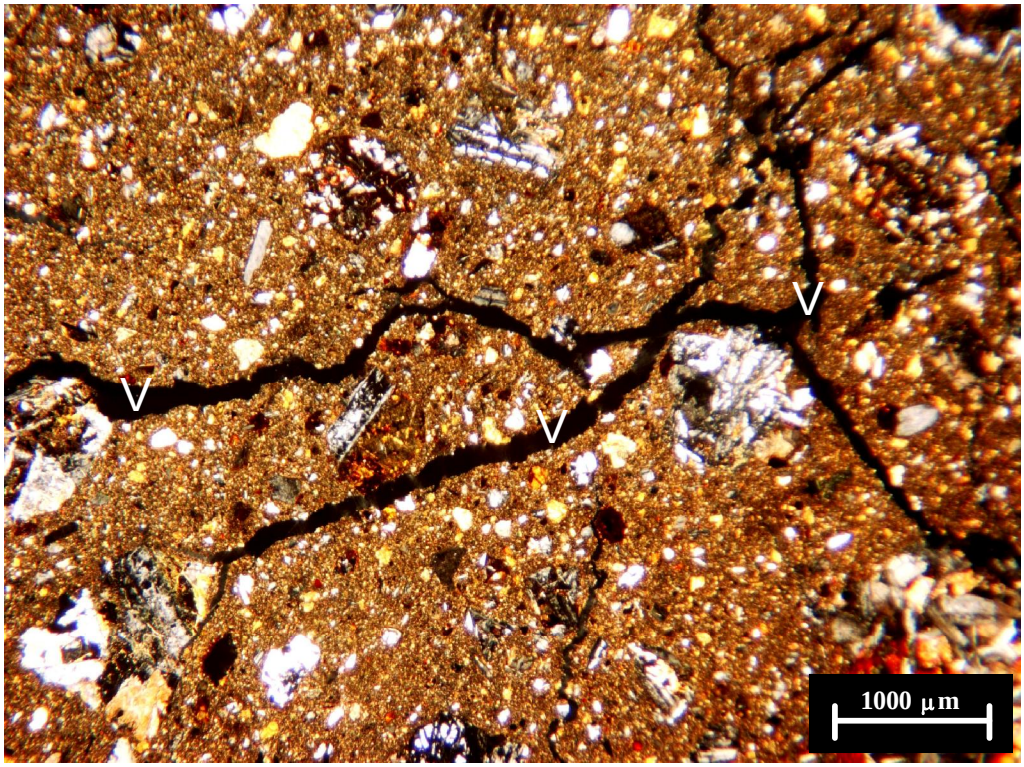



**Figure 6.16** An example of plane voids in trench 3 at 125 cm depth taken in XPL (v = void).

The main rock type is basalt and the average size of particles ranges from 2700 µm in trench 3 at 125 cm depth to 3200 µm in trench 2 at 90 cm depth and trench 3 at 80 cm depth. The colour of the fine material is yellowish brown and displays a speckled limpidity. The c/f ratio indicates that the material is predominantly coarse-grained and double spaced porphyric. Silt cappings are present in all three samples and cover <10% of grains. They are non-laminated in trench 2 at 90 cm depth and trench 3 at 125 cm depth, however are laminated on particles within trench 3 at 80 cm depth. Infillings are loose discontinuous passage features and there are few crystals present in trench 2 at 90 cm

depth and trench 3 at 125 cm depth, whilst there are some crystals present in trench 3 at 80 cm depth (Figure 6.17). Several rotation structures are also present in trench 3 at 125 cm depth (Figure 6.18). The upper photos in Figure 6.18 indicate the rotation of finer particles around the basalt clasts as well as lineation of particles. The shadow represents finer material which is older than the groundmass and has been incorporated and then rotated, breaking the intraclast into smaller pieces as highlighted in the photo. The lower two photos indicate a rotation structure around a small clast and rotation within the matrix. The lineation of particles represents a shear and a pressure shadow is also evident as highlighted on the photo. The mineral which is encircled may be a secondary growth which is indicated by the compressed fabric around it and the fact that it crosses the lineation.

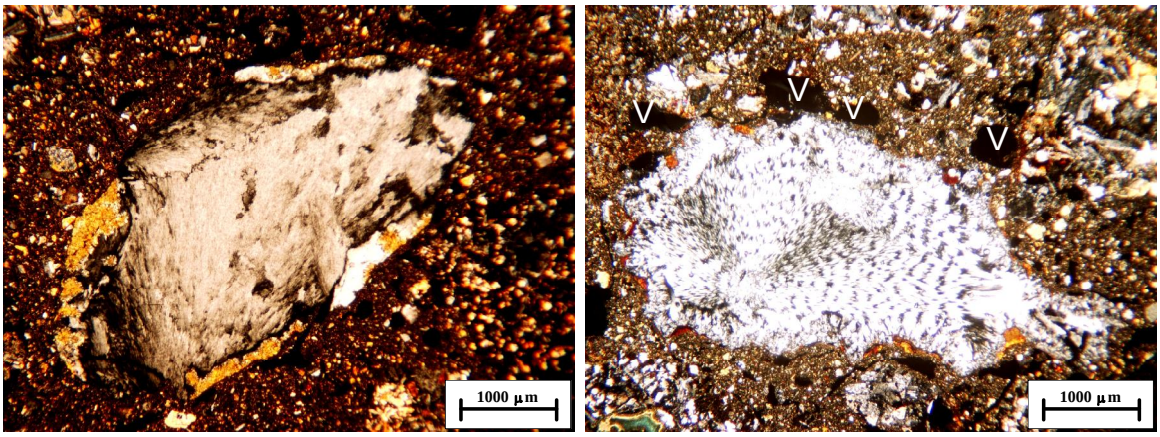



**Figure 6.17** Single crystals within groundmass at Sekhokong Site 1, trench 3, taken in XPL.

### 6.2.7 Radiocarbon dating

An AMS age of 12370 ± 60 radiocarbon yrs BP was obtained for trench 1 at a depth of 1.6 m (Table 6.10), which represents the maximum depth of the trench. This yields a calibrated age of 14 700 yrs BP.

### 6.2.8 Summary

A site summary of the sedimentary characteristics of the Sekhokong Site 1 deposit is presented in Table 6.11. All three trenches consist of a present-day soil overlying a medium to coarse grained diamict, which is very poorly sorted. The sediment in all three

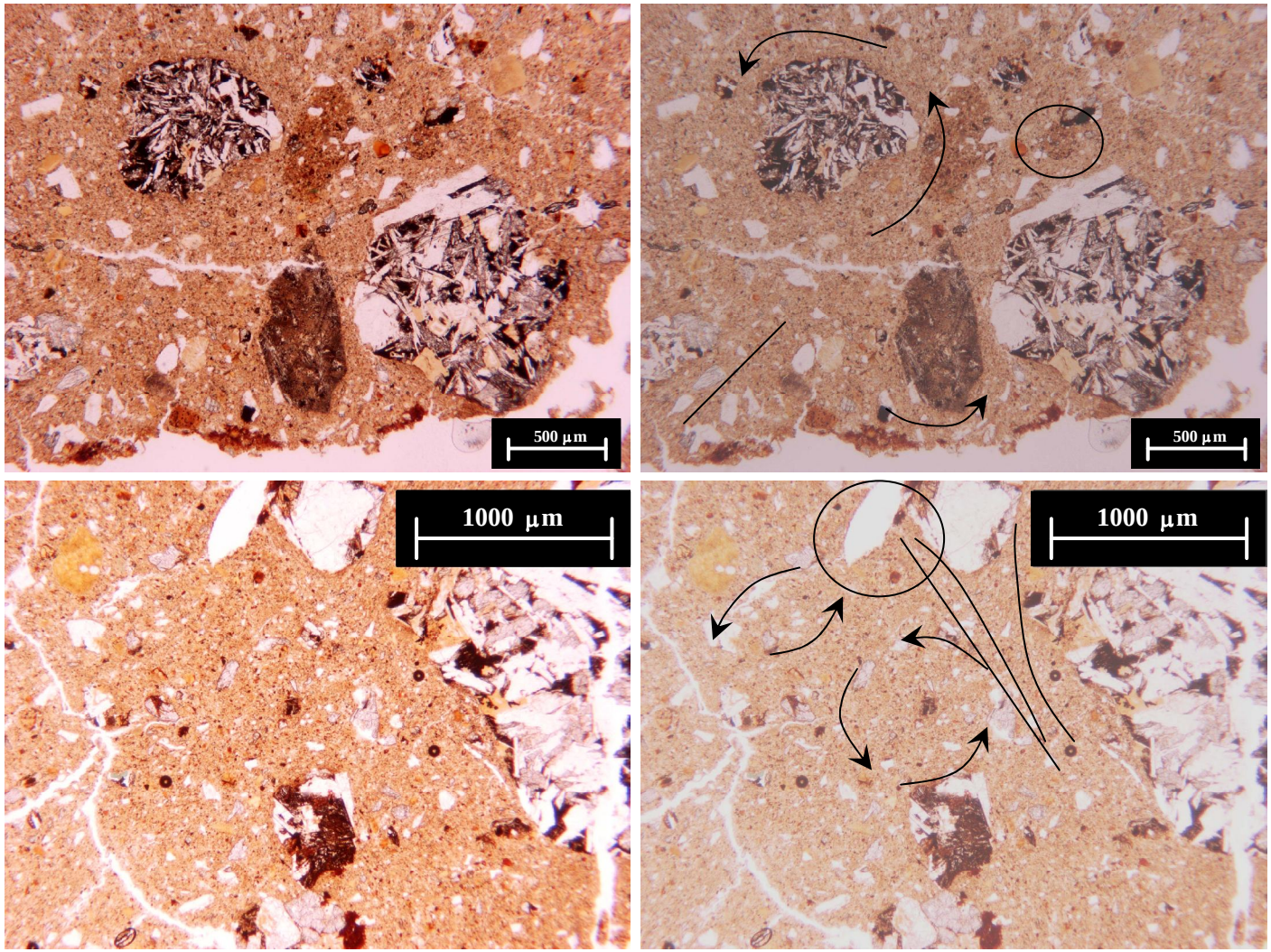



**Figure 6.18** Rotation structures within trench 3 at 125 cm depth. Note images are paired with original and annotated versions.

**Table 6.10** AMS and calibrated ages for the Sekhokong Site 1 deposit (Sampling depth: T1 = 1.6 m).

| Anal. No. [1] Gr-A | Sample designation | $\delta^{13}C$ (‰ PDB) | Radiocarbon Age yrs BP | 1σ yrs BC | 2σ yrs BC | Calibrated yrs BP |
|---|---|---|---|---|---|---|
| 24894 | Sekhokong Site 1 | -18.7 | 12370 ± 60 | 12 834 – 12 676 | 12 913 – 12 597 | 14 700 |

**Table 6.11** A summary of the sedimentary characteristics at Sekhokong Site 1.

| | Trench 1 | Trench 2 | Trench 3 |
|---|---|---|---|
| **Lithofacies** | Soil overlying medium - gravely diamict | Soil overlying medium - gravely diamict | Soil overlying medium - gravely diamict |
| **Particle Size** | -1 Phi (Gravel) | -1 Phi (Gravel) | -1 Phi (Gravel) |
| **Sorting** | Very poorly sorted | Very poorly sorted | Very poorly sorted |
| **Fabric** | In direction of ridge crest | Random | Random |
| **Dip** | 0° - 30° | 10° - 60° | 0° - 40° |
| **Shape** | Bladed | Bladed | Bladed |
| **Roundness** | Angular | Sub angular | Sub angular |
| **Micromorphology** | Few cappings | Few cappings | Few cappings, rotation structures |
| **AMS dating** | 14 700 yrs BP | | |

trenches becomes coarser with depth. The sediment in Trench 2 is predominantly made up of gravel, however trenches 1 and 3 also contain a significant amount of finer material and there are several bimodal distributions. Clast orientation within the trenches varies from in the direction of the ridge crest in trench 1, to random in both trenches 2 and 3 and mean dip tends to be between 0° and 40° in trenches 1 and 3, and 0° and 60° in trench 2. Clast shape is predominantly bladed in all three trenches; however roundness is predominantly angular in trench 1 and subangular in trenches 2 and 3. All three trenches contain few cappings in thin section and trench 3 also contains several rotational structures. The calibrated AMS age of 14 700 yrs BP indicates that the deposit is pre-Holocene.

## 6.3 SEKHOKONG SITE 2

### 6.3.1 Morphology

The Sekhokong Site 2 ridge (Figures 6.19 and 6.20) is 150 m in length and varies in width between 20 m and 43 m. The deposit reaches a height of 12 m on its eastern aspect. The altitudinal range of the deposit varies from 3019 m a.s.l. to 3076 m a.s.l. The slope gradient on the western aspect of the deposit ranges from 7º (cross section D-D; Figure 6.20) to 25° (cross section B-B; Figure 6.20), whereas the gradient on the eastern aspect ranges from 30º (cross section B-B; Figure 6.20) to 35° (cross sections C-C and D-D; Figure 6.20). Although the longitudinal profile (cross section A-A; Figure 6.20) indicates that the slope deposit may be as steep as 36° in some areas, the average gradient of the deposit is 22º. This cross section also illustrates that the deposit possesses slight ridges and furrows. Cross section E-E represents the slope profile of the area. The slope profile begins with an interfluve unit, which has a slope angle of 0º, increasing to 4º on the seepage slope unit. The slope angle increases to 16º on the convex slope unit and reaches a maximum of 26º on the transportational midslope. The slope angle on the colluvial footslope ranges from 20º to 8º, becoming gentler on the alluvial toeslope where it is 2º. There is then a second convex slope unit with a slope angle of 19º and a second colluvial footslope unit where the slope angle is 6º. The slope deposit occurs within both the transportational midslope and the colluvial footslope units and the total slope length is 2.1 km down to the small stream.

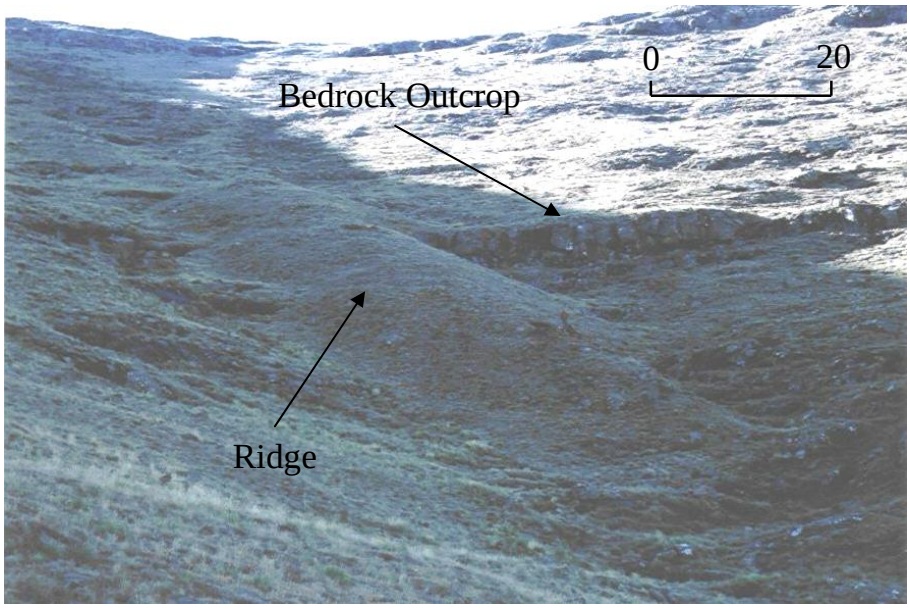



**Figure 6.19** The Sekhokong Site 2 slope deposit (photo by S. Mills).

The Sekhokong Site 2 deposit is unusual, given that it lies on a large bedrock outcrop and does not possess the secondary ridges which are typical of the Tsatsa-La-Mangaung and Sekhokong Site 1 deposits.

### 6.3.2 Field observations

The lithofacies at the three trenches at the Sekhokong Site 2 consist of a present-day soil, underlain by a gravelly diamict which was excavated to a depth between 150 cm and 190 cm (Figures 6.21 to 6.23). This is not the depth at which bedrock was reached, but the depth at which it became increasingly difficult to excavate boulders. Within this diamict, a variety of different sized boulders are present, ranging in size from 2 cm to over a 100 cm in length, and which are held together by a sandy matrix. There were once again considerably fewer clasts present than within the Tsatsa-La-Mangaung deposit.

The diamict unit in trenches 1 and 2 (Figures 6.21 and 6.22) is very similar and is massive, matrix-supported, clast rich, loose and poorly sorted. The soil is a yellowish brown colour when dry. Trench 3 is unlike anything described so far. Boulders excavated

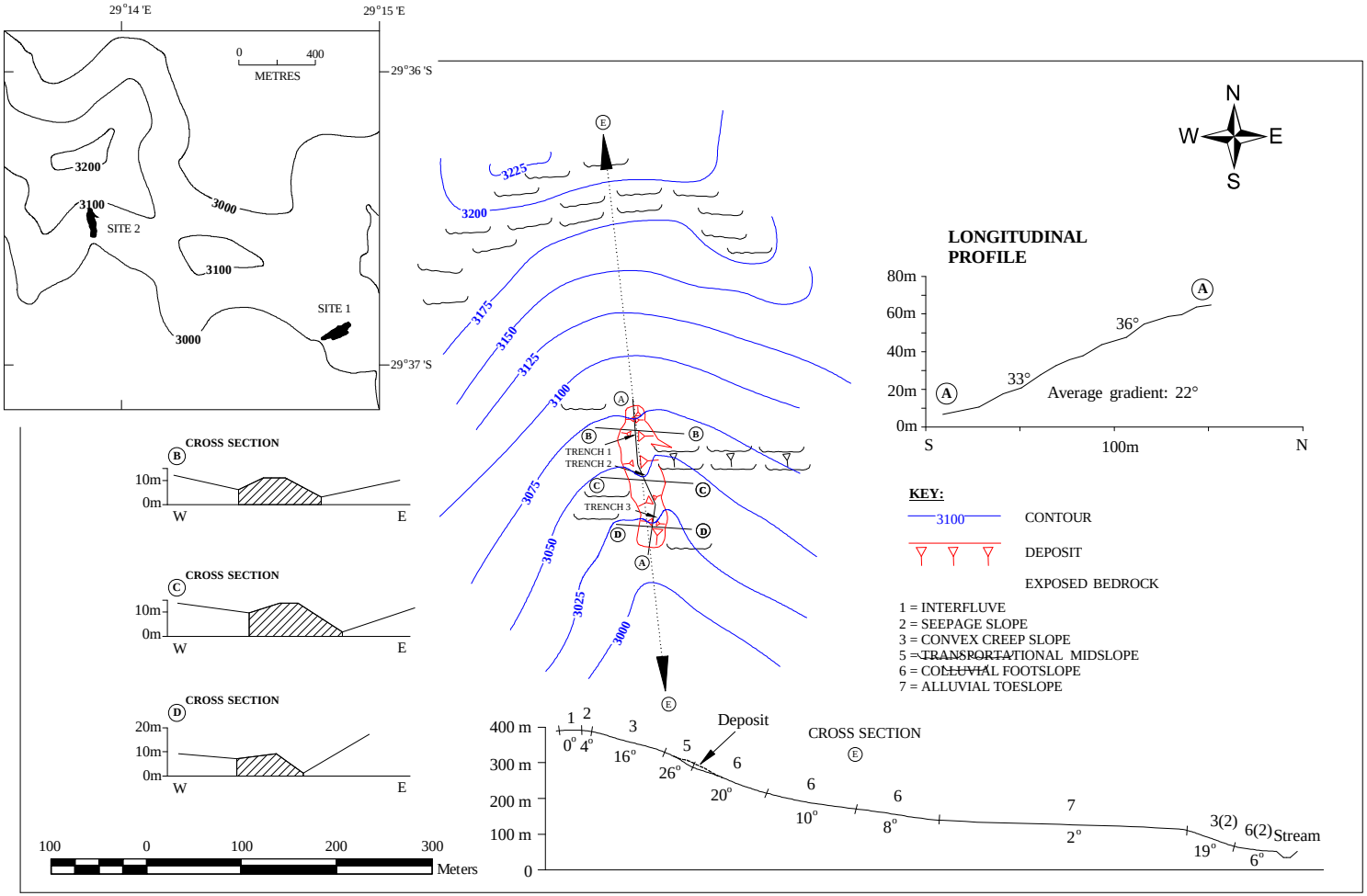



**Figure 6.20** Morphological map of the Sekhokong Site 2 deposit.

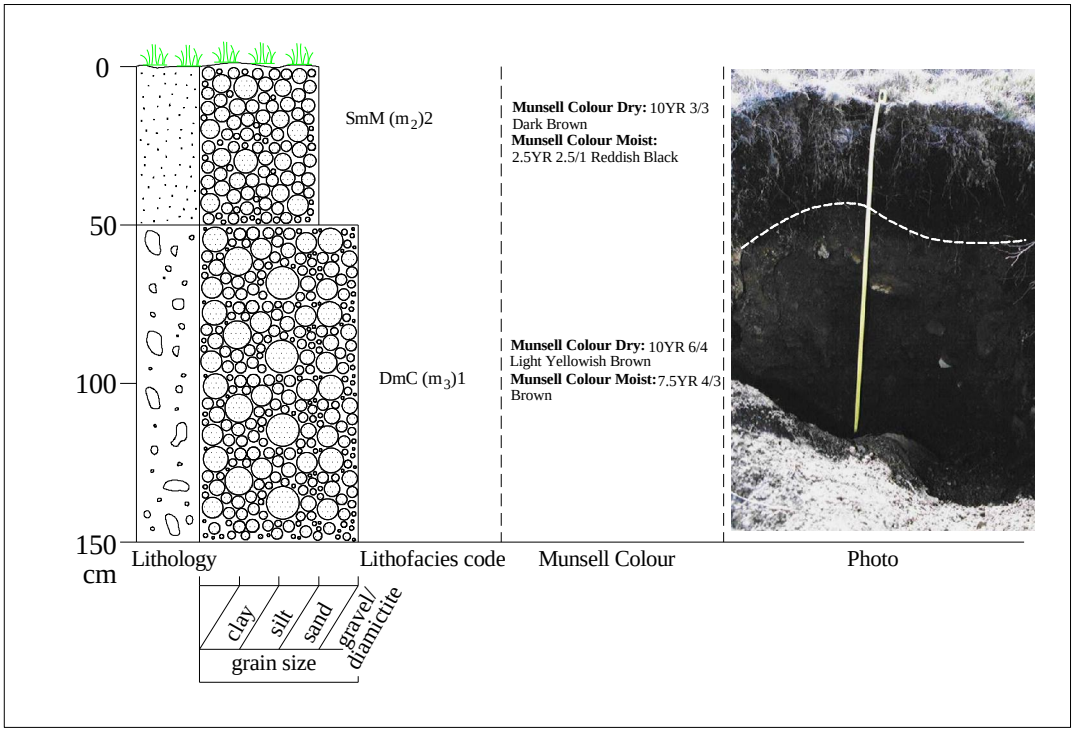



**Figure 6.21** Sedimentological and stratigraphical data for trench 1 at Sekhokong Site 2.

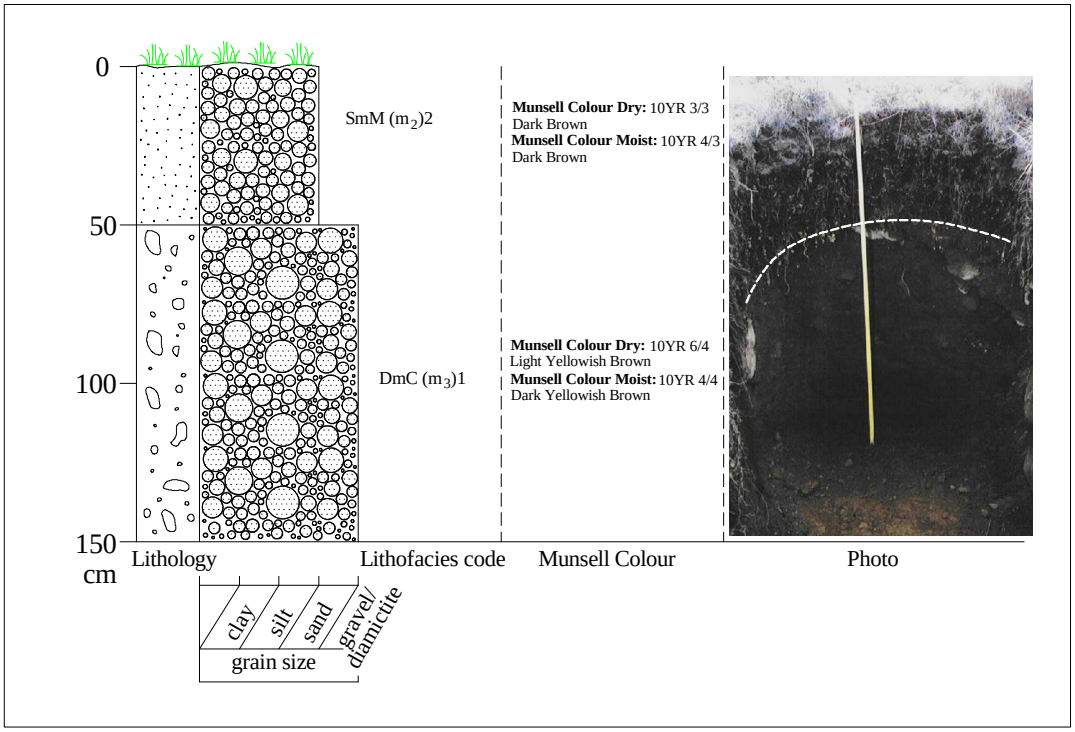



**Figure 6.22** Sedimentological and stratigraphical data for trench 2 at Sekhokong Site 2.

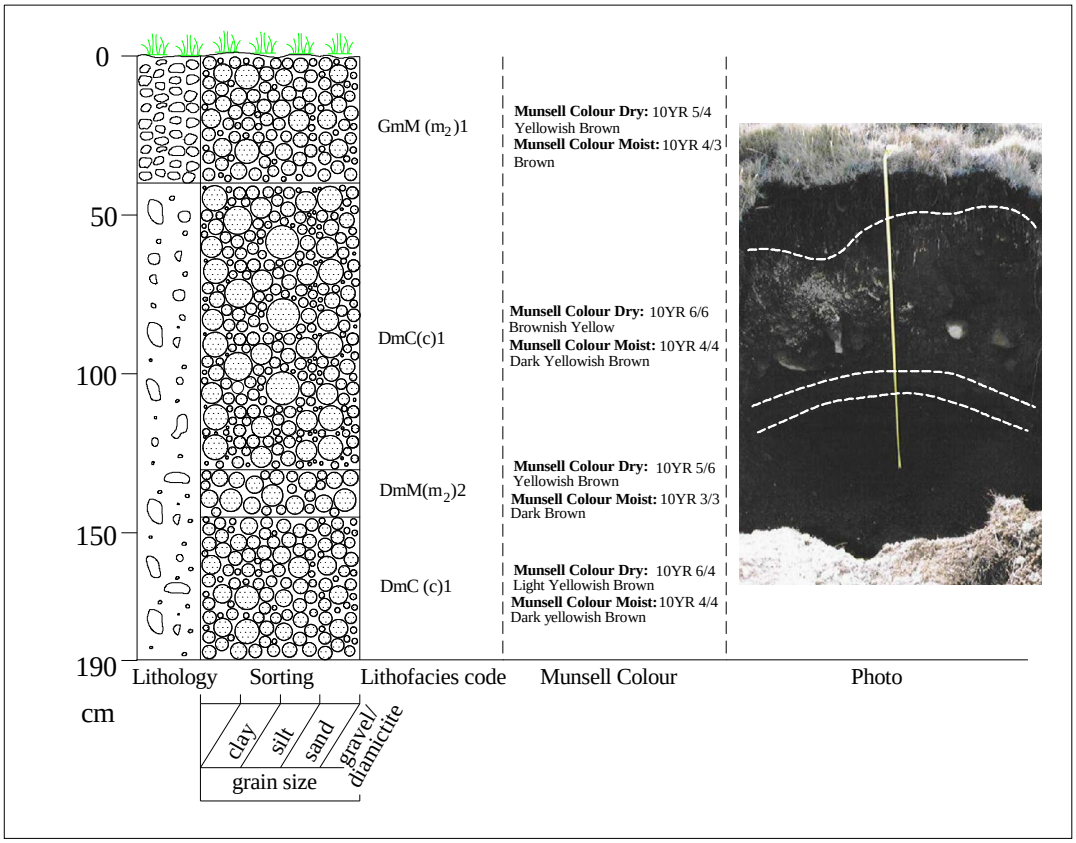



**Figure 6.23** Sedimentological and stratigraphical data for trench 3 at Sekhokong Site 2.

from the trench were fewer in number so it was possible to excavate down to 190 cm. However, it was not possible to excavate deeper than this as the sediment became loose. The diamict unit in this trench is divided by a 15 cm horizon of slightly finer material (Figure 6.23). The upper diamict unit is massive, coarse-grained, clast supported and loose. The soil is dark yellowish brown when moist and brownish yellow when dry. Below this unit is a 15 cm horizon which is massive, medium grained, matrix supported with moderate clasts and friable. The soil is yellowish brown when dry. Below this is a diamict unit which is massive, coarse-grained, clast supported and loose. The soil is light yellowish brown when dry.

### 6.3.3 Particle size analysis

The particle size analysis results are very similar for trenches 1 and 3, however trench 2 displays considerably different results (Figures 6.24 to 6.26 and Table 6.12). Gravel is the main constituent in trenches 1 and 3 and constitutes over 69%, with the exception of trench 3 at 140 cm depth. Combined silt and clay values constitute less

than 9% of the total samples, with the exception of trench 3 at 140 cm depth. There is a noticeable difference in trench 3 at 140 cm depth, where the sediment is much finer. There are no secondary peaks in trenches 1 and 3 with the exception of trench 3 at 140 cm depth. Although this sample has a slight secondary peak at 4 phi, the bimodality index is 1.22 which indicates that the sample is unimodal (Table 6.12). In contrast, trench 2 displays very different sedimentary characteristics to trenches 1 and 3. Gravel constitutes between 25% and 48% of the samples whilst combined silt and clay values range from 14% to 37% of the total samples. Although all samples within trench 2 have secondary peaks, only trench 2 at 80 cm depth is truly bimodal.

The graphic mean (Table 6.12) indicates that the sediment in trenches 1 and 3 range from very coarse sand to gravel. Because the samples are coarse and negatively skewed in these trenches, the mode is a better indication of the sample size. The mode for all the samples in trenches 1 and 3 is -1 phi, which means the sediment is primarily gravel. Further statistical analyses have been undertaken in the form of sorting, skewness and kurtosis (Table 6.13 and 5.3). The sediment sorting in trench 1 is poorly sorted to moderately sorted, whilst sediment sorting is very poorly sorted. In contrast, sorting in trench 3 ranges from well sorted to very poorly sorted. Values are all very negatively skewed for the three trenches (Table 6.13), with the exception of trench 2 at 80 cm depth, which is almost symmetrical. Kurtosis varies from extremely leptokurtic to very platykurtic to platykurtic. The mean values in Table 6.14 indicate that the sediment at Sekhokong Site 2 is primarily composed of gravel in trenches 1 and 3 and medium sand in trench 2. The sediment is poorly sorted in trenches 1 and 3 and very poorly sorted in trench 2. The sediment in the three trenches is very negatively skewed. The sediment in trench 1 is extremely leptokurtic, the sediment in trench 2 is very leptokurtic and the sediment in trench 3 is platykurtic.

### 6.3.4 Clast fabric and fabric eigenvalues

Clast a-axis orientation and dip were plotted as an equal-area stereographic scatter plot and an equal-area stereographic contour plot (Figure 6.27). Orientation of the clasts measured in trenches 1 and 2 indicates no preferred orientation. Alternatively, clasts in trench 3 display a preferred orientation transverse to the debris deposit ridge. Most clasts within the three trenches dip between 0° and 40°. The chi-square test was used in order to determine whether clast orientation is statistically significant. Clasts

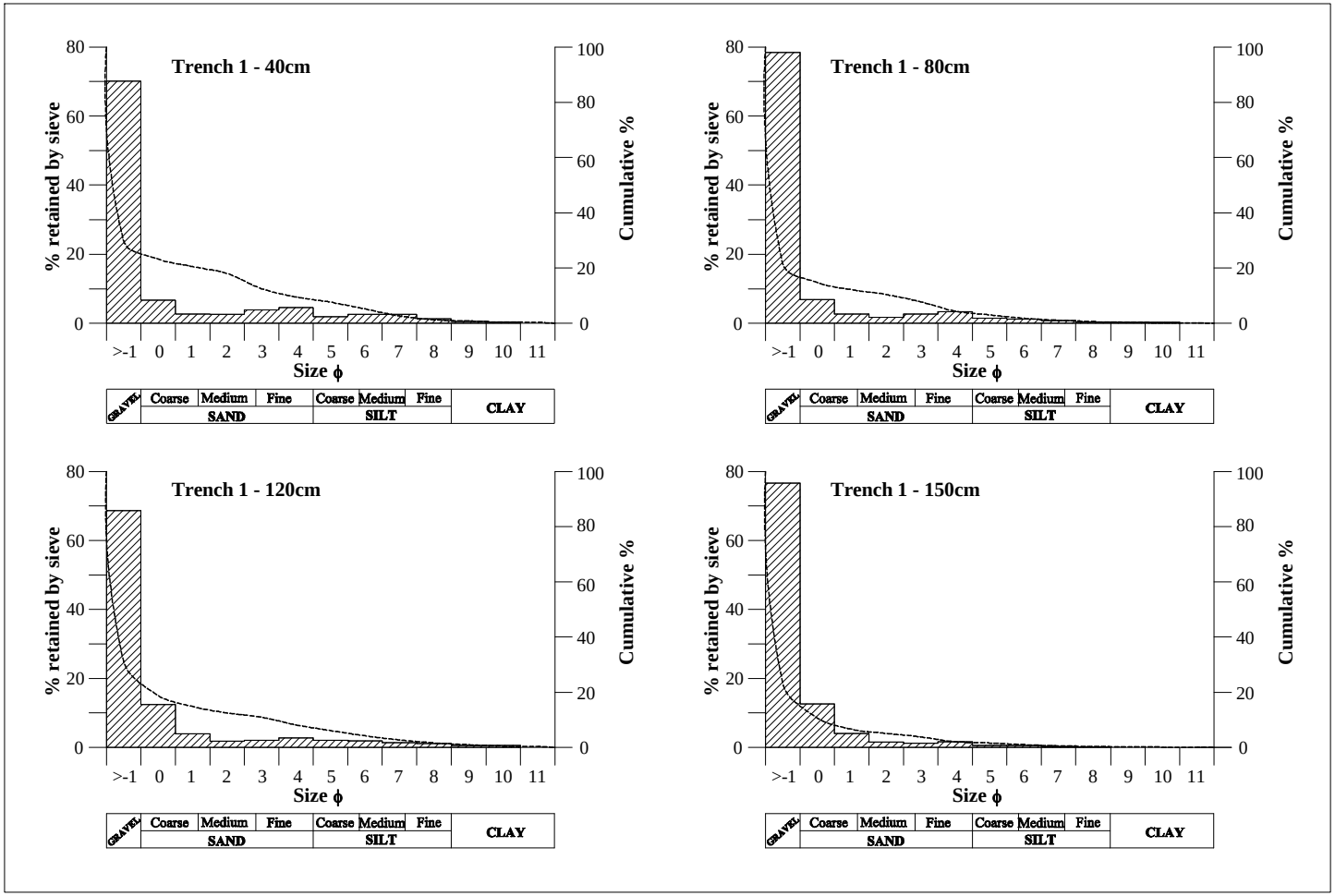



**Figure 6.24** Grain size distributions for the sediment from trench 1 at Sekhokong Site 2.

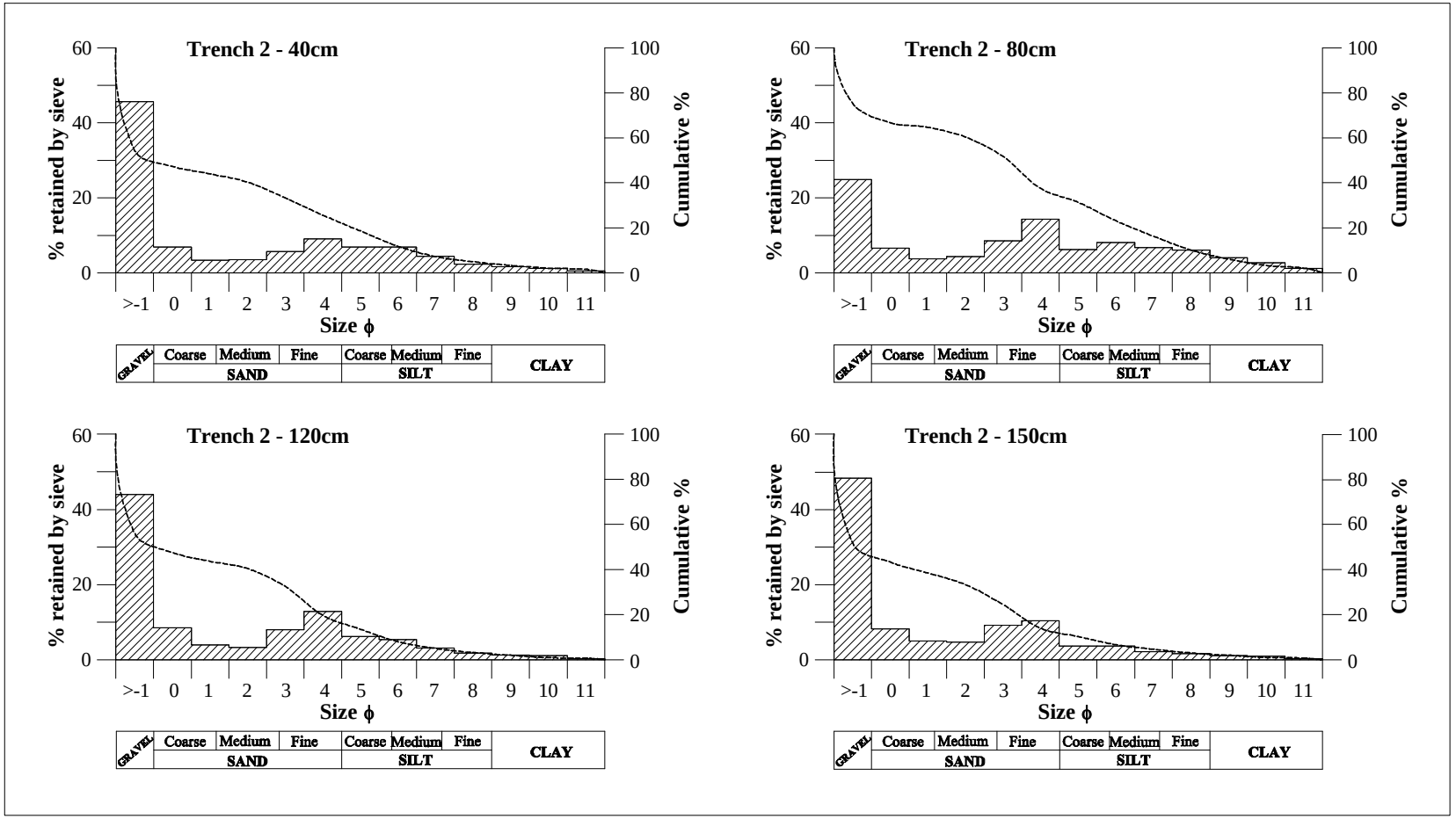



**Figure 6.25** Grain size distributions for the sediment from trench 2 at Sekhokong Site 2.

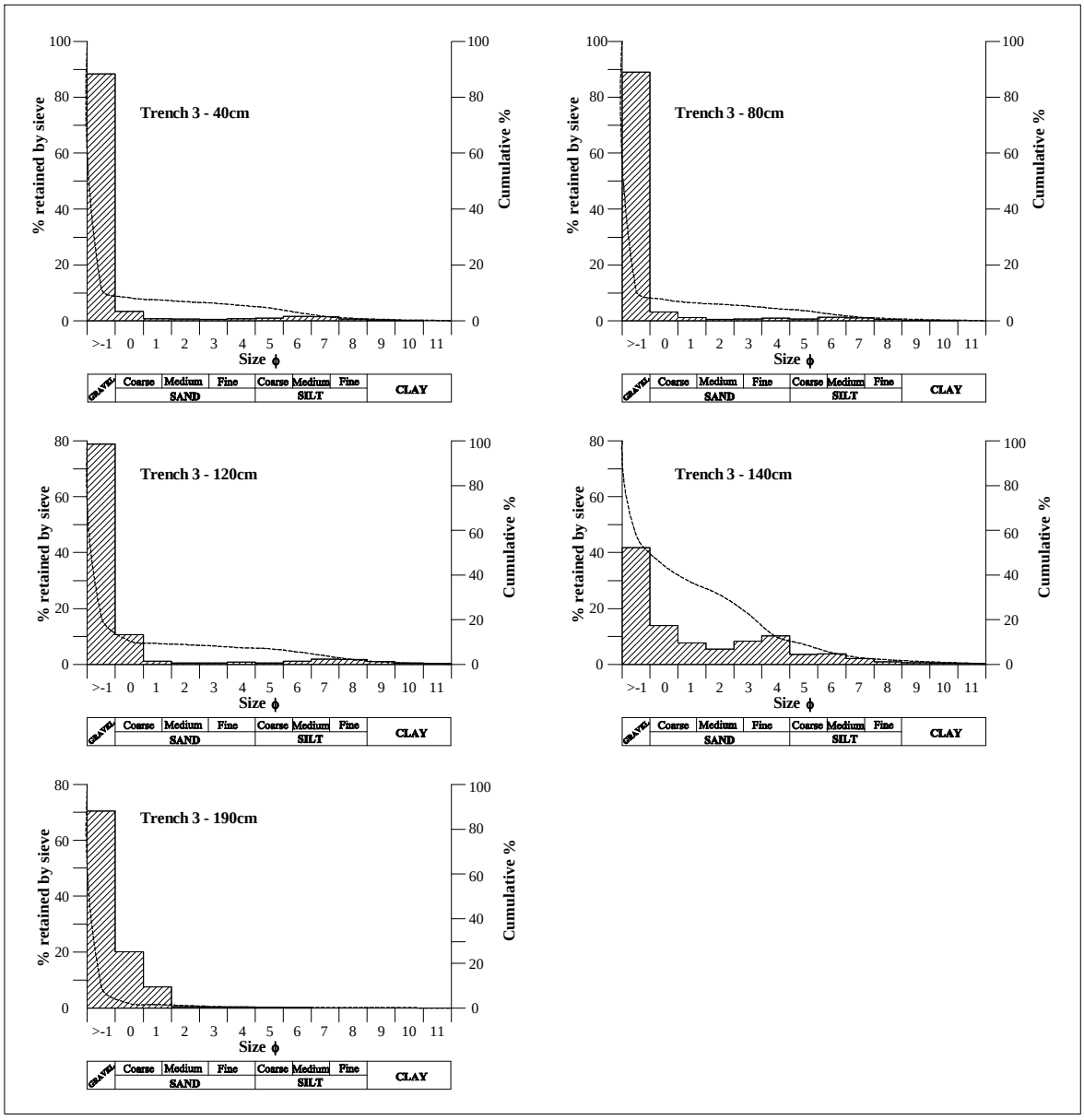



**Figure 6.26** Grain size distributions for the sediment from trench 3 at Sekhokong Site 2.

**Table 6.12** Particle size statistical analysis for Sekhokong Site 2.

| Sample | Depth | Gravel (%) | Sand (%) | Silt (%) | Clay (%) | Mean (phi) | Mode (phi) | Peaks (phi) | Bimodality Index ($B^*$) |
|---|---|---|---|---|---|---|---|---|---|
| Trench 1 | 40 cm | 70 | 20 | 9 | 1 | 0.17 | -1 | -1 | 0.32 |
| | 80 cm | 79 | 17 | 4 | 0 | -0.75 | -1 | -1 | 0.21 |
| | 120 cm | 69 | 23 | 7 | 1 | -0.45 | -1 | -1 | 0.20 |
| | 150 cm | 77 | 21 | 2 | 0 | -0.84 | -1 | -1 | 0.11 |
| Trench 2 | 40 cm | 46 | 29 | 22 | 3 | 1.32 | -1 | -1, 4 | 0.99 |
| | 80 cm | 25 | 38 | 31 | 6 | 3.08 | -1 | -1, 4, 6 | 2.9, 1.1 |
| | 120 cm | 44 | 36 | 18 | 2 | 1.10 | -1 | -1, 4 | 1.5 |
| | 150 cm | 48 | 38 | 12 | 2 | 0.66 | -1 | -1, 4 | 1.1 |
| Trench 3 | 40 cm | 88 | 6 | 5 | 1 | -1 | -1 | -1 | 0.13 |
| | 80 cm | 89 | 6 | 4 | 1 | -1 | -1 | -1 | 0.10 |
| | 120 cm | 79 | 14 | 6 | 1 | -0.91 | -1 | -1 | 0.19 |
| | 140 cm | 42 | 46 | 11 | 1 | 0.72 | -1 | -1, 4 | 1.22 |
| | 190 cm | 70 | 29 | 1 | 0 | -0.79 | -1 | -1 | 0.03 |

**Table 6.13** Further particle size statistical values for Sekhokong Site 2.

| Sample | | Sorting | Skewness | Kurtosis |
|---|---|---|---|---|
| Trench 1 | 40 cm | 1.94 | -0.82 | >3.00 |
| | 80 cm | 0.91 | -1 | >3.00 |
| | 120 cm | 1.41 | -1 | >3.00 |
| | 150 cm | 0.59 | -1 | >3.00 |
| Trench 2 | 40 cm | 2.95 | -0.83 | 0.73 |
| | 80 cm | 3.58 | -0.08 | 0.63 |
| | 120 cm | 2.61 | -0.79 | 0.71 |
| | 150 cm | 2.38 | -0.95 | 0.81 |
| Trench 3 | 40 cm | 0.86 | -1 | >3.00 |
| | 80 cm | 0.66 | -1 | >3.00 |
| | 120 cm | 1.19 | -1 | >3.00 |
| | 140 cm | 2.24 | -0.83 | 0.78 |
| | 190 cm | 0.36 | -1 | 2.73 |

**Table 6.14** Mean and Standard deviation for the particle size statistical analysis at Sekhokong Site 2.

| Trench | Mean | | Mode | | Sorting | | Skewness | | Kurtosis | |
|---|---|---|---|---|---|---|---|---|---|---|
| | *x* | *s* | *x* | *s* | *x* | *s* | *x* | *s* | *x* | *s* |
| Trench 1 | -0.47 | 0.46 | -1 | 0 | 1.21 | 0.59 | -1 | 0 | >3 | 1.08 |
| Trench 2 | 1.54 | 1.06 | -1 | 0 | 2.88 | 0.52 | -0.66 | 0.40 | 0.72 | 0.07 |
| Trench 3 | -0.55 | 0.84 | -1 | 0 | 1.24 | 0.70 | -0.96 | 0.09 | 2.44 | 1.11 |

in trenches 1 and 2 have a probability of being randomly distributed at a level >0.05%, whilst clasts in trench 3 have a statistically significant orientation (<0.05%).

$S_1$ values, which measure the strength of clustering about the mean axis range between 0.526 at trench 1 to 0.585 at trench 2, which means that these fabrics trend towards girdles, where the points are almost evenly distributed around a great circle and $S_1 \approx S_2 \gg S_3$. Alternatively, the $S_1$ value at trench 3 is 0.712, which indicates that the clast fabric represents a linear cluster, where all observations are approximately parallel and $S_1 \gg S_2 \approx S_3$. The normalised eigenvalues were then plotted onto a general shape diagram (Figure 6.28) and indicate that the sediment in all three trenches has a low isotropy value. Clasts within trenches 1 and 2 have a relatively low elongation value, however clasts within trench 3 have a moderate elongation value. Fabric shape ellipsoids are compared with plotted data from various published sources (Figure 6.28C), which indicates that the sediment within trenches 1 and 2 falls within the

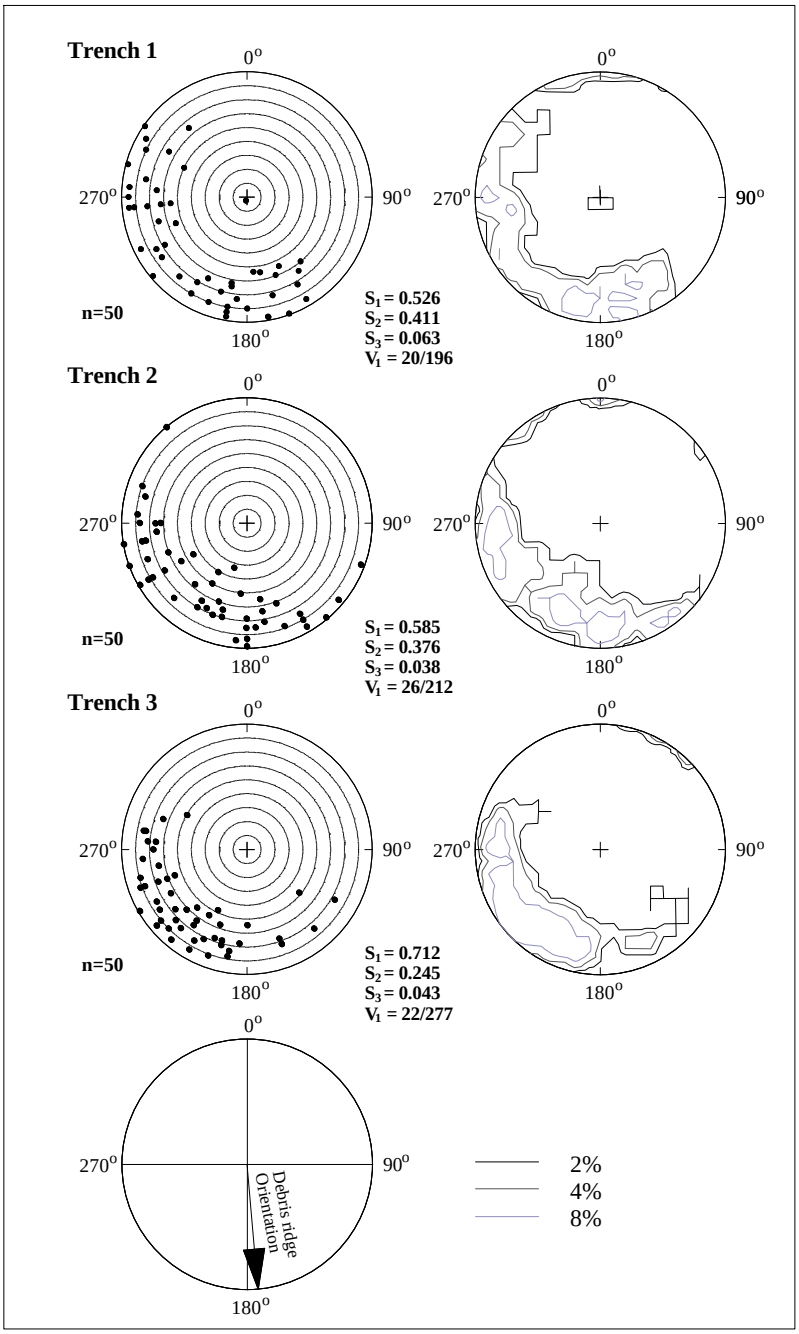



**Figure 6.27** Clast orientation, dip and contouring at trenches 1, 2 and 3 at Sekhokong Site 2.

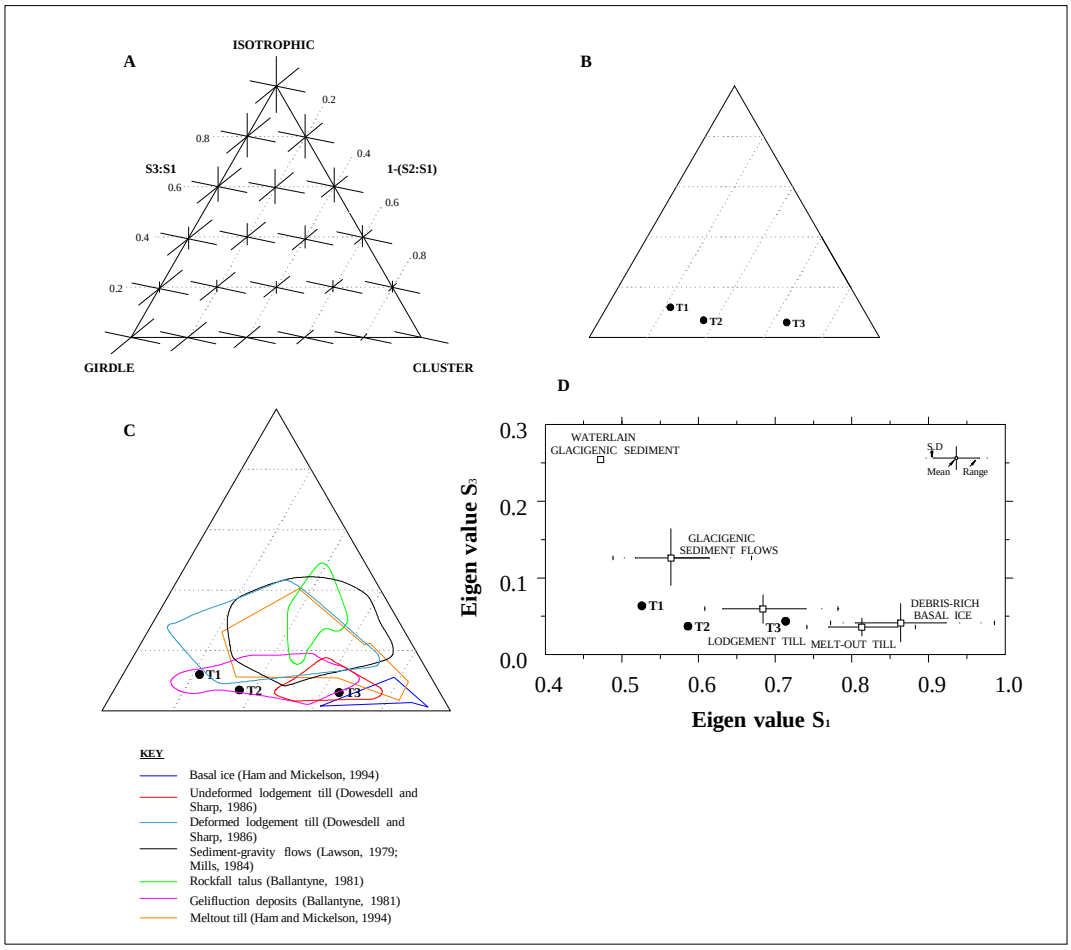



**Figure 6.28** Till fabric using eigenvalue data. (A) The range of orthorhombic fabric shapes. (B) Fabric data from the three trenches. (C) Comparison with envelopes from a range of deposits. (D) Comparison with modern data fabrics from various environments (Dowdeswell *et al.*, 1985).

gelifluction deposit envelope, whilst the sediment within trench 3 falls on the limit of this envelope and within the undeformed lodgement till envelope. When compared with Figure 6.28D, only the sediment in trench 3 falls within the boundaries of lodgement till. A triangular plot of normalised eigenvalues was also generated in order to further compare the Sekhokong Site 2 eigenvalues to envelopes produced by previous authors for various deposits (Figure 6.29). The sediment in trench 3 falls within the internal fabric of rock glaciers envelope, however the sediment in trenches 1 and 2 fails to fall within any envelope.

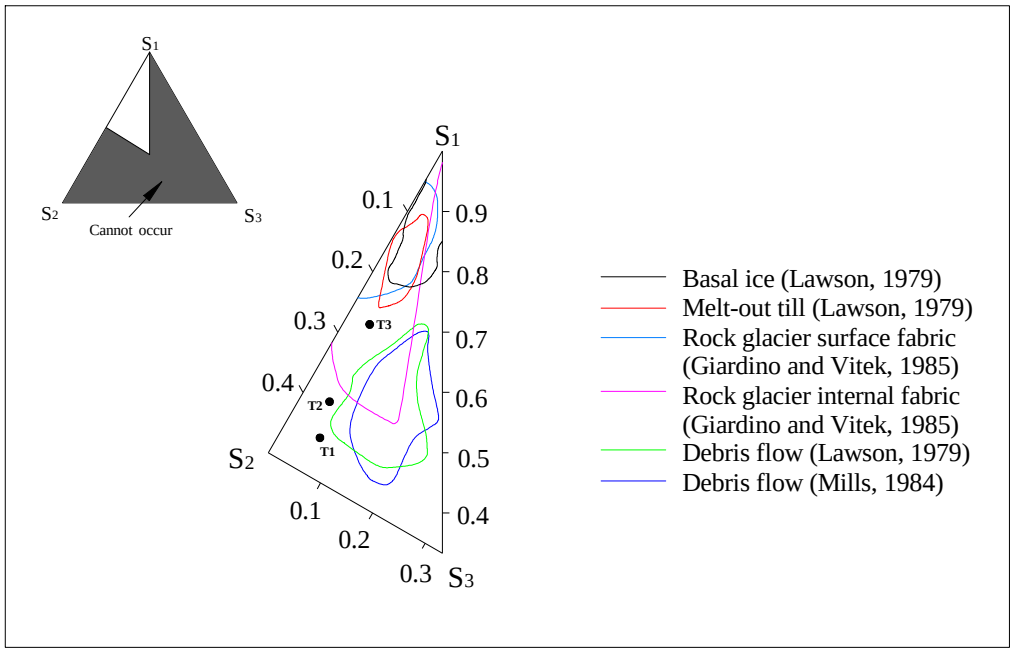



**Figure 6.29** Triangular plot of normalised eigenvalues for the Sekhokong Site 2 deposit, showing envelopes suggested by various authors. The usable field diagram occupies one sixth of the diagram because $S_1 > S_2 > S_3$.

### 6.3.5 Particle shape

Particle form was plotted onto triangular diagrams using Tri-plot v1.3 (Graham and Midgley, 2000) and representing the descriptive classes defined by Sneed and Folk (1958) (Figure 6.30) and the isolines of the Oblate-prolate (OP) index of Dobkins and Folk (1970) (Figure 6.31). All three trenches contain a wide range of clast shape; however the majority of clasts fall within the bladed category (Table 6.15). Particle shape in trenches 1 and 2 is fairly similar and bladed shapes constitute >54% of the sample. Trench 3 in contrast displays similar quantities of platy, bladed and elongate

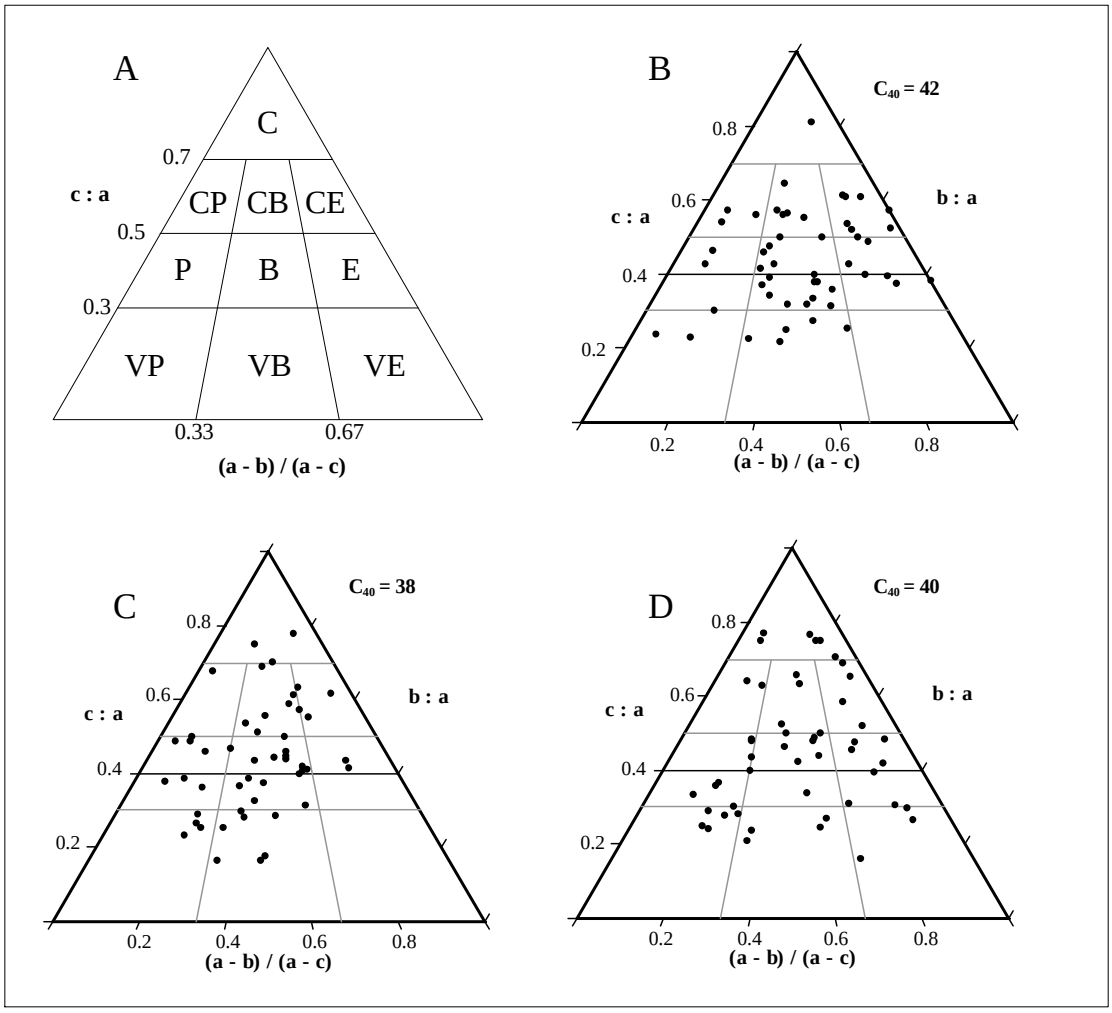



**Figure 6.30** Triangular diagrams after Sneed and Folk (1958). (A) The descriptive classes according to Sneed and Folk (1958) where C = compact, P = platy, B = bladed, E = elongate and V = very. (B-D) Triangular diagrams for Trenches 1, 2 and 3 respectively at Sekhokong Site 2. $C_{40}$ is the percentage of sample with c:a ≤ 0.4 (Benn and Ballantyne, 1993) (n = 50).

**Table 6.15** The percentage of clasts falling within the various shape categories at Sekhokong Site 2.

| Shape | Trench 1 (%) | Trench 2 (%) | Trench 3 (%) |
|---|---|---|---|
| Compact | 2 | 6 | 10 |
| Platy | 16 | 26 | 30 |
| Bladed | 54 | 58 | 32 |
| Elongate | 28 | 10 | 28 |

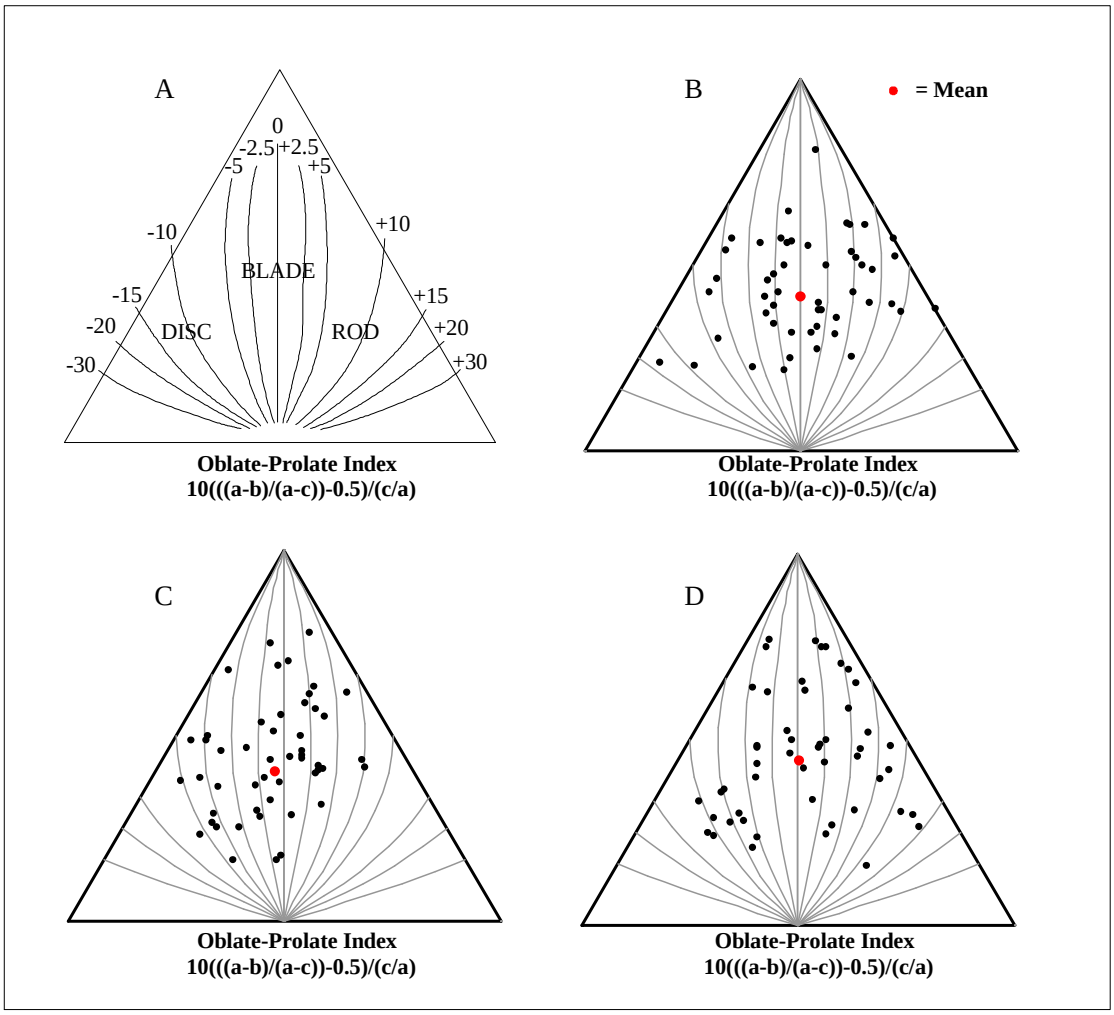



**Figure 6.31** Triangular diagrams after Sneed and Folk (1958). (A) Isolines of the Oblate-prolate index according to Dobkins and Folk (1970). Triangular diagrams for Trenches 1, 2 and 3 respectively at Sekhokong Site 2 (n = 50).

clasts and also a higher proportion of compact clasts than trenches 1 and 2. Figure 6.31 and Table 6.16 once again indicate the greater proportion of platy (disc-like) clasts present in trenches 2 and 3, in contrast to trench 1. This is further reinforced by the Oblate-prolate values, which range from -0.52 in trench 1 to -1.58 in trench 2 (Table 6.16). The maximum projection sphericity is represented in Figure 6.32. These results are varied, with the clasts in the three trenches falling between 0.2 and 1. The mean maximum projection sphericity ranges from 0.64 in trench 1 to 0.68 in trench 3 (Table 6.16).

Clast roundness is represented in Figure 6.33 and Table 6.17. The majority of clasts in trenches 1 and 2 fall within the angular and subangular categories; however trench 2 also contains 4% of clasts in the rounded category. Trench 3 only contains 2% of very angular clasts and the modal class is subangular, with 42% of the total sample. This trench also contains 30% subrounded and 10% rounded clasts which indicates rounding of clasts towards the snout of the deposit. This is further reinforced in Table 6.16, where the visual roundness mean ranges from 1.64 in trench 1 to 2.30 in trench 3, which means that the clasts in trench 1 fall between the angular and subangular categories, whilst those in trench 3 fall within the subangular and subrounded categories.

The t-test was performed to determine whether the sediment samples in the three trenches for form, sphericity and roundness was statistically significant (<0.05%), and whether there was a relationship between the sediment in the trenches (Table 6.18) and between deposits (Table 6.19). It is clear from Table 6.18 that the results for clast shape in the three trenches are statistically significant in all but visual roundness where the results are not significant between trenches 1 and 3 and trenches 2 and 3.

Table 6.19 indicates that the Oblate-prolate index is not significant between trench 1 for the Tsatsa-La-Mangaung deposit and all three trenches of the Sekhokong Site 2 deposit. Similarly, results are not significant between trenches 2 and 3 of the Tsatsa-La-Mangaung deposit and trench 2 of the Sekhokong Site 2 deposit. Oblate-prolate results are statistically significant between the Sekhokong Site 1 and 2 deposits.

**Table 6.16** The shape of clasts measured at the Sekhokong Site 2 slope deposit. *x* = mean, *s* = standard deviation.

| | Number In Sample | Oblate-prolate Index | | Maximum Projection Sphericity | | Visual Roundness (Powers, 1953) | |
|---|---|---|---|---|---|---|---|
| | | *x* | *s* | *x* | *s* | *x* | *s* |
| Trench 1 | 50 | -0.52 | 5.82 | 0.64 | 0.11 | 1.64 | 0.85 |
| Trench 2 | 50 | -1.58 | 4.79 | 0.65 | 0.13 | 1.68 | 0.98 |
| Trench 3 | 50 | -0.86 | 5.68 | 0.68 | 0.14 | 2.30 | 0.93 |

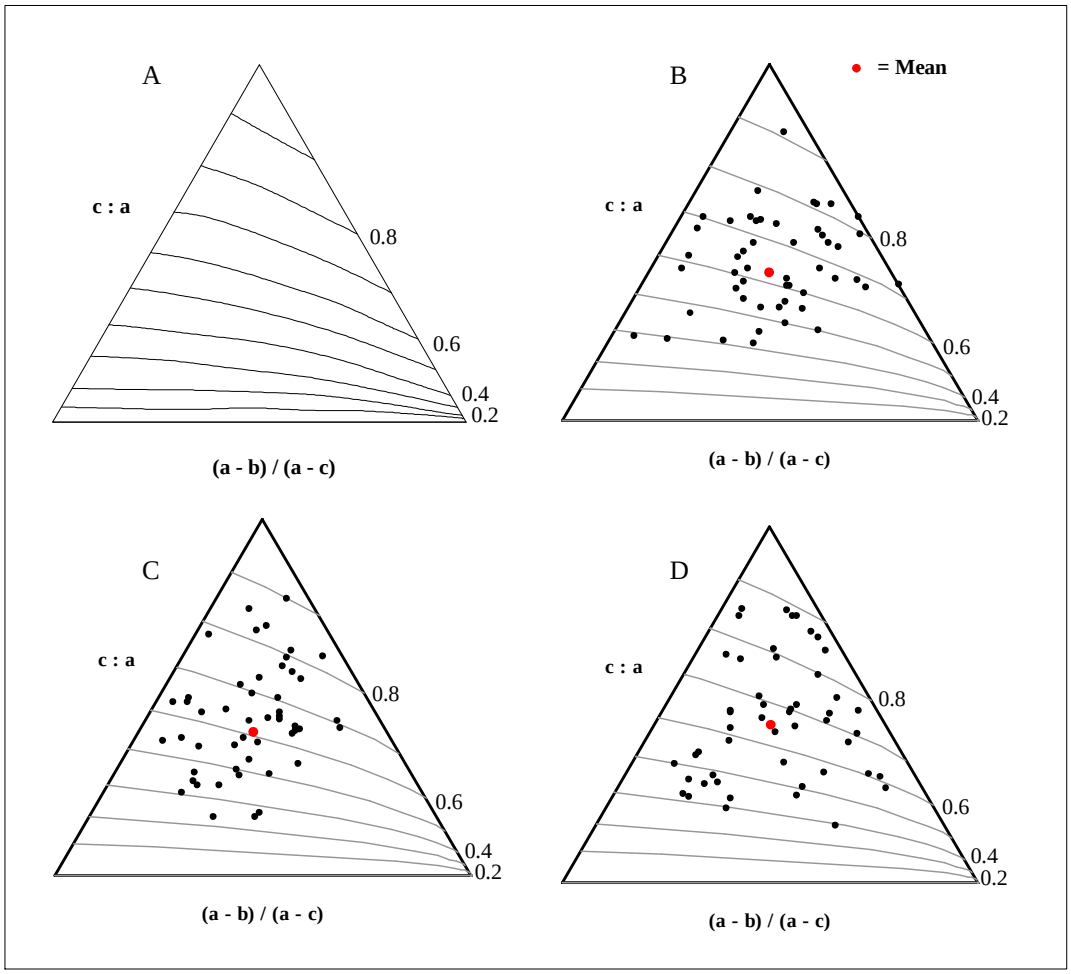



**Figure 6.32** Triangular diagrams after Sneed and Folk (1958). (A) Isolines of the maximum projection sphericity according to Sneed and Folk (1958). Triangular diagrams for trenches 1, 2 and 3 respectively at Sekhokong Site 2 (n = 50).

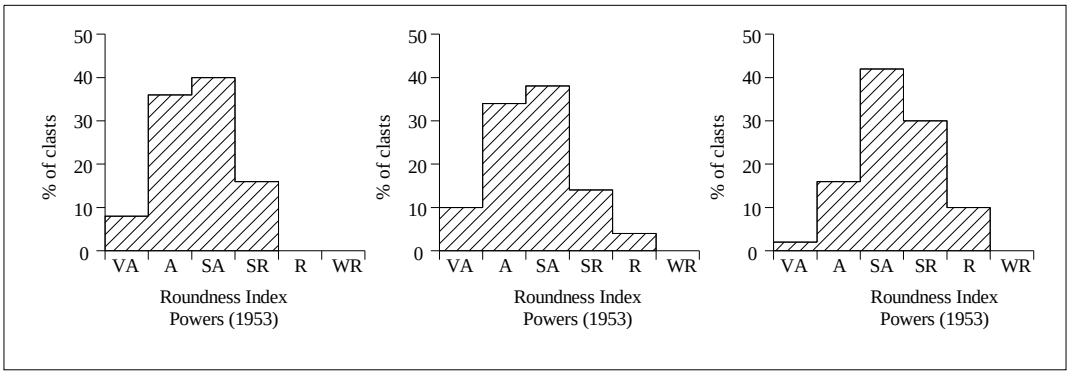



**Figure 6.33** Graphs representing visual roundness of clasts (after Powers 1953) in trenches 1 (A), 2 (B) and 3 (C) at Sekhokong Site 2. VA = Very Angular, A = Angular, SA = Sub Angular, SR = Sub Rounded, R = Rounded, WR = Well Rounded. n = 50.

**Table 6.17** The percentage of clasts falling in the roundness categories at Sekhokong Site 2.

| | VA (%) | A (%) | SA (%) | SR (%) | R (%) | WR (%) |
|---|---|---|---|---|---|---|
| Trench 1 | 8 | 36 | 40 | 16 | - | - |
| Trench 2 | 10 | 34 | 38 | 14 | 4 | - |
| Trench 3 | 2 | 16 | 42 | 30 | 10 | - |

**Table 6.18** The statistical significance calculated by the t-test of the shape of clasts sampled in the three trenches in the Sekhokong Site 2 deposit (SS = statistically significant, NS = Not significant).

| Trenches | Oblate Prolate Index | Maximum Projection Sphericity | Visual Roundness |
|---|---|---|---|
| T1-T2 | SS | SS | SS |
| T1-T3 | SS | SS | NS |
| T2-T3 | SS | SS | NS |

Maximum projection sphericity is not significant between Tsatsa-La-Mangaung trench 2 and Sekhokong Site 2, trench 3. Results are also not significant between the Sekhokong Site 1 and 2 deposits between trenches 1 and 3 and trenches 2 and 3. Visual roundness is also not significant between trench 2 of the Tsatsa-La-Mangaung deposit and trench 3 of the Sekhokong Site 2 deposit. In addition, visual roundness is not significant between trench 1 of the Sekhokong Site 1 deposit and all trenches of the Sekhokong Site 2 deposit. Visual roundness is also not significant between trench

**Table 6.19** The statistical significance calculated by the t-test of the shape of clasts sampled in the three trenches in the Tsatsa-La-Mangaung and Sekhokong Site 1 deposits (SS = statistically significant, NS = Not significant).

| Site and Trenches | Oblate Prolate Index | Maximum Projection Sphericity | Visual Roundness |
|---|---|---|---|
| TstatsaT1-Sek2T1 | NS | **SS** | **SS** |
| TsatsaT1-Sek2T2 | NS | **SS** | **SS** |
| TsatsaT1-Sek2T3 | NS | **SS** | NS |
| TsatsaT2-Sek2T1 | **SS** | **SS** | **SS** |
| TsatsaT2-Sek2T2 | NS | **SS** | **SS** |
| TsatsaT2-Sek2T3 | **SS** | NS | NS |
| TsatsaT3-Sek2T1 | **SS** | **SS** | **SS** |
| TsatsaT3-Sek2T2 | NS | **SS** | **SS** |
| TsatsaT3-Sek2T3 | **SS** | **SS** | NS |
| Sek1T1-Sek2T1 | **SS** | **SS** | NS |
| Sek1T1-Sek2T2 | **SS** | **SS** | NS |
| Sek1T1-Sek2T3 | **SS** | NS | NS |
| Sek1T2-Sek2T1 | **SS** | **SS** | **SS** |
| Sek1T2-Sek2T2 | **SS** | **SS** | **SS** |
| Sek1T2-Sek2T3 | **SS** | NS | NS |
| Sek1T3-Sek2T1 | **SS** | **SS** | **SS** |
| Sek1T3-Sek2T2 | **SS** | **SS** | **SS** |
| Sek1T3-Sek2T3 | **SS** | **SS** | NS |

2 of the Sekhokong Site 1 deposit and trench 3 of the Sekhokong Site 2 deposit and between trenches 3 of both deposits. No meaningful conclusions can be made in terms of statistical differences between deposits as some aspects are statistically significant and others are not. However, given the results are mainly statistically significant, it is suggested that similar processes took place.

### 6.3.6 Micromorphology

Samples were collected in trench 2 at 140 cm depth and in trench 3 at 118 cm and 150 cm depth (Table 6.20). The fabric pattern is random and particles have a broad degree of parallelism with weakly expressed orientations. The c/f related distribution is double spaced porphyric and the dominant size fraction is coarse sand. Particle sorting ranges from poorly sorted to unsorted and particle shape is blocky. Particles are subangular with an undulating surface roughness. Peds are spheroidal and weakly separated, whilst void type is vughy in trench 2 at 140 cm depth, and channel and vughy in trench 3. The sediment in trench 2 has a vughy microstructure, whilst the

**Table 6.20** Micromorphological description of the Sekhokong Site 2 samples.

| Micromorphological features → | Skeleton | | | | | | | | | Aggregates | | Voids | | | Parent Material | | | | Groundmass | | | Pedofeatures | | | | | |
|---|---|---|---|---|---|---|---|---|---|---|---|---|---|---|---|---|---|---|---|---|---|---|---|---|---|---|---|
| | Fabric | | | | | | Shape | | | | | | | | | | Fine | | | | | | | | | Infillings | | |
| Sample No. ← | Pattern | Degree of parallelism | Quantity of oriented particles | C/F related distribution | Dominant size fraction | sorting | Shape | Degree of roundness | surface roughness | peds | ped seperation and pedality | Void type | Microstructure | % total area occupied by voids | Rock type | Average size um | Colour | Limpidity | C/F 2mm | C/F 10um | C/F related distribution | Cappings | Texture | laminated | Classification | Descriptive criteria | Crystals |
| T2 140 | R | BA | W-E | DSP | CS | P/U | B | SA | U | S | WS | V | VM | 10 | B | 2500 | YB | SP | 4:1 | 9:1 | DSP | ● | SL | NL | LD | PF | ● |
| T3 118 | R | BA | W-E | DSP | CS | P/U | B | SA | U | S | WS | C&V | CM | 20 | B | 2700 | YB | SP | 4:1 | 9:1 | DSP | ● | SL | NL | LD | PF | ● |
| T3 150 | R | BA | W-E | DSP | CS | P/U | B | SA | U | S | WS | C&V | CM | 20 | B | 2500 | YB | SP | 4:1 | 9:1 | DSP | ● | SL | NL | LD | PF | ● |

KEY:

**Pattern:**
R = Random

**Degree of parallelism:**
BA = Broad angle

**Quantity of oriented particles:**
WE = Weakly expressed:<33% of particles are oriented

**C/F related distribution:**
SSP = Single spaced porphyric
DSP = Double spaced porphyric

**Size:**
CS = Coarse sand

**Sorting:**
PS = Poorly sorted
U = Unsorted

**Shape:**
P = Platy
B = Blocky

**Degree of roundness:**
A = Angular
SA = Subangular

**Surface roughness:**
U= Undulating

**Peds:**
S = Spheroidal Peds

**Ped seperation and pedality:**
WS = Weakly seperated

**Void type:**
C = Channels
CM = Chambers
V = Vughs
VCM = Vugh and Chamber
P = Planes

**Microstructure:**
VM = Vughy microstructure
CM = Channel microstructure

**Mineral type**
B = Basalt

**Colour:**
YB = Yellowish Brown

**Limpidity:**
SP = Speckled

**Cappings:**
● <10%
●● <10-20%
●●● >20%

**Texture:**
SL = Silt

**Laminated:**
NL = Nonlaminated
L = Laminated

**Infillings classification:**
LD = Loose discontinuous

**Descriptive criteria:**
PF = Passage features

**Crystals:**
● Few
●● Some
●● Many

**Crystal intergrowth:**
P = Parallel

sediment in trench 3 has a channel microstructure. The total percentage area occupied by voids ranges from 10% in trench 2 to 20% in trench 3.

The rock type is basalt and the average size of particles ranges between 2500 µm in trench 2 at 140 cm depth and trench 3 at 150 cm depth to 2700 µm in trench 3 at 118 cm depth. The colour of the fine material is yellowish brown and displays a speckled limpidity. The c/f ratio indicates that the samples are very coarse with very little material <10 µm (Figure 6.34). The c/f related distribution is double spaced porphyric. Pedofeatures include non-laminated silt cappings which occur on <10% of particles and loose discontinuous passage features. Crystals within the thin sections are few in all trenches.

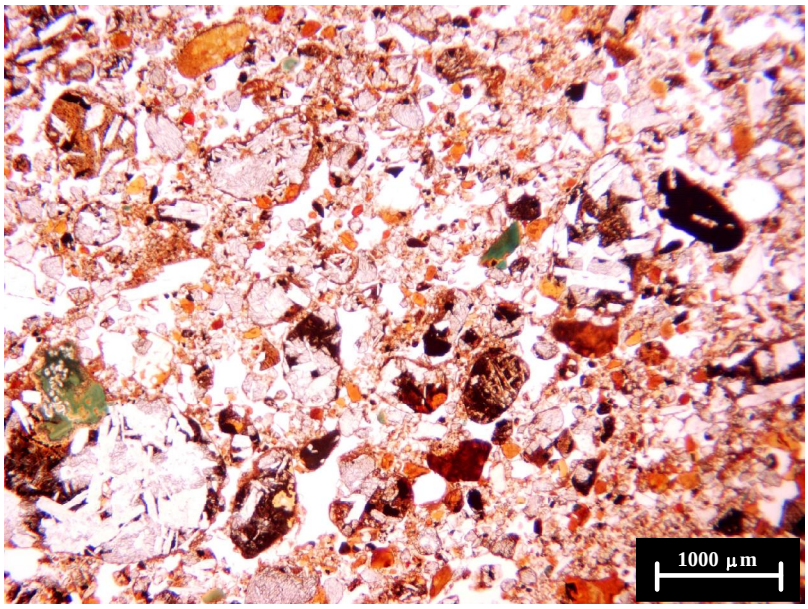



**Figure 6.34** Coarse material with very little fine fractions taken in PPL in trench 3 at 150 cm depth.

### 6.3.7 Radiocarbon dating

An AMS age of 16 270 ± 70 radiocarbon yrs BP was obtained from trench 3 at 1.9 m depth (Table 6.21), which represents the maximum depth of the trench. The calibrated age indicates that the deposit is younger than 19 350 yrs BP.

### 6.3.8 Summary

A Site summary of the sedimentary characteristics of the Sekhokong Site 2 deposit is presented in Table 6.22. Trenches 1 and 2 exhibit very similar characteristics, which

**Table 6.21** AMS and calibrated ages for the Sekhokong Site 2 deposit (Sampling depth: T3 = 1.9 m).

| Anal. No. [1] Gr-A | Sample designation | $\delta^{13}C$ (‰ PDB) | Radiocarbon Age yrs BP | 1σ yrs BC | 2σ yrs BC | Calibrated yrs BP |
|---|---|---|---|---|---|---|
| 24892 | Sekhokong Site 2 | -19.6 | 16270 ± 70 | 17 476 – 17 315 | 17 557 – 17 235 | 19 350 |

**Table 6.22** A summary of the sedimentary characteristics at Sekhokong Site 2.

| | Trench 1 | Trench 2 | Trench 3 |
|---|---|---|---|
| **Lithofacies** | Soil overlying gravely diamict | Soil overlying gravely diamict | Soil overlying gravely diamict with a medium grained horizon present |
| **Particle Size** | -1 Phi (Gravel) | -1 Phi (Gravel) | -1 Phi (Gravel) |
| **Sorting** | Poorly – moderately sorted | Very poorly sorted | Well - very poorly sorted |
| **Fabric** | Random | Random | Transverse to the ridge |
| **Dip** | 0° - 40° | 10° - 30° | 0° - 30° |
| **Shape** | Bladed | Bladed | Bladed, platy, elongate |
| **Roundness** | Sub angular | Sub angular | Sub angular |
| **Micromorphology** | Few cappings | Few cappings | Few cappings |
| **AMS dating** | | | 19 350 yrs BP |

consist of a present-day soil overlying a gravely poorly sorted diamict. Gravel is the main constituent in both trenches, however trench 2 also consist of a significant amount of finer material with some bimodal distributions. Clast orientation in trenches 1 and 2 is random and clasts tend to dip between 0° and 40°. Clast shape is predominantly bladed and subangular, however there is also a considerable amount of angular clasts present. There are also very few cappings present in thin section. In contrast, although the sediment in trench 3 also consists of a gravely diamict, there is also the presence of a medium grained horizon within this diamict unit. The diamict unit also contains a significantly higher proportion of gravel compared to trenches 1 and 2. Sorting ranges from well sorted to very poorly sorted and clasts tend to be oriented transverse to the ridge crest with dips between 0° and 30°. Clast shape is variable, with equal amounts of bladed, elongate and platy clasts, whilst roundness tends to be subangular. The coarse nature of the material is reflected in thin section and there are also a few cappings present. The calibrated age of 19 350 yrs BP for the deposit indicates that it is pre-Holocene.